2009

comparison of bio-oil produced in a fractionated bio-oil collection system

Anthony Joseph Sherwood Pollard
Iowa State University

Comparison of bio-oil produced in a fractionated bio-oil collection system

by

Anthony Joseph Sherwood Pollard

A thesis submitted to the graduate faculty

in partial fulfillment of the requirements for the degree of

MASTER OF SCIENCE

Co-majors: Mechanical Engineering, Biorenewable Resources and Technology

Program of Study Committee:
Robert Brown, Major Professor
Steven Hoff
Gregory Maxwell

Iowa State University

Ames, Iowa

2009

TABLE OF CONTENTS

LIST OF FIGURES

LIST OF TABLES

ACKNOWLEDGEMENTS

I dedicate this thesis to my wife, Jenny. She has supported me and allowed me to fully concentrate on this project and I am eternally grateful for that. I thank her for everything that she has done.

Secondly, I would like to thank Dr. Brown for the opportunity to work on this project. Sam Jones for offering guidance and input throughout the process. All of my fellow graduate students who have provided insight, information and help. I would like to specifically like to thank Lysle Whitmer and Andrew Olthoff for all of their help during the testing of the system. I would also like to thank Marge Rover and Patrick Johnston who helped me immensely with analytical equipment and analysis and Bruce Erickson and Dick Egger for helping me with the manufacturing and design of my fast pyrolysis system. Finally, all of the undergraduate assistants that I have worked with. Without the help of these students, there is no way that this research would have gotten finished.

ABSTRACT

Fast pyrolysis bio-oil, char and non-condensable gases were produced from a 8 kg/hr fluidized bed reactor. The bio-oil was collected in a fractionating bio-oil collection system that produced multiple fractions of bio-oil. This bio-oil was fractionated through two separate, but equally important, mechanisms within the collection system. The aerosols and vapors were selectively collected by utilizing laminar flow conditions to prevent aerosol collection and electrostatic precipitators to collect the aerosols. The vapors were successfully collected through a selective condensation process. The combination of these two mechanisms has created the ability to effectively fractionate the bio-oil into distinct fractions with improved characteristics. The fractions of bio-oil each contained different properties. Bio-oil properties that were improved included the energy content, water content, acid content and distribution of certain carbohydrates (levoglucosan and acetic acid). The improved properties that are associated with the fractionated bio-oil could allow bio-oil to be used in new markets, preferably without further upgrading. The decreased water and acid contents in the first four (of five) fractions could allow for easier upgrading of the bio-oil into transportation fuels or other valuable products.

CHAPTER 1. OVERVIEW

1.1 Introduction

Fractionated bio-oil collection is a method of bio-oil collection, produced through the fast pyrolysis of biomass, that has been used very sparingly in research and industry. Most bio-oil collection systems that are currently in use purposefully collect only a single fraction. This single fraction of bio-oil contains all of the water from the process as well as all of the over 300 compounds[2] that are found in fast pyrolysis bio-oil. This can lead to many problems, including low energy contents and bio-oil instability.

The encompassing goal of fractionating bio-oil collection is to separate the bio-oil into distinct fractions that contain different families of compounds. Each fraction has different properties that make that fraction unique. For instance, one of the main goals of the system is to collect the vast majority of the water in the final fraction. This will increase the energy content of the other fractions because of the lack of water in those fractions of bio-oil. This system operates by making a distinction between vapors and aerosols as well as collecting the vapors based on the boiling point. By collecting the vapors based on the boiling point, it is possible to separate the compounds that are found in the vapor phase into distinct fractions.

1.1.1 Hypothesis

Hypothesis: The separation of bio-oil components is possible through the utilization of cooling surfaces that have elevated temperatures that are analogous with the dew point of certain compounds.

Discussion of hypothesis: Each bio-oil component that is present in the vapor phase has a certain vapor pressure that is constantly changing. If the vapor pressure of that component is lower than atmospheric pressure, then the dew point of that component will be lower than its boiling point at atmospheric pressure. This phenomena is described

with the Clausius-Clapeyron relationship. Using this principle, this thesis will show that it is possible to collect bio-oil in distinct fractions, separating compounds like acetic acid, water and levoglucosan.

1. 2 Definition of Terms

Fast Pyrolysis: A high temperature process that converts raw biomass into bio-oil, char and non-condensable gases. This process takes place between 450 and 550^{o}C in the lack of oxygen.

Biomass: Mixture of cellulose, hemicelluloses, lignin and small amounts of minerals. Biomass can range from agricultural wastes (cornstover, bagasse) to energy crops (switchgrass, wood).

Bio-oil: The liquid product from fast pyrolysis reactions. Bio-oil is composed of up to 300[2] organic compounds that include anhydrosugars, phenolics, carboxylic acids, pyrolytic lignin, ketones, aldehydes and water.

Char: Solid byproduct of fast pyrolysis. Consists mainly of carbon, but can also contain other compounds including minerals and ash.

Non-Condensable Gases: Gaseous product of fast pyrolysis reactions. Contains hydrogen, carbon monoxide, carbon dioxide, methane and other light hydrocarbon gases.

Cyclones: Solid-gas separation filters that utilize centrifugal forces to remove solid particulate from gas flow. Most utilize a tangential entrance to force the gas to move around the outer walls at high velocities.

Diffusion: The macroscopic result of random thermal motion on a microscopic scale.[3] Products are drawn from high concentrations to lower concentrations.

Condensation: Physical change of state from a gaseous phase to a liquid. The energy that is released during condensation is referred to as the enthalpy of vaporization.

Electrostatic Precipitator (ESP): Filter that utilizes electrostatic forces to clean gases. Has the ability to remove either solid particulate or liquid aerosols. Typical operating voltages: 15-40 kVDC.

Heat Exchanger: Device designed to transfer heat from one medium to another. Requires a temperature gradient between mediums.

Gas Chromotography: Method for separating and analyzing organic compounds that can be detected in the gas phase without decomposition. Can be used to analyze either gases or liquids.

GC-MS: A method that combines both gas chromatography and mass spectrometry. Used to analyze liquid samples to identify compounds that are present. Can only detect compounds that can volatilize without degradation.

GC-FID: A method that combines both gas chromatography and flame ionization detection. Analyzes a sample by detecting the electrical current that is generated by the electrons that are generated from burning the carbon in said sample.

Modified Acid Number (MAN): Amount of potassium hydroxide (KOH) that is required to neutralize the organic acids that are present in one gram of sample. Typically used for petroleum, but recently gaining interest in bio-oil analysis. This analysis is used to detect weak, carboxylic acids.

Moisture Content: Amount of moisture, in weight percent, that is present in a sample.

% Water Insolubles: Amount of water insoluble components, in weight percent, that are present in bio-oil after complete washing in water. In bio-oil, these insolubles are thought to be products of the lignin and possible secondary reactions.

Higher Heating Value: Amount of heat that is released when the product is combusted and returned to atmospheric temperature. This value takes into account the latent heat of vaporization water which makes the higher heating value a strong function of moisture content.

Solids: Solid particulate that escaped the solid-gas separation filter. The solids found in bio-oil are typically considered char, ash and even some condensed organic residues can act as solids.

Viscosity: Measure of resistance a fluid feels when it is being deformed through either shear forces or other forces.

CHAPTER 2. REVIEW OF LITERATURE

2.1 Introduction

There is a large amount of literature available on general biomass fast pyrolysis and the associated reactors that are used, but there are very few articles that discuss the collection of bio-oil directly. The concept of fractionated bio-oil collection is new, thus there is no literature to directly compare the results. Comparisons will be made with whole bio-oil which is well documented from many biomasses.

2.2 Fast Pyrolysis and Fast Pyrolysis Reactors

Fast pyrolysis is the rapid thermal decomposition of carbonaceous organic matter in the absence of oxygen. This process occurs at moderate temperatures (450-550^{o}C) and in a very short amount of time (1-2 seconds). Fast pyrolysis produces three main products which include char, bio-oil and non-condensable gases. The amount of these products produced is dependent on many factors including reactor temperature, feed stock and residence time. The best results for biomass occur when the reactor is operated in the temperature range of 450^{o}C to 550^{o}C, the reactor can provide high heating rates and there is a method of rapidly cooling the pyrolysis vapors after the char has been sufficiently removed.[2]

Fast pyrolysis of biomass occurs in multiple steps.[4] First, heat is transferred from the heat source to the biomass. This causes an increase in temperature in the entire biomass particle. The increase in temperature leads to primary pyrolysis reactions. These reactions lead to the release of volatiles and the initial formation of char. The flow of the volatiles out of the biomass particle results in heat transfer between the hot volatiles and liquids and the cool un-reacted biomass. Finally, there are autocatalytic secondary reactions that are caused by the interaction of bio-oil vapors and liquids with the char that is produced.

Typical fast pyrolysis systems include a reactor, solid particulate removal and bio-oil collection system. There are many reactor configurations currently available for fast pyrolysis. These include bubbling fluidized bed, circulating fluidized bed, vacuum reactors, ablative reactors, auger reactors and free fall reactors. All of these reactors have their benefits and pitfalls. Each of these fast pyrolysis reactors are very distinct in their operating parameters and conversion techniques. Bubbling fluidized beds offer high heat transfer rates, good mixing, good temperature control and good elutriation of char particles. These factors make a bubbling fluidized bed a good reactor for fast pyrolysis. Many fast pyrolysis systems, both in industry and research, utilize fluidized beds because of their beneficial attributes and ease of operation.[5-8]

Circulating fluidized beds use fluidization velocities that are sufficiently high enough to elutriate both the sand and char particles.[9] This mixture of sand and char then enter a cyclone which removes all of the particulate from the gas flow. The gases then proceed to a system to collect the bio-oil. Typically, the char and sand are then sent to a separate reactor where the char is combusted, thus heating the sand. The sand then is sent back into the pyrolysis reactor already preheated. The circulating fluidized bed shares some of the same benefits as a bubbling fluidized bed, but has the added value of pre-heated sand. There are some disadvantages to using a circulating fluidized bed as well. Circulating fluidized beds require large amounts of inert gases (nitrogen, CO_2, etc.) to act as a fluidizing gas. This large amount of gas dilutes the vapors even further. This dilution creates a higher amount of heat that must be removed from the product stream as the bio-oil vapors are condensed. Industrial companies who have utilized this technology include Ensyn and Dynamotive.[9]

Vacuum reactors utilize a negative pressure (a vacuum) to remove the vapors from the reactor. Vacuum pyrolysis uses relatively slower heating rates but utilizes the vacuum pressure to lower the vapor pressure of the products. This removal of vapors keeps the vapor residence time similar to that of other fast pyrolysis reactors. Vacuum pyrolysis

reactors typically only have a 60-65% liquid yield with higher yields of solid particulate.[9, 10] These yields may be due to the lower heating rates found in vacuum pyrolysis.

Ablative reactors utilize hot plates and large particle sizes to "melt" the biomass on the ablative plate. This process requires both a large amount of force to be applied to the biomass as well as a large relative motion between the biomass and the heated surface. The bio-oil that is deposited on the plate is then evaporated and later condensed. This process works very well with large particle sizes and is only limited on the amount of heat that can be applied to the rotating disc. Some benefits to ablative reactors is a compact size and a lack of carrier gas. The disadvantages include poor control and moving parts that are at an elevated temperature.[11]

Auger reactors are a fairly new technology in the biomass pyrolysis industry. Auger reactors, also referred to as mechanically fluidized beds, use either one or two auger configurations to mix and move hot sand and biomass particles.[9] The biomass particles mix with the hot sand, causing the fast pyrolysis reactions. Typically, very little or no carrier gas is used in the process. These reactors could be very useful because of their small size, lack of fluidizing gas and a possible lower operating temperature.

The free fall reactor that has recently gained interest in the research of fast pyrolysis.[12] This reactor utilizes radiant heat to quickly heat free falling particles of biomass. The major benefit of this system is its simplicity and lack of moving parts. There are questions that are associated with scale-up to commercial scale though.

2.3 Fluidized Bed and Cyclone Design

Fluidized bed design is a well developed methodology that has been used for many applications. Even though bubbling fluidized beds have been used quite frequently for the fast pyrolysis of biomass, there is not much information in the literature concerning the sizing of the fluidized bed for certain biomass feed rates. For the fluidized bed fast pyrolysis reactor that was designed, the amount of heat required for fast pyrolysis was the determining factor when sizing the fluidized bed. According to Daugaard[13], the enthalpy of pyrolysis for cornstover was determined to be 1.35 MJ/kg (dry). This design required an assumed convective heat transfer coefficient in the range of 100-250 W/m^2-K.[14] The final heat transfer coefficient was selected to be 150 W/m^2-K. This heat transfer coefficient is between the sand particles and the reactor walls. Heat transfer between the bed media and a surface is dependent on the particle size as well as other fluidization characteristics. Figure 1 depicts the relationship between particle diameter and the bed-to-surface heat transfer coefficient.

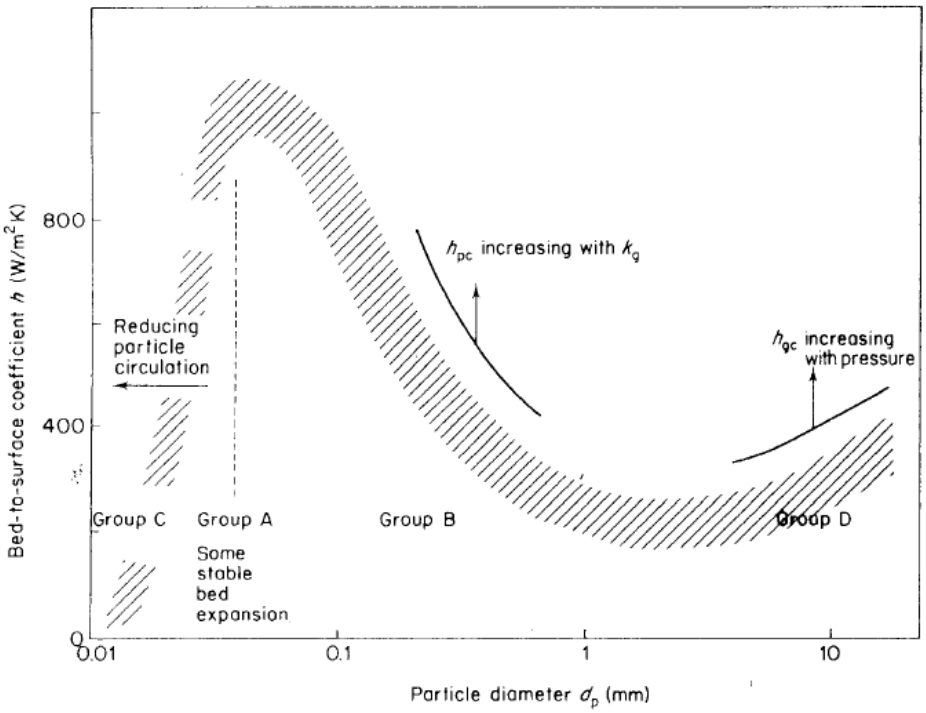

Figure 1 Heat Transfer from Fluidized Bed[14]

Fluidized bed design is based on the combination of bed media properties and fluidizing gas properties. A bed of sand is fluidized when the forces due to gravity on the particles is equal to the drag forces generated by a fluid passing by the particle. This balance has been studied extensively and is shown in an empirical formulation in Equation 1.[14]

$$U_{mf} = \left(\frac{\mu_f}{\rho_f d_v}\right)\left[(1135.7 + 0.0408 \cdot Ar)^{1/2} - 33.7\right] \quad \textbf{Equation 1}$$

This equation for the minimum fluidization velocity (U_{mf}) is a function of the fluid properties, the particle diameter and the Archimedes number (Ar). The Archimedes number (Equation 2), is used to determine the motion of fluids due to differences in densities. This can apply to solids that are within a fluid as well.

$$Ar = \frac{\rho_f {d_v}^3 (\rho_p - \rho_f) g}{{\mu_f}^2} \qquad \textbf{Equation 2}$$

Gas cyclones have long been used in industry for the removal of solids from a gas flow. The solids are removed from the flow through the application centripetal forces. Gases enter the cyclone tangentially and are forced to flow around the outside, creating large centripetal forces that force the solid particulate towards the walls. There are many methods of designing cyclones. One method that is presented by L. Svarovsky[14] makes a distinction between high flow and high efficiency. The difference between these cyclone designs is the distance the gases have to travel within the cyclone as well as the inlet and outlet velocities. Cyclone calculations can be seen in Appendix A. It has been shown that a series of multiple cyclones will produce a better overall efficiency than a single cyclone.[15]

2.4 Condenser Technology

One of the most important processes in fast pyrolysis, which is typically viewed as secondary compared to the reactor, is the bio-oil collection system. To be able to use the bio-oil, you must be able to condense it from the vapor form in a reliable and fast manner. If the vapors are left at high temperatures for a prolonged period of time, secondary reactions can occur. These secondary reactions occur either when larger, heavier molecules break down into lighter molecules and eventually into a non-condensable gas, or when bio-oil vapors react with char.

Bio-oil collection has long been a challenge for fast pyrolysis researchers. The product stream exiting a reactor is a combination of vapors, aerosols and polar molecules that are bonded to water vapor molecules.[11] ESPs are commonly used to collect the aerosols droplets.[5, 7, 11] There are problems that can occur with ESPs, including electrical arcing across the bio-oil. Currently, there are a few different options available in the literature for bio-oil collection systems. These bio-oil collection systems can be broken down into two main categories: spray towers and heat exchangers. Large scale systems typically utilize quench systems that are designed specifically for the reactor that they service. Bridgwater[11] summarized the use of heat exchangers by stating that slow cooling can lead to the preferential collection of lignin-derived components, but that can lead to blockages in the heat exchanger equipment due to the high viscosity of the lignin-derived components.

A spray tower is a commonly used bio-oil collection system that many authors have presented in the literature. These systems are presented in this section. Spray tower or spray quench systems utilize a re-circulated spray of bio-oil to cool and collect all of the bio-oil at once. An example of a spray quench system can be seen in Figure 2. The already condensed bio-oil is sprayed in a countercurrent manner in a spray column. Westerhof et al.[16] used two jacketed spray columns along with an intensive cooler to cool their gases and collect their bio-oil. Shell Ondina 941 was used by Westerhof et al. as a start-up liquid for their spray tower. This solvent was used because it had a low

solubility in bio-oil. Zheng et al.[17] used a similar system in their research of cotton stalk fast pyrolysis. Their spray system featured a heat exchanger that had cool bio-oil sprayed over it from the top. The bio-oil was initially collected by the spray and all of the bio-oil was cooled by the heat exchanger. This allows the sprayed bio-oil to be cool in temperature when it is sprayed again.

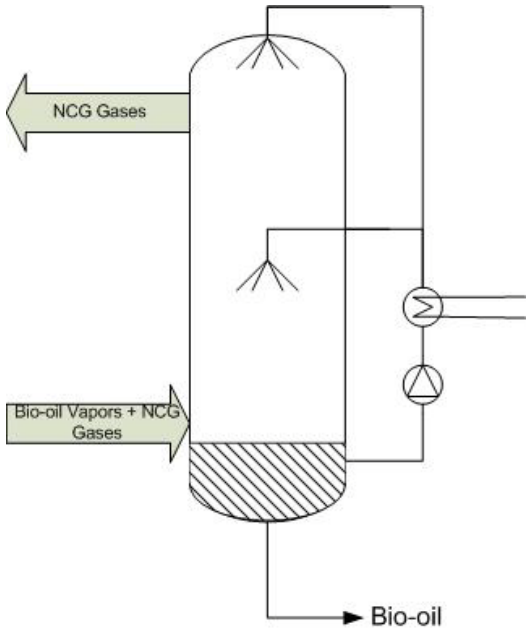

Figure 2 Spray Quench System

Heat exchangers utilize a cool surface to cool the gases and condense the bio-oils. This can be a very effective manner of cooling and collecting bio-oil for any size of system. Boateng et al.[5] used a series of four identical impingers (see Figure 3) that were submersed in a water bath that was chilled by dry ice. Boateng used a bench scale, 2.5 kg/hr, fluidized bed fast pyrolysis reactor.

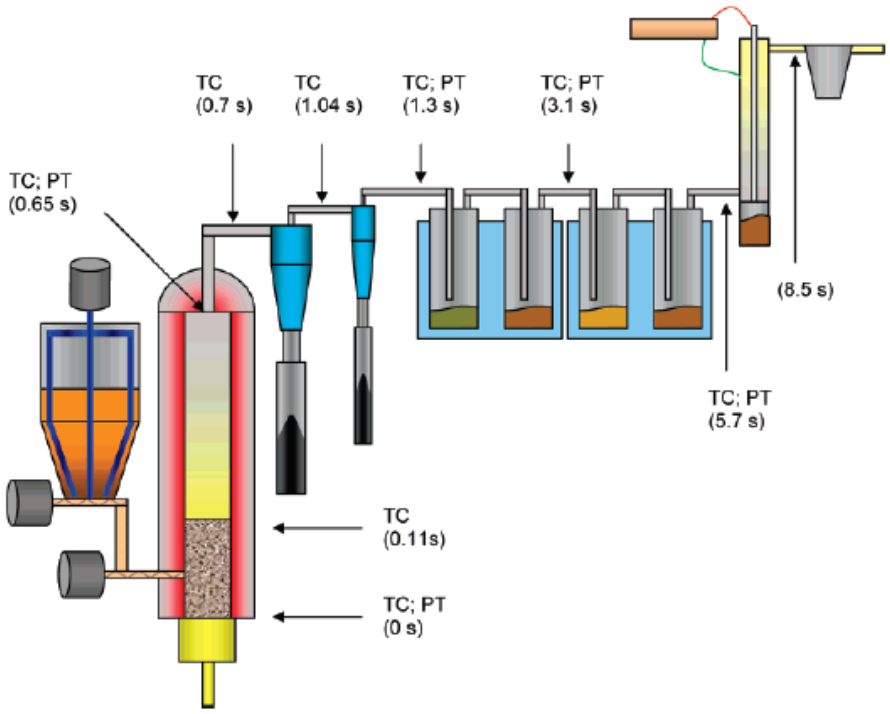

Figure 3 Example of Fluidized Bed with Impingers[13]

Scott et al.[8] utilized two separate water cooled condensers with their 3 kg/hr fluidized bed reactor. The first condenser used water that could be kept at temperatures up to 100°C. The second condenser utilized a chilled water bath that was kept at 0°C to finish cooling the gases and oil product. Lede et al.[18] used a series of three water cooled heat exchangers with their 1 kg/hr cyclone fast pyrolysis reactor. Each of these heat exchangers was approximately 0.5 meters long and had a diameter of 0.01 meters. Lede then used an air cooled condenser to cool and collect the last of the bio-oil. Predel and Kaminsky[7] utilized a slightly different configuration when cooling the bio-oil from their 1-3 kg/hr fluidized bed fast pyrolysis system. Predel and Kaminsky utilized an initial cooler followed by two electrostatic precipitators. The ESPs were then followed by two more coolers. Z. Luo et al.[6] used a pipe bundle quencher to collect the bio-oil produced from their 3 kg/hr fluidized bed fast pyrolysis system. Miao et al.[19] used a hot water condenser followed by an ice water condenser to collect the bio-oil that was created in

their system. Gerdes et al.[20] designed a process development unit that utilized both a heat exchanger and an intensive cooler to cool and collect their bio-oil.

One common theme that was found among all of the bio-oil collection systems that were found was that all of the bio-oil was either collected in one container or eventually mixed together. The system that is used in this study fractionates the bio-oil as it is being collected. Another commonality that can be found in most of these systems is an electrostatic precipitator. ESPs are commonly used to collect the aerosol droplets that are present when the bio-oil vapors leave the fast pyrolysis reactor.

Separating whole bio-oil (post condensation) into separate compounds or fractions can be a costly and difficult proposition. Bio-oil is very sensitive to changes in temperature. Heating bio-oil can cause an array of reactions that include decomposition, polymerization and oxygenation. These reactions cause difficulties when traditional distillation is attempted on whole bio-oil. There is a high probability for coking and polymerization, which prevent full distillation from occurring.

Recent research has shown that molecular distillation is possible at small scales.[1, 21] Molecular distillation has been historically used for purification of chemicals when there were concerns about thermosensitivity, usage of high molecular weight materials, high viscosity and high boiling points. According to Wang et al.[1] molecular distillation has historically been used in the following industries: fine chemical, petrochemical, pharmaceutical, oil and grease, food processing and light industry. Molecular distillation is a process where the bio-oil is heated to moderate temperatures (50-130^{o}C) under a vacuum (10-60 Pa) in a thin film (1mm) on a plate. A second cool plate is placed at a specified distance from the warm plate. The distance between the plates is the distance a light molecular weight molecule can travel before colliding with another molecule. This allows for purification compounds in complex mixtures like bio-oil.

Table 1 Results from Molecular Distillation (Adapted from Wang et al.)[1]

Wang et al. and Guo et al. were able to separate bio-oil into three distinct fractions. These fractions were analyzed and the results are shown in Table 1 Results from Molecular Distillation (Adapted from Wang et al.)[1]. Note the removal of water and acid from two of the fractions. The water and acid is concentrated in the first fraction. The second fraction was a dark-red liquid that was combustible with a low moisture content. The final fraction was a solid at room temperature and was high in carbon and levoglucosan.

2.5 Biomass and Bio-oil Components

Biomass is comprised of three main components that have a specific function integral to the life and survival of a plant material. These components include cellulose, hemicelluloses and lignin.

Cellulose

Cellulose is a linear polymer comprised of β-(1-4)-D-glucopyranose units that are linked in the $^4C_1$ conformation.[9] The linear polymers make fibers that provide strength to plant material. Wood, which is a strong material, is comprised of between 40-50% by weight of cellulose. Cellulose has the propensity to form crystalline structures through hydrogen bonding, making it insoluble to normal solvents. Cellulose decomposes at temperatures that range between 240-350^{o}C. The degradation of cellulose produces anhydrosugars including levoglucosan. Figure 4 is an example of the cellobiose unit which is the building block for cellulose polymers.

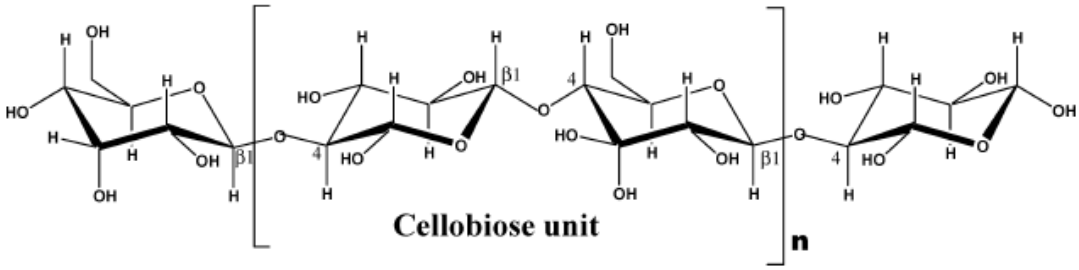

Figure 4 Cellulose Structure[9]

Hemicellulose

Hemicellulose is a polymer that is comprised of five and six carbon sugars. These sugars include glucose, mannose, galactose, xylose, arabinose and glucuronic acid. These sugars form a polymer that can comprise between 25-35% by weight of the biomass. Thermal degradation of hemicellulose occurs between 200-260^{o}C. The thermal degradation of hemicellulose is thought to produce most of the acetic acid that is produced during the fast pyrolysis of wood.[9] There is some levoglucosan that is produced during the fast pyrolysis of hemicellulose as well. Figure 5 shows the six main components that comprise the hemicellulose polymer.

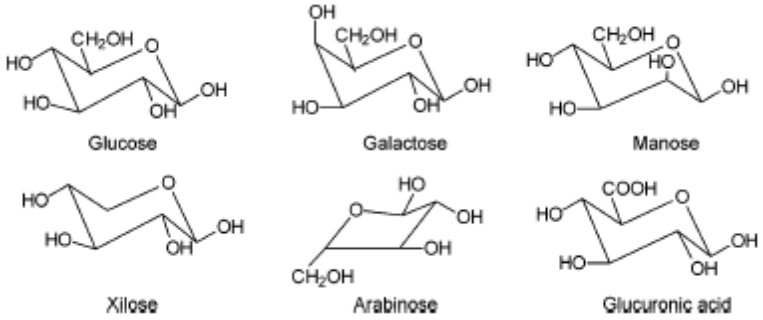

Figure 5 Hemicellulose components[9]

Lignin

Lignin is the final major component of biomass. Lignin can comprise between 16 and 33% of woody biomass. Lignin is an amorphous cross-linked resin that has no exact structure.[9] Figure 6 is a partial lignin molecule from a hard wood. Lignin is thermal decomposed at temperatures that span a wide range, from 280-500^{o}C. Lignin is specific to the biomass that is being pyrolyzed.[22] Hardwoods have a significantly different lignin structure than cornstover, switchgrass or even softwoods. Hardwoods typically favor the production of both guaiacols and syringols while softwoods typically favor only the production of guaiacols.[22] Lignin is thought to be responsible for the bio-oil that is collected in the aerosol form. Lignin is also responsible for the production of guaiacols and phenols from fast pyrolysis.[23]

There are many ways to break down the compounds and components of bio-oil. It has been suggested in the literature that the GC/MS compounds can be broken down into major and minor carbohydrates, furans, phenols, guaiacols and syringols.[22] Table 2 denotes the breakdown of compounds that are in these groups. Other major bio-oil constituents that can be documented include water content, solids content, water insoluble content and ash.

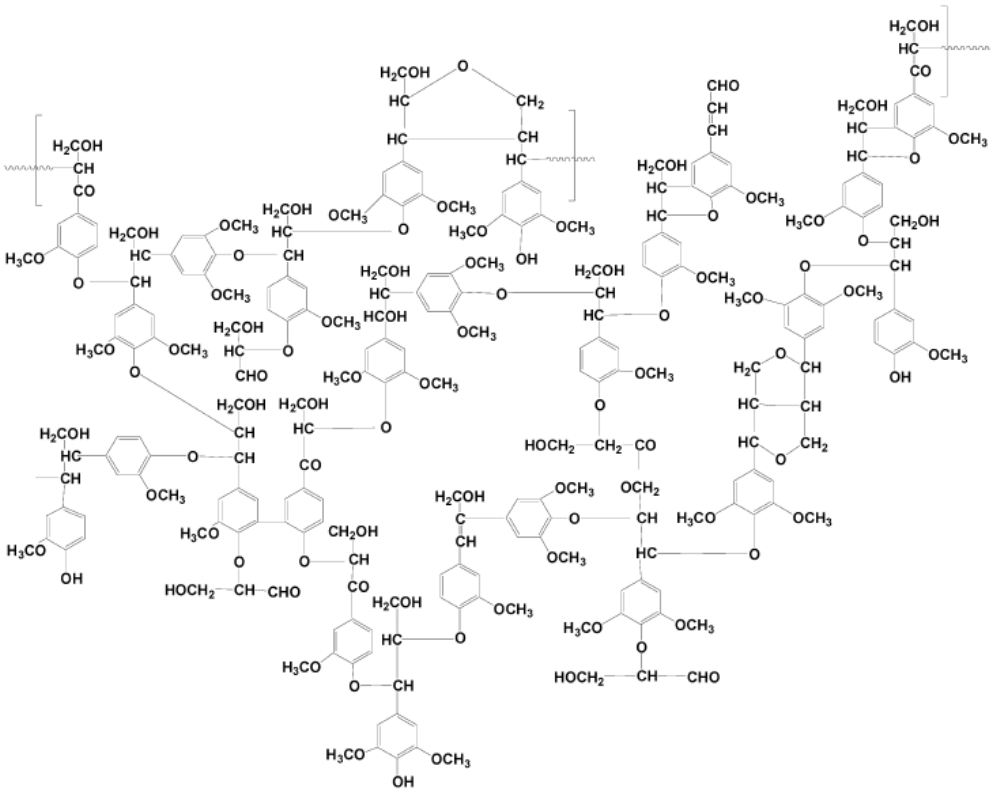

Figure 6 Partial Lignin Molecule[9]

Table 2 GC/MS Compound Groupings[22]

Major Carbohydrates	Minor Carbohydrates	Furans
hydroxyacetaldehyde	3-ethyl-2-hydroxy-2-cyclopentenone	2-acetylfuran
hydroxypropanone	acetoxyacetone	5-methyl-2-furaldehyde
acetic acid	propionic acid	2-furaldehyde
levoglucosan	2-methyl-2-cyclopentenone	furantetrahydro-2,5-dimethoxy *cis*
	3-methyl-2-cyclopentenone	furantetrahydro-2,5-dimethoxy *trans*
	1-hydroxy-2-butanone	furfuryl alcohol
	formic acid	2(5*H*)-furanone

Phenols	Guaiacols	Syringols
phenol	guaiacol	syringol
o-cresol	4-acetoneguaiacol	syringaldehyde
p-cresol	4-ethylguaiacol	acetosyringone
m-cresol	4-methylguaiacol	4-methylsyringol
2-methyl-4-propylphenol	isoeugenol *cis*	
3,4-dimethylphenol	isoeugenol *trans*	
2,5 or 2,4-dimethylphenol	eugenol	
2-ethylphenol	vanillin	
hydroquinone		

Other GC/MS Detectable Compounds
1,2-Cyclopentanedione, 3-methyl-
2-Propanone, 1-(acetyloxy)
2H-Pyran-2-one
Acetol
Methanol

Acetic Acid

Acetic acid is one of the simplest carboxylic acids. It is a two carbon acid that has a molecular formula of $C_2H_4O_2$. Acetic acid is classified as a major carbohydrate, as shown in Table 2. Acetic acid has a molecular weight of 60.05 grams/mol and a boiling point of 118.1°C at atmospheric pressure. Current understanding shows that acetic acid is formed through the thermal degradation of hemicellulose, lignin and cellulose.[9, 22, 24] Figure 7 denotes the chemical structure of acetic acid.

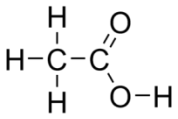

Figure 7 Acetic Acid Molecule[25]

Levoglucosan

1,6-anhydro-β-D-glycopyranose (commonly known as levoglucosan) is a product of the thermal degradation of cellulose.[24] Levoglucosan is classified as a major carbohydrate as shown in Table 2. The chemical formula is $C_6H_{10}O_2$, with a molecular weight of 114 grams/mol. The chemical structure of levoglucosan can be seen in Figure 8. When heated, levoglucosan proceeds through single phase change. It has been shown that levoglucosan has a melting point of 113°C.[26] As the temperature of levoglucosan is increased further, it degrades into smaller compounds before it reaches the boiling point. Suuberg has estimated that the true boiling point of levoglucosan is approximately 260°C with an enthalpy of vaporization of 120 kJ/mol.[26] The enthalpy of vaporization was based on the Clausius-Clapeyron equation, which relates the enthalpy of vaporization to the boiling point at a give pressure.

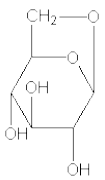

Figure 8 Levoglucosan Molecule[27, 28]

Formic Acid

Formic acid is the simplest carboxylic acid with a chemical formula of CH_2O_2. It has a molecular weight of 46 grams/mol and a boiling point of 101.3°C at atmospheric temperature. The production of formic acid is due to dehydration and elimination reactions of cellulose and hemicelluloses.[22] Figure 9 denotes the chemical structure of formic acid.

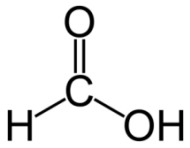

Figure 9 Formic Acid Molecule[29]

Furans

Furans are a heterocyclic organic compound that has an oxygen molecule and two double bonds. An example of a furan is shown in Figure 10. Furans are aromatic compounds that are very flammable and volatile. Furans have low boiling points (31.4°C for pure furfural). Furans are the product of the thermal decomposition of hemicellulose[22] and are commonly found in bio-oil. A list of other furans can be found in Table 2.

Figure 10 Furfural Molecule[30]

Phenolic Compounds

There are many phenolic compounds that can be found in bio-oil. These can include phenols, syringols and guiacols. Phenols are aromatic rings that have a single hydroxyl group. A list of phenols typically found in bio-oil can be seen in Table 2. The chemical structures of many phenolic compounds can be found in Figure 11. Phenols can be relatively acidic and can have more than one hydroxyl group attached to the same

aromatic ring. Phenols also have a relatively high boiling point with the boiling point for phenol being 181.7°C. Phenolic compounds in bio-oil originate from the lignin that was originally in the biomass. Inspection of the lignin molecule in Figure 6 shows that there are many aromatic rings that are available to become phenolic compounds.

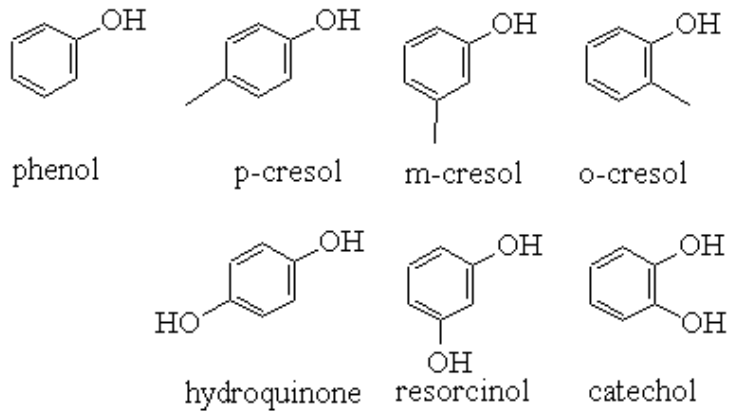

Figure 11 Phenolic Compounds[31]

Guaiacols are phenolic compounds that have a methoxy group that is located one carbon away from the hydroxyl group on the #2 carbon. Gusiacol is shown in Figure 12. Other guaiacols can be found in Table 2. Guaiacols typically have boiling points that are greater than 200°C. Guaiacols, like phenols, are a product of the breakdown of lignin.

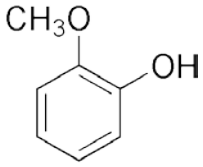

Figure 12 Guaiacol Molecule[32]

Syringols are very similar to phenols and guaiacols with a single main difference. Syringols have two methoxy groups that surround the hydroxyl group. The two methoxy groups are located on the 2nd and 6th carbons. Syringol has a boiling point of 261°C at atmospheric pressure. The chemical structure for syringols can be seen in Figure 13 and

a list of other syringols can be seen in Table 2. Syringols are products of lignin degradation. Both syringols and guaiacols can be seen in the lignin structure in Figure 6.

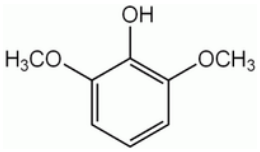

Figure 13 Syringol Molecule[33]

Water insoluble content is a term that has been coined for the large molecular weight products that are not soluble in water. Some researchers feel that these compounds are derivatives of lignin.[34] Typically, these compounds are very large molecules that are products of lignin thermal degradation. Attempts to identify these compounds through GC/MS have not been successful.

2.6 Bio-oil Challenges and Stability

Bio-oil presents many challenges based on its complex make-up. Combinations of certain compounds can cause adverse reactions. These undesired reactions can cause both an increase in water content as well as an increase in viscosity. Other challenges that are present due to the complex nature of bio-oil include low energy content and low pH.

Water content can have both positive and negative impacts on bio-oil. Water has the ability to lower the viscosity of bio-oil which is a major benefit when considering the challenges related to pumping bio-oil. Water, though, negatively affects the heating value and pH.[9] Water can also cause problems with homogeneity and separation of the bio-oil. Water also acts as a reagent in some reactions that can occur after the bio-oil has been collected.[35] Water contents have been reported to be as high as 15-30 wt% of the bio-oil.

The acid content of bio-oil is a challenge that has been prevalent in fast pyrolysis for many years. There are two different methods of determining the acid content of bio-oil. Many researchers have used pH[9] to determine the severity of acid content. It has been reported that whole bio-oil can have a pH as low as 2.5. Another method that is starting to be commonly used for determining acid content is the Total Acid Number (TAN).[5] The TAN is a titration that measures the amount of KOH that is required to neutralize the organic acids in a sample. This method has only been used recently, but gives a true value of the amount of acids that are present in bio-oil. The total acid number is a measure of all of the acids including strong, weak and very weak acids.

Most of the acids that are found in bio-oil are organic acids. These acids include acetic, formic and propanic acid[22] as well as other hydrocarbon molecules that have acidic qualities. Acetic acid is the most prevalent acid found in bio-oil. Carboxylic acids cause problems associated with corrosion of materials and stability of bio-oil. Aubin[36] studied the corrosiveness of bio-oil and found that stainless steel resisted corrosion of pyrolysis bio-oil from wood. It was also reported that increasing the temperature of the bio-oil to 45^{o}C significantly increased corrosion activity.[36] Stainless steel is widely used to prevent corrosion of metal in bio-oil collection systems. There are some olefin polymers that can stand up to the large concentration of organic acids that are present in bio-oil as well.[9] Acids can act as a catalyst for bio-oil reactions as well as reactants. Almost all of these reactions have a negative effect on the stability of bio-oil over long periods of time.

Bio-oil's low energy content can be attributed to two separate sources. First, bio-oil has a large amount of water. This water has an enthalpy of vaporization of 2.257 MJ/kg. This becomes lost energy when considering the energy content present in bio-oil. The oxygen content of bio-oil also has a negative effect on the energy content of bio-oil. Energy content is measured by combusting the bio-oil. Combustion takes place when oxygen reacts with carbon and hydrogen to create carbon dioxide and water. Oxygen, which is considered excess weight, lowers the heating value because it is counted into the mass of

the sample but does not contribute any energy to the combustion reactions that occur when the reaction is operated under fuel lean conditions.

The presence of solids in bio-oil has many negative effects. Solids are typically suspended char particles that were able to escape the solids removal process. Solid char can act as a catalyst for bio-oil reactions that can take place during storage. Solid particulate can also cause erosion, equipment blockages, slower rates of combustion and clogging of spray nozzles.[9]

There has been a recent emphasis on the stability of bio-oil and the reactions that occur in whole bio-oil as it ages. As whole bio-oil ages, it increases in viscosity and water content at the same time.[35] These changes act as a double-edged sword for bio-oil. The increase in viscosity makes it more difficult to pump the bio-oil; while the increase in water content lowers the heating value of the bio-oil and it also has the possibility of causing the bio-oil to separate into phases. Stability studies include analysis of initial bio-oil followed by accelerated aging at elevated temperatures.

There are many adverse reactions that can occur between the numerous compounds that are present in bio-oil. The list below, adapted from an NREL report written by J.P. Diebold[35], is a list of probable chemical mechanisms that contribute to bio-oil instability:

- Organic acids with alcohols to form esters and water
- Organic acids with olefins to form esters
- Aldehydes and water to form hydrates
- Aldehydes and alcohols to form hemiacetals, or acetals and water
- Aldehydes to form oligomers and resins
- Aldehydes and phenolics to form resins and water
- Aldehydes and proteins to form oligomers
- Organic sulfur to form oligomers

- Unsaturated compounds to form polyolefins
- Air oxidation to form more acids and reactive peroxides that catalyze the polymerization of unsaturated compounds

The list above denotes that many of the reactions that produce water as a byproduct of reactions that naturally occur in bio-oil. Esters, which have a low boiling point, are also produced by the reactions that are listed above. Esters will easily volatilize from the bio-oil, thus increasing the overall viscosity of the bio-oil. It should also be noted that resins, oligomers and polyolefins are produced by many of these reactions. These compounds are high molecular weight compounds that increase the overall viscosity of the bio-oil. These compounds are also typically not soluble in water which increases the chances of phase separation.

CHAPTER 3. METHODS AND PROCEDURES

3.1 Introduction

The system utilized to fractionate the bio-oil for this study is shown below in Figure 14 and a complete detailed description is given. Selected engineering drawings can be seen in Appendix B. The system consisted of multiple components:

- Reactor
- Particulate Removal
- Bio-oil Collection System
- Gas Analysis
- Data Acquisition and Automated Controls System

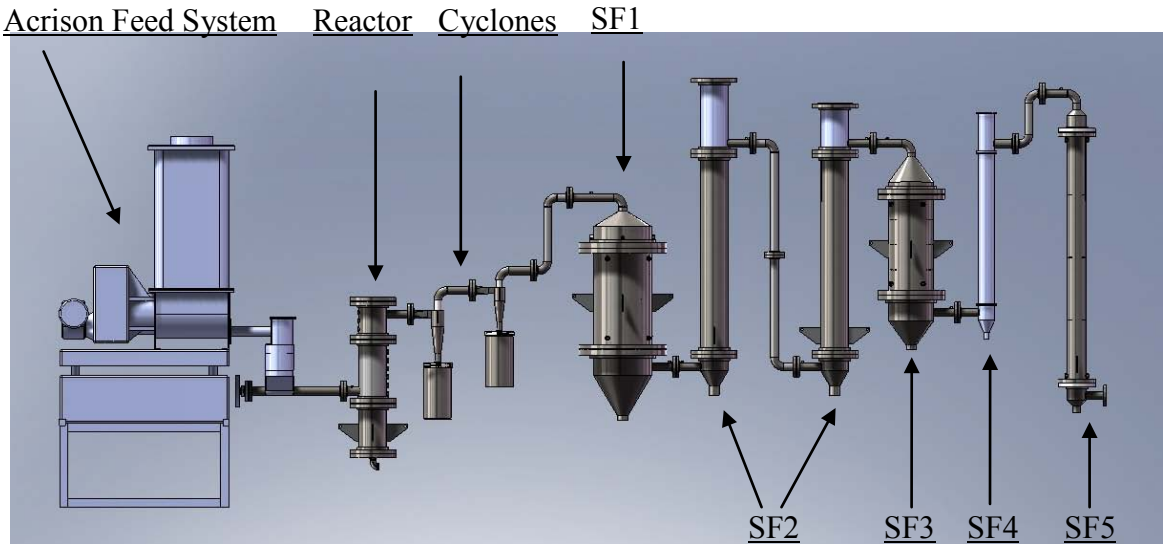

Figure 14 System Schematic

3.2 System Design

The fast pyrolysis system was designed with many goals in mind. The initial goal was to build a reliable system that could produce bio-oil from any biomass in significant quantities. Large amounts of bio-oil are needed to progress the end-uses of bio-oil.

Determining the end uses of bio-oil needs to be a top priority for fast pyrolysis to become a solution to energy and resource problems. This system was designed for an 8 kg/hr throughput of biomass into the reactor. The reactor is a fluidized bed that can provide high heat transfer rates from a nearly isothermal bed to the biomass. Particulate removal is accomplished with gas cyclones that were designed to remove 99% of the solid particulate from the product flow out of the reactor.

Bio-oil collection is being performed with a fractionating bio-oil collection system. This system has the ability to fractionate bio-oil vapors and aerosols based on dew point and phase. The fractionating bio-oil collection system collects the bio-oil in five distinct fractions. Each of these fractions has unique characteristics, both physical and chemical. This research project is acting as a proof of concept for the fractionating bio-oil collection system.

3.3 Experimental Apparatus

3.3.1 Reactor

The reactor that was utilized and designed for this project was a bubbling fluidized bed. This reactor utilizes silica sand and nitrogen as a bed medium and fluidization gas. The complete set of design calculations can be found in Appendix A.

The reactor is an assembly of stainless steel pipes and flanges. The reactor is split into three pieces, including the plenum, fluidized bed and freeboard. The bottom section is the plenum. Heated gases enter the bottom of the plenum through a distributor pipe. Calcium silicate insulation, that is 3″ thick, surrounds the outside of the plenum. The plenum is constructed of standard (schedule 40) 6″ stainless steel pipe welded to standard 150# flanges. This pipe has a nominal outer diameter of 6.625″ and a nominal inner diameter of 6.065″. The overall height of the plenum is 12″. The purpose of the plenum is to allow the fluidization gas to expand before passing through the distributor plate.

This section has a thermocouple and a pressure transducer to allow for temperature and differential pressure readings.

Located at the top of the plenum is a distributor plate that separates the plenum from the fluidized bed. The distributor plate is designed to provide proper pressure drop and gas distribution for fluidization. The distributor plate is 0.3175 cm (1/8 inches) thick and has 55 holes that each have a diameter of 0.15875 cm (1/16 inches). The holes are placed in an equilateral triangle orientation where all holes are equally spaced from each other. This is represented in Figure 15.

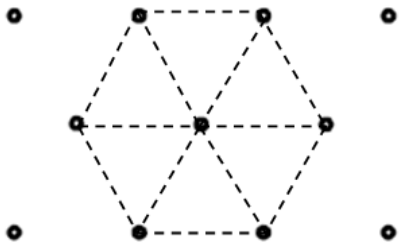

Figure 15 Distributor Plate Hole Distribution

The second section of the fluidized bed reactor is the actual fluidized bed. This section of the reactor houses the fluidized sand bed. The sand is silica sand with a mean particle size of 500 microns. This section is constructed from 15.24 cm (6 inch) schedule 40 stainless steel pipe. The fluidized bed section of the reactor is 38.42 cm (15.13 inches) tall. Standard pipe and flanges were used throughout the system for two different reasons. Standard pipe is readily available which allows for quick turnaround time for replacement parts. Standard flanges were used because there is already an industry for high temperature gaskets that will provide a gas tight seal with relative ease.

The fluidized bed is heated with electric clam shell heaters. Clam shell heaters provide radiant heat to the outside of the reactor. There are five thermocouples located within the fluidized bed which provide temperature measurement throughout the fluidized bed. There is also a thermocouple that is located between the reactor and the clam shell heaters. The purpose of this thermocouple is to prevent the heater from overheating. This array of thermocouples will allow for constant monitoring and precise control of the fluidized bed temperature.

The top section of the reactor is referred to as the "freeboard". The purpose of the freeboard is to provide the proper volume of gas to prevent the fluidizing media from elutriating from the reactor. The total disengagement height (TDH) is a correlation that determines the height above a fluidized bed that is required to prevent entrainment. The TDH is a balance between the forces that were applied on a particle within the fluidized bed and gravity once the particle has entered the freeboard. For the reactor conditions that were used, the TDH was calculated to be 8.35 cm (3.288 inches). The height of the freeboard is 15.24 cm (6 inch). Gases exit the freeboard through a 3.8 cm (1.5 inch) pipe that is located at the top of the freeboard. The freeboard is heated with another set of clam shell heaters and there are three thermocouples that allow for temperature measurement and control within the freeboard. There is also a differential pressure transducer that measures the pressure drop across the fluidized bed and distributor plate.

The required heat for the reactor is provided from two different heat sources. Initially, the fluidization gases are pre-heated to the process temperature with a pair of inline gas immersion heaters. The Watlow Starflow heaters are each powered with 208 volts to generate 2,600 watts of heat. Preheating the gas before it enters the fluidized bed will allow for better fluidization. Preheating also reduces the amount of heat that has to be transferred into the fluidized bed from other sources. The heaters utilize a rotating star configuration to cause turbulence and transfer heat to the gas from the heating coil.

The fluidized bed and the freeboard are both heated with "clam shell" ceramic fiber heaters. These electric heaters are semi-circular heaters that fit the outer diameter of the reactor. A 2.54 cm (1 inch) space was left between the reactor wall and the heater. The pair of clam shell heaters that provide heat to the fluidized bed are powered with 208 volt electricity. Each heater is rated to provide 1,972 watts of heat. The reactor heaters have two main purposes. The main purpose is to provide the heat required for the fast pyrolysis reactions. The secondary purpose of the reactor heaters is to act as active insulation. The active insulation is to prevent any heat loss. The pair of heaters that are located on the freeboard are 60 volt heaters that are placed in series. This configuration creates a 120 volt heater that can provide 2600 watts of heat. The overall heat load at the freeboard is minimal and the heater will act solely as active insulation.

3.3.2 Feed System

The need of a consistent biomass feed rate led to the design of a complex continuous feed system. This system is designed to provide continuous feeding of biomass throughout the duration of a test. For this study, though, the system was operated as a batch system that was refilled after each test.

There are three major challenges that have to be overcome when designing and implementing a continuous feed system. The first challenge that must be overcome is the consistent feeding of biomass into the reactor. Obstacles that must be overcome for consistent feeding include varying bulk densities and biomass bridging. The biomass bridging can be prevented by inserting an agitator in the hopper, directly above the auger, to keep the biomass moving down to the auger. The feeder that is being used is a weigh and loss feeder that was purchased from Acrison. This feeder utilizes a scale and ballast system that can accurately determine the change in biomass weight within the hopper. The system operator has the ability to input a desired feed rate and the control system will actively adjust the auger speed to provide that feed rate.

The second challenge that is addressed with this feed system is continuous, rather than batch, operation of the system. The biggest challenges to continuous feeding are associated with refilling the hopper. The hopper on the Acrison feeder has a capacity of 8 cubic feet, thus it must be refilled if the test runs longer than a few hours. To accomplish the refilling of the feeder, a surge hopper system was installed. This system consists of two slide-gate valves, a surge hopper with two agitators, a bucket elevator and a refill hopper. Biomass is loaded into the refill hopper. This hopper is a large hopper, on wheels, that utilizes three augers in the bottom that can feed the bucket elevator. The bucket elevator then lifts the biomass into the surge hopper, which has a 15.24 cm (6 inch) slide gate valve on the top. The surge hopper resides directly above the Acrison feeder, separated by a 25.4 cm (10 inch) slide gate valve. When the feeder signals for more biomass, the surge hopper closes the upper 15.24 cm (6 inch) valve and becomes pressurized with nitrogen. The surge hopper will be pressurized so that it is at the same pressure as the feeder to prevent back flow. The lower 25.4 cm (10 inch) valve then opens and the agitators in the surge hopper empty the surge hopper into the Acrison feeder. Once the surge hopper is emptied, the agitators stop and the lower valve closes. The surge hopper is then allowed to release its pressure and is once again refilled by the refilling hopper and bucket elevator. This extensive process allows the system to continue to operate while more biomass is added to the feeder.

Finally, the ability to seal the feed system to prevent back flow is essential to successful operation of a fast pyrolysis system. This was done by using two different approaches. First, there was a nitrogen purge that passed nitrogen straight into the feeder. This purge was high enough in flow that it always generated positive gas flow into the reactor. Secondly, rubber coated nylon sleeves were used to the inlet and outlet of the feeder. These sleeves kept the feeder isolated from any vibrations or outside forces. They also kept the hopper sealed.

3.3.3 Cyclones

The design of the two gas cyclones was based off of standard gas cyclone design methodology. According to Hoffman and Stein[37], the design methodology requires 4 design parameters: gas flow rate, particulate density, desired efficiency and desired pressure drop. The gas flow rate for the cyclones was determined by estimating the amount of gas (volumetrically) that would be produced during the fast pyrolysis reaction. The bio-oil vapors were assumed to be ideal gas with a molecular weight of 98.9 gram per mole. The non-condensable gases were also modeled as an ideal gas but with a molecular weight of 29.4 gram per mole. The calculations for the flow can be seen in Appendix A. The design flow rate for the cyclones was determined to be 500 liter per minute when the bio-oil vapors, the non-condensable gases and the nitrogen were added together. The char was then assumed to have a density of 240 kg/m^3. This value was determined both through experimentation with char produced on a separate fast pyrolysis reactor and from the literature.[38]

The actual design of the cyclone is traditionally based on the diameter of the cyclone. The other dimensions are then determined by using pre-determined ratios. There are two different ratios that were used and the use of either was determined by the Stokes number. For a high flow cyclone, a Stokes number of 0.006 is used; a high efficiency cyclone will have a Stokes number of 0.000117. The overall efficiency is then determined by the allowable pressure drop. The higher the pressure drop, the lower the 50% cut diameter of the cyclone. The efficiency of a gas cyclone can be described by comparing the 50% cut diameter of the cyclone particle size distribution of the particulate. The 50% cut diameter is the diameter of particle in which exactly 50% of the particles of that size are collected. Figure 16 illustrates the efficiency for the high efficiency cyclone with a 50% cut diameter of 1.6 microns. Larger particles will experience a more thorough removal while smaller particles will have a high probability of passing through the cyclone. The calculated 50% cut diameter of the two cyclones that were designed and built for this project were 11 microns and 1.6 microns.

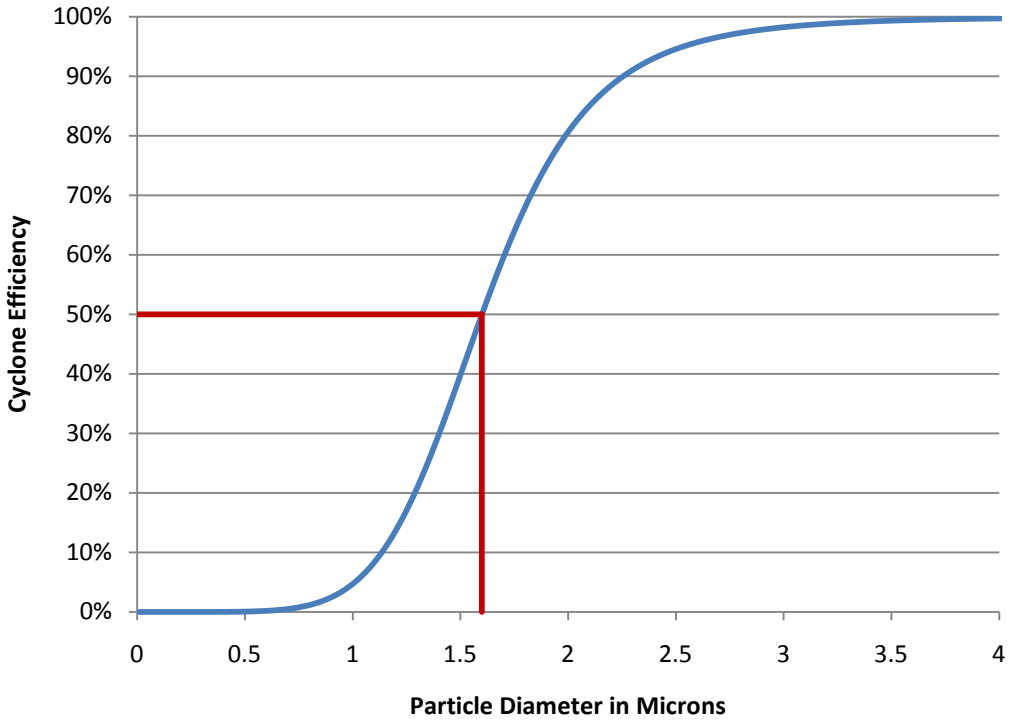

Figure 16 Cyclone Efficiency for 1.6 Micron 50% Cut Diameter

3.3.4 Bio-oil Collection System

The product stream entering the bio-oil collection system consists of the products of the reactions that have occurred in the fluidized bed fast pyrolysis reactor. The product stream has passed through the gas cyclones to remove up to 99% of the solid particulate (char) that was present in the bulk flow. The product stream entering the bio-oil recovery system includes three main components classified by their physical state: non-condensable gases, vapors and aerosols. Also entering with the product stream are the fluidization gases from the reactor. The non-condensable gases include hydrogen, carbon monoxide, carbon dioxide and light hydrocarbons created during pyrolysis. The non-condensable gases represent 10-20 wt-% of pyrolysis products.[9]

Vapors include water and organic compounds that can be condensed upon cooling the gas stream exiting the pyrolyzer. The organic compounds tend to be of "medium" molecular

weight and include carboxylic acids, alcohols, esters and phenolic compounds. Aerosols are micron and submicron liquid droplets[39] of organic compounds that either have too high of boiling point to evaporate in the pyrolyzer (typically operated around 500°C) or have condensed from vapor after leaving the reactor because the gas stream has cooled. Aerosols tend to consist of carbohydrates, highly substituted phenolic compounds and lignin oligomers.

The relative amounts of vapor and aerosol are difficult to ascertain, partly because each can transform into the other depending upon the temperature and nucleation environment. It has been reported that up to 90% of the flow exiting a fluidized pyrolyzer is in the form of aerosols, although this depends upon feedstock and reaction conditions.[40] The bio-oil collection system exploits the different behavior of vapors and aerosols exiting the fast pyrolysis reactor in order to collect "stage fractions" that are partitioned according to saturation temperature.

Operation of the bio-oil collection system is based on setting the temperature in each stage fraction to correspond to the saturation temperature of specific compounds that are thought to exist as vapors in the product stream from the pyrolyzer. Compounds will condense from the product gas stream whenever the surface temperature drops below the saturation temperature of the compound in the product gas stream. Saturation temperature, T_{sat}, is calculated from the vapor pressure, P_v, of the compound in the product gas stream using the Clausius-Clapeyron equation:

$$\ln\left(\frac{P_v}{P_o}\right) = \frac{\Delta H_{vap}}{R}\left(\frac{1}{T_o} - \frac{1}{T_{sat}}\right) \qquad \textbf{Equation 3}$$

where P_o is the saturation pressure corresponding to a standard temperature, T_o, and ΔH_{vap} is the enthalpy of vaporization of the compound. The vapor pressure is estimated

from the mass fraction of the compound in the bio-oil, m_f, and the mass concentration of bio-oil, C_{oil}, in the product gas stream using the ideal gas law:

$$P_v = \frac{m_f C_{oil} R_u T_o}{MW} \qquad \textbf{Equation 4}$$

where R_u is the Universal gas constant, T_o is the standard temperature at which the volumetric flow rate of the product gas is determined, and MW is the molecular weight of the compound. Table 3 denotes some of the constants used in the design of the system.

Table 3 Boiling Point and Enthalpy of Vaporization for Selected Compounds[41]

	T_b(K)	H_{vap} (kJ/mol)
Water	373.15	40.657
Phenol	454.95	45.69
Acetic Acid	391.15	23.7
Methanol	338.15	35.21
Acetaldehyde	293.25	25.76
Formic Acid	374	22.69

Figure 17plots saturation pressure vs. temperature, as determined by Equation 3, for several important bio-oil components. Theoretical vapor pressures (horizontal lines in Figure 17) were determined using Equation 4. The intersection of the saturation pressure curves and vapor pressure lines indicates the temperatures at which the various compounds will condense. For the case shown in Figure 17, levoglucosan is expected to condense at 200^{o}C, phenol will condense at 80^{o}C and water will condense at 50^{o}C.

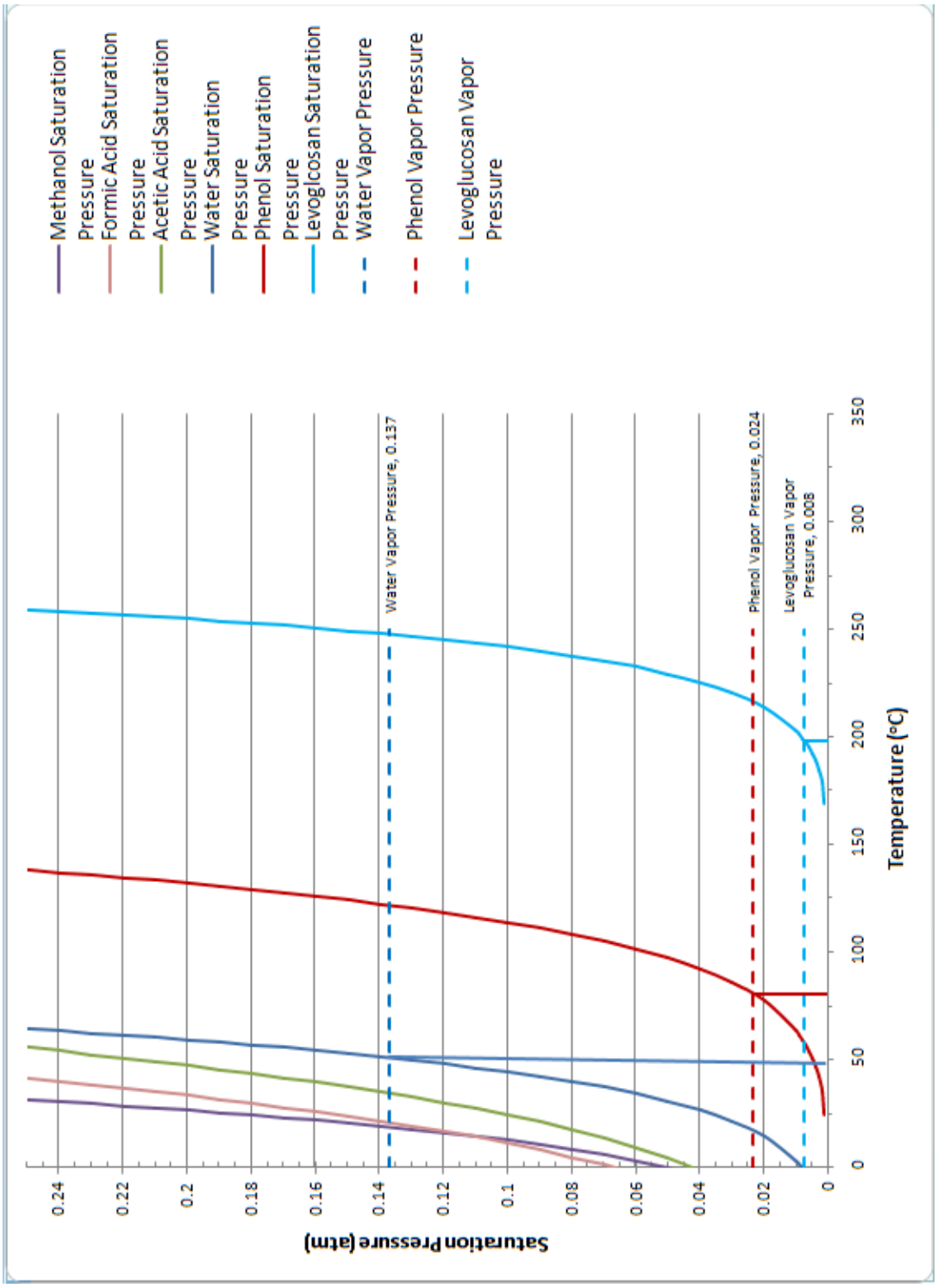

Figure 17 Saturation pressure vs. Temperature for Vapors Entering the First Condenser Stage

The design of each condenser fraction is based on a constant surface temperature shell and tube heat exchanger. Standard design procedure was used to model the heat flow through the heat exchangers. Assumptions made for the design include inlet temperature, outlet temperature, wall temperature, flow composition and mass flow rate. The heat transfer analysis proceeded as follows (All equation were taken from Incropera[3]):

1. The total heat flow (Equation 5) was calculated from both assumed and theoretical values. This value included both the sensible heat associated with the total flow and the latent heat of vaporization of the liquid that was being condensed. It was assumed that only 95% of the desired compound was condensed.

$$q = m_{N2} \cdot C_{pN2} \cdot (T_{in} - T_{out}) + 0.95 \cdot m_L \cdot H_{vapL} \qquad \textbf{Equation 5}$$

2. The configuration of the heat exchanger was assumed. This value was eventually compared to the final solution. The configuration parameters included diameter of tubes, number of tubes and length of tubes.
3. The Reynolds Number was then calculated. If the Reynolds Number did not indicate the desired flow regime, the heat exchanger configuration parameters were adjusted. The first two heat exchangers were designed as laminar flow systems, while the last heat exchanger was designed as a turbulent flow system. The Reynolds Number equation for flow through a pipe is shown in Equation 6.

$$Re_D = \frac{4 \cdot m_{N2}}{\pi \cdot D \cdot \mu_{N2} \cdot N} \qquad \textbf{Equation 6}$$

4. The Nusselt Number (Equation 7) is the ratio of convection to pure conduction heat transfer. When rearranged, the Nusselt Number can be written as a function of the Reynolds Number, tube length, tube diameter and Prandtl Number. There are special correlations that have been derived from experimental data that are applicable for laminar and turbulent flow in a pipe. These two correlations can be

seen in Equation 8 and Equation 9. A friction factor is used for turbulent flow because the higher velocities will be affected more by the friction forces along the walls of the pipe. This friction force has the ability to create eddy currents and enhance mixing – thus enhancing the heat transfer of the fluid.

$$Nu = \frac{h \cdot L}{k_f}$$ **Equation 7**

$$Nu_{Laminar} = 1.86\left(\frac{Re \cdot Pr}{\frac{L}{D}}\right)^{1/3}$$ **Equation 8**

$$Nu_{Turbulent} = \frac{\left(\frac{f}{8}\right)(Re - 1000)Pr}{1 + 12.7\left(\frac{f}{8}\right)^{1/2}\left(Pr^{2/3} - 1\right)}$$ **Equation 9**

f= friction factor

5. The convection coefficient (h) can be found by rearranging Equation 7. Heat flow is then equal to the convection coefficient multiplied by the area and the log-mean temperature difference. This equation was then used to determine length of tubes required for the number and size of tubes that were assumed. If the length was not similar to the assumed length, then the heat exchanger configuration parameters were iterated to design an appropriate heat exchanger.

$$A_s = \frac{q}{h \cdot \Delta T_{log-mean}}$$ **Equation 10**

Heat transfer was only half of the design for the heat exchangers. The mass transfer from the bulk flow to the heat exchanger walls was equally important to the design of the condensers. The mass transfer design was completed with the Reynolds Analogy (as seen in Equation 11) which is a relationship between mass transfer and heat transfer. The Reynolds Analogy is a function of the Nusselt, Prandlt, Sherwood and Schmidt Numbers.

$$\frac{Nu}{Pr^n} = \frac{Sh}{Sc^n}$$ **Equation 11**

Through the Reynolds Analogy, relationships for the Nusselt Number can be transformed into relationships for the Sherwood Number. The Sherwood Number (Equation 12) is a dimensionless concentration gradient at the surface in which mass transfer is occurring.[3] This transformation is completed by replacing the Nusselt Number (Nu) with the Sherwood Number (Sh). Similarly, the Prandlt Number (Pr) is replaced with the Schmidt Number (Sc). To complete the transformation, the conductive heat transfer coefficient (k) is replaced with mass diffusivity (D).

$$Sh = \frac{h \cdot L}{D}$$ **Equation 12**

$$Sh_{Laminar} = 1.86\left(\frac{Re \cdot Sc}{\frac{L}{D}}\right)^{1/3}$$ **Equation 13**

$$Sh_{Turbulent} = \frac{\left(\frac{f}{8}\right)(Re - 1000)Sc}{1 + 12.7\left(\frac{f}{8}\right)^{1/2}\left(Sc^{2/3} - 1\right)}$$ **Equation 14**

f= friction factor

To transfer vapors through the boundary layer, from the bulk flow to the condenser walls, a driving force is needed. For this analysis, partial pressure was used as the driving force. Differences in concentration are also commonly used as a driving force for mass transfer calculations. Concentration and partial pressure can be related through the ideal gas law. The partial pressures were calculated as noted earlier in this section with Equation 4. Like temperature, a log-mean partial pressure difference is required to determine the surface area required for mass transfer. The mass transfer (Equation 15) is calculated by multiplying the mass transfer coefficient, surface area and log-mean pressure difference.

$$m = h_m \cdot A_s \cdot \Delta P_{log-mean} \qquad \textbf{Equation 15}$$

At the inlet of the Stage 1, the product stream temperature ranges from 350-500^{o}C and the pressure at the inlet between 1.2 - 5 kPa (5 and 20 inches of water column). The goal of the first condenser is to collect levoglucosan, the most prevalent anhydrosugar in bio-oil, and other high boiling point compounds that exist as vapors in the product stream exiting the pyrolyzer. Levoglucosan and the other high boiling point compounds are challenging to collect using a traditional condenser as they are solid at temperatures below approximately 75^{o}C. Thus, to prevent build up on the condenser walls, the condenser walls must be operated at temperatures higher than 75°C. If the condenser wall temperature exceeds temperatures greater than approximately 100°C, the condensed liquid may begin to thermally decompose to char and non-condensable gases. Hence, the condenser must have a wall temperature between 75 and 90°C. This temperature is just above the saturation temperature of phenol at its calculated partial pressure, shown in Figure 17. The condenser is designed to operate with a coolant maintained at 75-90°C and the ability to cool the inlet stream temperature from 350-500°C to 170-125°C. To significantly decrease the chances that the aerosol droplets would impact the walls and collect in the first condenser, laminar flow conditions were chosen.

For the 8 kg/hr process development unit, a shell and tube heat exchanger was utilized to collect the bio-oil in stage 1. The tubes were 2.54 cm (1 inch) diameter thin-walled stainless steel tubes while the shell was constructed from 35.56 cm (14 inch) schedule 40 stainless steel pipe. According to both design calculations that can be found in Appendix A and testing, 30 tubes were required to cool the product stream from the 450^{o}C inlet temperature to the desired outlet temperature of 150^{o}C. The product stream entered through a cone that distributed the vapors evenly to all tubes. The gases flowed in a downward direction, pushing the liquid down the tubes to the collection bottle. This downward flow aided the collection of the bio-oil. The downward gas flow also helped to keep the tubes clear by encouraging the bio-oil to flow towards the bottom of the condenser. There was a second cone at the bottom that funnels the bio-oil into the collection bottle. This cone had a pipe that exited from the side that allowed the gas to proceed to the ESP.

The stream exited the first stage, at a temperature between 150-125^{o}C, and entered the second stage, which was a pair of electrostatic precipitators (ESP). The purpose of the second stage was to collect all of the aerosols present in the product stream without additional vapor condensation. To accomplish this, the second stage was heat traced to prevent the vapor stream from cooling. These aerosols contain phenolics, anhydrosugars and pyrolytic lignin formed during the pyrolysis process.

An ESP consists of two main components. The pipe that the gas and vapors flow through will act as a ground and collection site for the aerosols. A cylindrical rod that is suspended in the center of the pipe will act as the high voltage (20-40 kV DC) electrode. The high voltage applied to the electrode causes an electrostatic field to be formed between the electrode and the grounding pipe. This field causes a force on any particle (aerosols or particulate) that passes through it. As the particle passes through the field, it moves towards the ground wall and thus collects on the wall. The liquids will flow down to the bottom of the ESP to be collected in a bottle. The walls of the ESP were kept at a

temperature between 150 and 125^{o}C to prevent the gases that are passing through the ESP from cooling before they leave. The ESP should only collect the aerosols in the flow.

For the 8 kg/hr process development unit, both ESPs were the same size and placed in series. The main pipe was a 15.24 cm (6 inch) schedule 40 stainless steel pipe. The cylindrical rod, in the center of the ESP, had a diameter of 2.54 cm (1 inch). The product stream flowed upward from the bottom of the ESP to the top. The bio-oil that was collected on the walls flowed downward to a cone at the bottom that funneled the bio-oil into the collection bottle.

The third stage has the same inlet temperature as both the inlet and outlet of the ESP (between 150 and 125^{o}C). The desired products that are obtained from the third stage are the remaining phenolic compounds and any other compounds that have a saturation temperature that is greater than the saturation temperature of water at the partial pressures present in the second condenser. The third stage was designed much like the first stage with the wall temperature of the tubes being determined by the saturation temperature of the undesired component of the bio-oil – in this case, water. The saturation temperature of water was approximately 55^{o}C at the given conditions. The wall temperature of the second condenser was held between 60 and 70^{o}C and the flow rate of the water passing through the shell is sufficient to keep a constant temperature on the inner tubes. The condenser was configured for laminar flow but was also capable of operating in a turbulent flow regime as well. The desired outlet temperature of the second condenser was between 75 and 100^{o}C. This outlet temperature should prevent any water from condensing in third stage.

The third stage of the 8 kg/hr process development unit was designed as a shell and tube heat exchanger in the same manner as the first stage. This stage operated with 24- 1.9 cm (¾ inch) tubes, but had the ability of adding or taking tubes away to adjust for different biomasses. The shell for the third stage was constructed from 25.4 cm (10 inch) schedule 40 stainless steel pipe.

The fourth stage was another ESP that acted as a final aerosol collection point within the bio-oil collection system. These aerosols could be aerosols that were not collected in second stage or they could have also been created while the fast pyrolysis vapors were cooled in the third stage. Stage four consisted of a shell, electrode and power supply. This stage was purely insulated with no heat tracing to prevent condensation. The gases and vapors exited stage four at temperatures between 75 to 100^{o}C. The design procedure for the second ESP was the same as the first ESP. The outer pipe is a 10.16 cm (4 inch) pipe. The inner cylindrical rod has a diameter of .635 cm (1/4 inches).

Stage five acted as a final stage removal of the remaining compounds. The fifth stage should collect the water, alcohols, acids and any other compounds that are still in the vapor form when the stream enters the third condenser. This condenser had an inlet temperature that ranged from 75 to 100^{o}C and an outlet temperature that will ranged between and 0 to 20^{o}C depending on coolant temperature. Stage five was designed to be a turbulent flow condenser rather than laminar. This was due to the lack of aerosols. The turbulent flow provides for better heat and mass transfer. The goal of the final condenser was to collect all of the remaining pyrolysis vapors.

The fifth stage of the bio-oil collection system was designed in the same manner as the first and third stages as a shell and tube heat exchanger. The fifth stage contained 8 tubes with an inner diameter of 0.9398 cm (0.37 inches). The shell is constructed of 10.16 cm (4 inch) schedule 40 stainless steel pipe. The shell can be filled with either cool water, chilled water or a chilled mixture of water and glycol (to reach wall temperature of less than 0^{o}C). The fifth stage flowed in a downward direction that aided in the collection of the liquids at the bottom of the condenser.

3.3.5 Gas Analysis

To determine the composition and amount of gases being produced, a Varian Micro-GC was used. A Micro-GC makes it possible to see relative amounts of gas on a semi-continuous basis. Two columns were used to detect the non-condensable gases. A MolSieve 5A (MS5A) detected the hydrogen, helium, oxygen, nitrogen, methane and carbon monoxide. A PoraPLOT Q (PPQ) was utilized to detect carbon dioxide, ethane and ethylene. The operating conditions of the two columns can be seen in Table 4.

Table 4 Micro-GC Operating Conditions

Column	MS5A	PPQ
Length of Column (m)	10	10
Pressure (kPa)	151.7	117.2
Oven Temperature (^{o}C)	100	58
Injector Temperature (^{o}C)	110	110
Injection Time (ms)	40	40
Run Time (s)	130	130
Length of sample (s)	30	30
Carrier Gas	Argon	Helium

To determine the actual flow rate of the non-condensible gases, a helium tracer was utilized. 1.5 standard liters per minute of helium was introduced into the reactor along with the fluidizing gases. Helium can be accurately detected with the MS5A. The MS5A can be calibrated to see accurate concentrations of helium as long as the carrier gas for the column is not helium. A typical percentage of helium that was measured was approximately 0.6%. By recording the input flow rate of helium, the output concentrations of the product gases can be calculated. This makes it possible for an accurate mass balance to be kept.

3.3.6 Data Acquisition and Control

The controls and automation system consisted of five main components. These components included the HMI (human-machine interface) server, historian server, work station, I/O racks and instrumentation. The controls and automation system was provided by Rockwell Automation and Van Meter Industrial. The system, which is still in place, was a PlantPAx Process Automation System. The two servers, the work station and the I/O racks are all connected on an Ethernet network. This system has the capabilities to monitor and control an entire array of digital and analog devices. Screenshots from the controls system can be seen in Appendix D.

Two servers, which include the HMI and historian servers, are required to operate the system on a continuous basis. The HMI server contained all of the control programming as well as the HMI control screens. The work station computer loaded the HMI interfaces from the HMI server. The historian server logged all of the data from the instrumentation while the I/O racks were powered. The historian logged new data points whenever it detects a change in the state of the instrumentation. If the process were to remain at a constant temperature for five minutes, only one data point would be logged.

The control of the fast pyrolysis system could be accomplished from a single work station computer. The I/O racks were located in three different enclosures. The main panel contained digital input and digital output cards as well as the controller. The controller housed the control program and controlled the other I/O racks. The other two sets of I/O racks were stored in remote enclosures. The remote enclosures were placed near the reactor and the last condenser. These remote panels contained two I/O racks each and received signals from almost all of the instrumentation that was utilized on the fast pyrolysis system.

The fast pyrolysis system utilized many types of instrumentation, motors and valves. For temperature measurement, Omega brand Type K thermocouples were used. Type K thermocouples are chromel-alumel which outputs 41 micro-volts/ ^{o}C.[42] The range of

Type K thermocouples is between -200 to +1350^{o}C. For pressure measurement, Dwyer Series 677 differential pressure transducers were utilized. The full system pressure was measured on a 0-100" of water column (0 – 24.88 kPa) transducer that had a 0.4% full scale accuracy. The other pressure transducers were 0-25" of water column (0 – 6.22 kPa) transducers with a 0.4% full scale accuracy. Liquid flow measurement of the hot water was accomplished with an Omega turbine flow meter (Omega part # FPR205-PC). This meter has a range of 5-50 gallon per minute (18.82 - 189.27 liter per minute) with 2% full scale accuracy.

3.4 Test Methods

3.4.1 Test Procedure

The test procedure to produce bio-oil from the fast pyrolysis system is a simple process that begins with the selection of operating conditions. Operating conditions that include the reactor temperature, heat tracing temperatures, biomass feed rate, condenser temperature set points and fluidization gas flow rate. For the study of fast pyrolysis products from different feed stocks, similar conditions were utilized for each experiment. The reactor was held at 500^{o}C and was fluidized with 183 standard liters per minute of nitrogen and 1.5 standard liters per minute of helium. The heat tracing lines were held at high enough temperatures to prevent any condensation of bio-oil before it was desired. The condenser walls were held at 85^{o}C for the first fraction. The walls of the first ESP were held at a high enough temperature to keep vapors and gases at 125^{o}C for the second fraction. The walls of the third fraction were held at 65^{o}C and the walls for the final fraction were held at 18^{o}C. This temperature corresponds to the temperature of the potable water that was available at the facility. The reactor was fed with the desired biomass at 4-6 kg/hr on a volumetric basis.

The desired volumetric flow rate was determined through a feeder calibration procedure that is meant to generate a mass flow versus auger speed. The feeder is set at a speed (25% to begin) and biomass is collected for 30 seconds three consecutive times. The feed

rate at that speed is calculated and this process is repeated for 50%, 75% and 100%. A linear fit is generated and the speed for the desired feed rate is calculated.

To start the actual fast pyrolysis system, the condenser coolant system is initiated first. This system has to be started ahead of time to allow the coolant to reach the desired operating temperatures. The water pumps are each set to 13 gallons per minute (49.21 liters per minute) and the hot water heaters are started. The control loops for the hot water heaters are set to heat the separate loops to their desired temperatures. Meanwhile, the heat tracing heat tapes are activated at this time as well.

Prior to fluidization, the mass of the feeder is recorded and the injection auger cooling water is turned on. Once the water control loops have both reached 60^{o}C, the startup sequence can proceed. First, the compressed air is started at 183 standard liters per minute and the injection auger is started. Once the fluidization gas is flowing through the reactor, the pre-heaters and clam shell heaters can be turned on.

Air is used to fluidize the bed at the beginning of the start-up to both conserve nitrogen and also to burn out any contaminates that could be located either in the fludized bed or in the piping between the reactor and the first condenser. The temperatures throughout the system are monitored and the fluidized bed is heated to 550^{o}C. When the system is at its proper temperature, the fluidization gas is switched from air to nitrogen and helium.

While the system is heating, the Micro-GC is prepared. The GC has to be taken out of bake-out and a calibration gas is used to verify that the Micro-GC is operating properly. While the verification is taking place, a cold trap is prepared with both glass wool and a desiccant filter. The desiccant filter and cold trap are used to prevent any moisture from reaching the Micro-GC. Once the verification has taken place, a leak check is performed on the entire system. This is done to make sure the vacuum pump is not drawing any air into the system.

With the gas analysis equipment and the fast pyrolysis system both ready, the biomass can be fed into the reactor at the desired feed rate. This will cause the reactor temperature to lower into the desired reactor temperature. Once the biomass feeder is started, the ESP power supplies must be started to ensure that the aerosol droplets are collected. A timer is started as well to keep track of the biomass that is fed into the system. The Micro-GC is then used throughout the test to monitor the gas production. Nalgene bottles are used to collect the bio-oil from each fraction.

For this study, a small sample of steady state bio-oil was used to perform the mass balance and bio-oil analysis. To perform the mass balance, the system was run for 45 minutes to allow the bio-oil collection system to reach a steady state. The bottles will then be switched and allowed to collect bio-oil for the duration of the test. At the same time that the bio-oil collection bottles were switched, the char catches were emptied as well. The char and bio-oil production were monitored to ensure that the containers do not overflow. After the test was completed 150 milliliters of bio-oil was placed into three separate containers to be used for bio-oil analysis.

When the test has been completed, the biomass feeding is stopped and the bed is allowed to clear itself of any biomass. The fluidized bed is allowed to stabilize and the clam shell heaters are stopped to allow the bed cool. Nitrogen is used as a fluidization gas until the fluidized bed is below 300^{o}C. This is done to prevent combustion inside the fluidized bed. Once the bed has cooled, the fluidization gas is transitioned from nitrogen to compressed air. The system is then cooled to room temperature while the bio-oil is allowed to continue to collect in the Nalgene bottles.

3.4.2 Set of Experiments

A set of 9 experiments were conducted with the fast pyrolysis system for this thesis. All of the tests were conducted with the same set-points. Three tests were run with each of the following biomasses: red oak, cornstover and switch grass. The three biomasses were chosen so that a comparison of biomass types could occur.

Each of the three biomasses that were selected is unique in their chemical and elemental analysis. Typical chemical analysis of each biomass is shown in Table 5 while a full elemental breakdown of these three biomasses is shown in Table 6. Each biomass contains similar amounts of lignin but significantly different amounts of cellulose and hemicellulose. It is believed that the lignin is responsible for the production pyrolytic lignin and other high molecular weight compounds. The pyrolysis of cellulose can produce many products that include levoglucosan and organic acids[38] as well as other low molecular weight compounds. Hard woods typically contain large concentrations of cellulose and low ash contents. The switchgrass and cornstover both contain lower concentrations of cellulose and higher amounts of ash and moisture.

Table 5 Typical Biomass Constituents

Wt% of Biomass	Hard wood (i.e. Red Oak)[43]	Cornstover[44]	Switchgrass[44]
Cellulose	45	35	33
Hemicellulose	30	23	26
Lignin	20	19	18

Table 6 Biomass Ultimate Analysis

Wt% of constituents	Red Oak	Clean Cornstover	Switchgrass
Ash	0.3	2.5	5.6
Percent Moisture	4.8	12.1	11.1
C	46.4	41.4	42.6
H	6.4	5.8	6.1
N	0.1	0.4	0.2
O	46.8	49.9	45.5

3.4.3 Bio-oil Analysis

The analysis of bio-oil is a process in which multiple tests are performed to determine the major components and qualities of the bio-oil. The testing methods are standard methods that are typically used in other industries (i.e. petroleum), but there are new methods that are being developed solely for the analysis of bio-oil.

GC/MS

To determine the major organic constituents that are contained in each bio-oil fraction, two separate instruments are used. These two devices are the Gas Chromatography/Mass Spectrometer (GC/MS) and the Gas Chromatography/Flame Ionization Detector (GC/FID). The GC/MS is used to determine specific compounds that are volatilized in an inert atmosphere. The GC/MS utilizes an ion trap that traps ions in a small volume. As the electrodes that are trapping the ions change voltages, different ions are ejected from the trap. The mass spectrometer then uses differences in mass to charge ratio of the ionized atoms to separate and determine the specific compounds that are present in the bio-oil. To prepare a sample for the GC/MS, bio-oil is mixed with methanol in a ratio of 4:96 bio-oil to methanol. The instrument, with an auto-sampler, then samples the mixture and performs the separation of ions. The amount of time between the injection and the detection of a specific compound is referred to as the retention time. The GC/MS then outputs results as shown in Figure 18.

.

Key:

1. Acetic Acid	4. Phenol 2, methoxy-4,methyl (Guaiacol)
2. Furfural	5. Phenol 2,6 Dimethoxy (Syringol)
3. Phenol	6. Levoglucosan

Figure 18 GC/MC Chromatograph for 1-20090731

The above chemical analysis was performed with a Varian Saturn 2200 GC/MS. The column used was a Varian capillary column CP8722 which was 60 meters in length, a 0.25 mm inner diameter, with a 0.25 mm film thickness. The carrier gas was helium (99.9995%) with a constant flow rate of 1.0 mL/minute. The oven temperature was programmed at 45ºC for 4 minutes to 235ºC at a heating rate of 3ºC/minute (63.3 minutes) and held at 235ºC for 13 minutes. The injector temperature was held at 250ºC and the GC/MS interface was kept at a constant temperature of 235ºC. Sample preparation was 4.5% pyrolysis liquid in 95.5% methanol for all samples except the fractions high in acetic acid. These fractions were 2.0% pyrolysis oil and 98% methanol. After sample preparation the samples were filtered with 0.45µm Corning micro filters. A sample volume of 1µL was injected utilizing a Varian CP 8400 auto sampler. There was a split ratio of 45. The MS was operated in the electron ionization mode scanning an *m/z* range from 30 to 300. The standard mass spectra with 70-eV ionization energy were recorded. Identification of the peaks was based on calibration standards purchased from Fisher Scientific. Calibrations were performed by injecting 4 standard solutions of each standard.

GC/FID

The GC/FID is another method and instrument that is used to determine the components that are present in a mixture. In this study, a Varian 430-GC with FID was used to analyze the water soluble fraction of the bio-oil. The GC/FID is used to analyze the water soluble portion of each fraction as well as the entire last fraction of the bio-oil. The GC/FID vaporizes the sample, which then passes through a capillary column. Hydrogen and standard breathing air are used to create a flame. The flame is used to produce ions as the organic compounds are heated to high temperatures. The detector on the instrument then responds to the number of ions that are released. This response can be used to determine the compounds that are present in the mixture. Column and system operating conditions can be seen in Table 7.

Table 7 GC/FID Operating Conditions

Column	Restek Stabilwax - DA (water tolerant)
Injection Volume	0.5 µL
Split mode	50:1
Injector Temperature	200°C
Oven Temperature Ramp	40-175°C
Ramping Rate	15°C /min
Detector Temperature	240°C
Column Flow	7.7 mL/min
Helium	25 mL/min
Hydrogen	30 mL/min
Air	200 mL/min

Moisture Content

To determine the amount of water in each of the bio-oil fractions, a Karl Fischer Moisture Titrator MKS-500 is utilized. This instrument follows ASTME E203 Standard Test Method for Water Using Karl Fischer Reagent.

To complete the analysis, the following procedure is used: The bio-oil sample is injected into the titration vial where it is dissolved by the solvent. In this case, the solvent is Hydranal Working Medium K which contains chloroethanol and chloroform. The mixture is then titrated with iodine (reagent) until the mixture is devoid of all water. The iodine and water react on a mole to mole basis, thus the percentage of water in the sample can be calculated from the initial sample weight. This specific instrument utilizes Hydranal Composite 5K as the reagent. A micro-processor in the instrument monitors the current change during the reaction for multiple reasons. The current can be an indicator for the end point of the reaction, and the amount of iodine produced and used in the reaction. The initial and final weight of the sample syringe is recorded and entered into the instrument. When the analysis is complete, the instrument outputs percent moisture.

Heating Value

A bomb calorimeter is used to determine the heating value of the bio-oil. The method for this test is ASTM D240 (Test Method for Heat of Combustion of Liquid Hydrocarbon Fuels by Bomb Calorimeter), suggested by ASTM Standard Specification for Pyrolysis Liquid Biofuel. The method of determining the heating value of a sample is to first combust the sample while monitoring the amount of heat that is released from the sample. A small sample of bio-oil is placed in a cup, which is then positioned inside of the calorimeter. For low heating value samples, mineral oil is mixed with the sample to encourage combustion. The sample is then ignited under fuel lean conditions and the temperature rise of the water surrounding the device is continuously monitored. An energy balance is completed on the system and the temperature rise in the water bath is used to determine the heating value of the sample. The units of measure for this test are MJ/kg.

Water Insolubles

The determination of the percentage bio-oil that is not soluble in water is important for the characterization and utilization of bio-oil. Water insoluble compounds typically contain more than six carbon molecules and an oxygen molecule. To determine the percent of water insolubles that are present in the bio-oil, a small sample of bio-oil is mixed with water in a ratio of 20:1 water to bio-oil. Hot water (~80^{o}C) is used for fractions that are near solid at room temperature. The bio-oil and water are mixed well using a vortex mixer, a sonicator, a mixing table and a centrifuge. The mixture is then passed through a 2.5 micron filter that will catch the water insoluble compounds as well as any particulate that is present. The vial and filter paper are dried. The percent water insolubles is the mass of the bio-oil that is not soluble in water divided by the total mass of bio-oil tested.

Solids

The determination of the solids content of bio-oil is integral to creating standards for bio-oil usage. Solid particulate can erode surfaces, which can cause a need for increased maintenance. The procedure for determining the solids content of bio-oil has been adapted from the standards that are in place for many hydrocarbon fuels. A known mass of bio-oil is mixed with methanol. The methanol acts as a solvent, thinning the bio-oil, making it easier to filter. The char and other solid particulate are typically either not soluble in methanol or too large to pass through the filter paper. The methanol-bio-oil mixture is then filtered and the mass of solid particulate that was collected is measured. The solid particulate that was collected is divided by the sample mass to determine the percent solids content.

Modified Acid Number

The modified acid number (MAN) is a measure of the amount of carboxylic acid that is present in a sample. The instrument that is used to determine the MAN is a Metrohm 798 Titrino. This instrument follows ASTM SMANdard D 664. The acid number is determined by potentiometric titration. The modified acid number represents the amount of potassium hydroxide (KOH) that is required to neutralize the acid present in 1 gram of a sample. The units of measure for MAN are mg KOH/gram of sample. A known mass of bio-oil is mixed with MAN solvent. The mixture of bio-oil and MAN solvent is placed on the device, where it is mixed vigorously. It is at this point that the titration occurs. The instrument monitors the amount of KOH that is injected into the mixture. A probe also monitors the reaction to determine when the reaction has been completed. When the reaction has been completed, the instrument outputs the MAN on the screen.

Elemental Analysis

Elemental analysis is completed for each fraction of bio-oil to determine the breakdown of carbon, hydrogen, nitrogen, sulfur and oxygen. This test was completed with a TruSpec Series instrument with a separate instrument for the measurement of sulfur. For

the measurement of carbon, hydrogen and nitrogen, bio-oil is prepared in a foil packet. The sample is dropped from an auto-sampler into a furnace that is held at 950^{o}C. The furnace is flushed with pure oxygen and the product gases are conditioned and analyzed. Carbon and hydrogen concentrations are determined with infrared detectors. Nitrogen concentration is determined by passing a small sample of the gas over a hot copper element that removes oxygen. This process also transforms NOx to N2. The conditioned gas is then passed by a thermal conductivity detector to determine nitrogen content. Oxygen is determined by summing the amount of ash, carbon, hydrogen, nitrogen and sulfur and subtracting that from 100.

ASH

The ash content of bio-oil is determined through thermal gravimetric analysis. A small sample (<5 micrograms) is placed in a crucible. The thermal gravimetric analyzer (TGA) places the crucible in a furnace that has the ability to measure heat flow with a differential scanning calorimeter. The sample is slowly heated through many stages. The stages are set-up to determine the moisture content, volatiles, fixed carbon and ash. Some of the heating occurs with a nitrogen purge to prevent combustion. Typical tests last between 1 and 3 hours.

Viscosity

The kinematic viscosity of bio-oil can be determined with a Cannon-Fenske Opaque viscometer. This viscometer is used in accordance to ASTM D 445, 446 and 2170.[45-47] The viscometer is a reverse flow viscometer that has a capillary tube that passes bio-oil through to the set of three bulbs. These tubes are used for opaque Newtonian fluids where the bottom of the meniscus cannot be seen. The viscosity is measured at 40^{o}C for all bio-oil except for the heavy bio-oil which is measured at 60^{o}C. The heavy bio-oil is measured at the elevated temperature, in a similar manner to asphalt.

To complete the viscosity test, the bio-oil is pulled into the upper bulb with a vacuum. The tube is placed in a warm oil bath that is held at a constant temperature. The tube is given 10-15 minutes to equilibrate to the bath temperature. Once the bio-oil has settled to the desired temperature, a plug is removed from the tube and the bio-oil flows through the three bulbs. The time that is required for the bio-oil to pass through the two upper bulbs in used to calculate the kinematic viscosity (cSt).

Mass Balance

Complete mass balances were kept for each fast pyrolysis trial. Each fraction was captured in a one liter Nalgene bottle that was weighed before and after the test. The char was collected during the test and weighed afterwards. The mass of the non-condensable gases was calculated using a helium tracer gas.

The helium gas flow was controlled with a mass flow controller that logged the continuous flow rate of helium into the system. The helium remained in the gas flow throughout the system as we detected in the non-condensable gases with the Micro-GC. Seeing the flow rate of the helium was known, as well as the concentration, the flow rate of the other gases could be determined utilizing the measured concentrations.

The mass balances from the fast pyrolysis trials are an indication that the reactor has not yet been optimized. Optimal yields for biomass fast pyrolysis are typically reported as 75% bio-oil, 12% char and 13% non-condensable gases (NCG).[2] Increased production of char and NCG act as an indication that the pyrolysis process has not been optimized. This could be a function of many operations within the reactor. These factors include fluidization gas flow rate, biomass feed rate, sand particle size, heating rates and even biomass particle size.

CHAPTER 4. RESULTS AND DISCUSSION

The hypothesis developed for this research states that separation of bio-oil components can be achieved through the utilization of cooling surfaces that have elevated temperatures that are analogous with the dew point of desired compounds. Bio-oil analysis indicates that is it possible to remove water and low molecular weight acids from some of the bio-oil by collecting it in a single fraction. The analysis also provided evidence that is possible to collect fractions that are rich in levoglucosan and water insoluble content. While the fractionation was not as clear cut as hoped, this data indicates that with further refining of the process high quality bio-oil can be produced on a large scale.

The full analysis included a mass balance of the bio-oil collection system, moisture content, energy content, modified acid number, elemental analysis, chemical analysis, water insoluble analysis, solids content analysis and measurement of the viscosity of each bio-oil fraction. Appendix C contains tables with the full analysis for each test. The following sections present and discuss the results from this analysis. The error bars shown in the graphs are based solely on the standard deviation of the data that was collected.

4.1 Mass Balance

The mass balances for the fast pyrolysis trials are shown in Figure 19, Figure 20 and Figure 21. These figures show each test as well as averages for the three biomasses. Visually significant differences can be seen between the results from each biomass.

Char production is one quality that varies between biomasses. The red oak produced less char than the other two biomasses (cornstover and switchgrass). One explanation for this is the fundamental differences between a hard wood and the grasses/agricultural wastes. Hard woods have been shown to produce more bio-oil, less char and a higher quality bio-oil in general.[48] There is also significantly less ash in the red oak than there is in either

the cornstover or the switchgrass (See Table 6). Ash can cause secondary reactions which lead to an increase in char yield. The removal of ash from the switchgrass char could lead to a similar percentage of char being produced from both the switchgrass and the red oak.

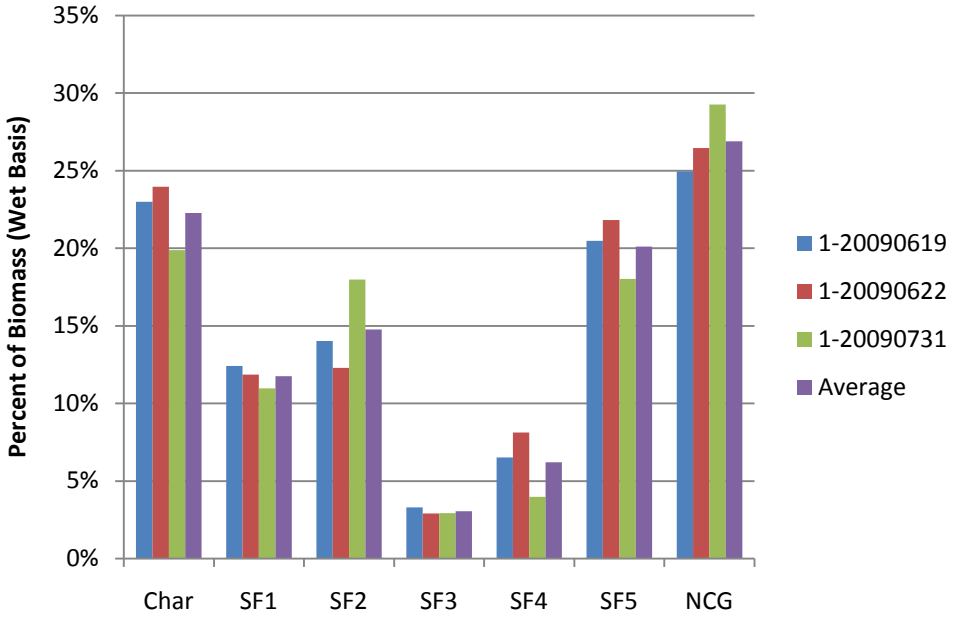

Figure 19 Red Oak Mass Balance

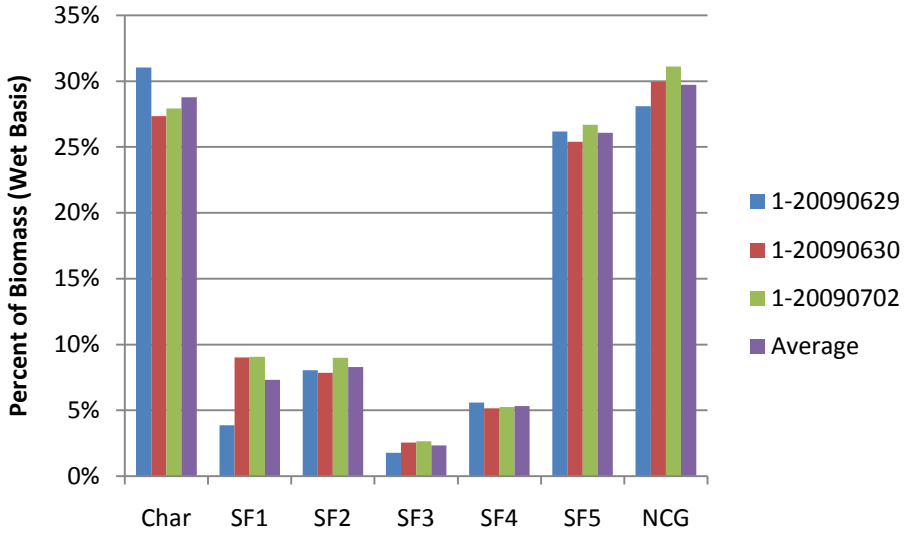

Figure 20 Cornstover Mass Balance

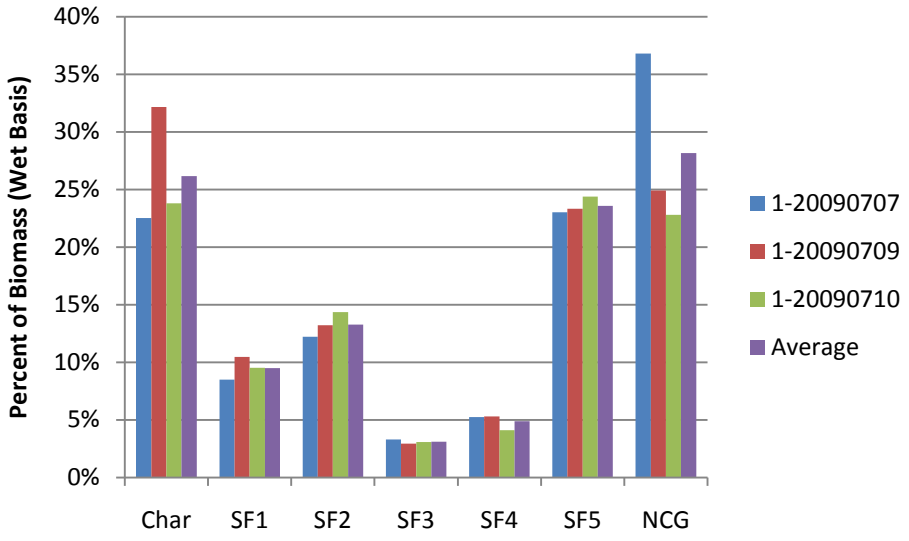

Figure 21 Switchgrass Mass Balance

The bio-oil production of the three biomasses was similar, but also very different. Each biomass produced around 50% bio-oil (55.89% for red oak, 49.35% for cornstover and 54.34% for switchgrass). The red oak did produce more bio-oil than the other biomasses, which is consistent with multiple values seen throughout the literature. This can also partially be attributed to the amount of ash that is present in the biomass. The secondary reactions that are catalyzed and caused by ash reduce the amount of bio-oil that is produced. These secondary reactions tend to produce a higher amount of char and non-condensable gases.[9]

The fractionation, though, performed similarly for each biomass. Large portions of bio-oil were collected in the first two fractions (SF1 and SF2) and the last fraction (SF5). This includes the large molecular weight compounds that can be found in the first condenser and ESP as well as the watery fraction found in the last condenser. A breakdown of the bio-oil collected in each fraction can be seen in Table 8. A similarity between each of the biomasses was the proportion of bio-oil that was collected in the third and fourth fractions (SF3 and SF4). SF3 collected approximately 5% during each test and SF4 collected nearly 10% of the bio-oil during each test. These fractions are

meant to contain the phenolic compounds (Figure 11) and any other compounds that have a higher dew point than water. This low percentage could be an indication that most of the phenolics produced have a higher boiling point than simple phenol. SF5 produced the largest volume and mass of bio-oil for each biomass. This was due to the large amount of water and light organic compounds that were collected in this fraction.

Table 8 Bio-oil Collection Mass Balance

Test #	Biomass	SF1	SF2	SF3	SF4	SF5
1-20090619	Red Oak	21.9%	24.7%	5.8%	11.5%	36.1%
1-20090622	Red Oak	20.8%	21.6%	5.1%	14.2%	38.3%
1-20090731	Red Oak	20.4%	33.4%	5.4%	7.4%	33.4%
	Average	**21.0%**	**26.6%**	**5.5%**	**11.0%**	**35.9%**
1-20090629	Cornstover	8.5%	17.7%	3.9%	12.3%	57.6%
1-20090630	Cornstover	18.0%	15.7%	5.1%	10.3%	50.8%
1-20090702	Cornstover	17.2%	17.1%	5.0%	10.0%	50.7%
	Average	**14.6%**	**16.8%**	**4.7%**	**10.9%**	**53.0%**
1-20090707	Switchgrass	16.2%	23.4%	6.3%	10.0%	44.0%
1-20090709	Switchgrass	19.0%	23.9%	5.3%	9.6%	42.2%
1-20090710	Switchgrass	17.2%	25.9%	5.6%	7.4%	44.0%
	Average	**17.5%**	**24.4%**	**5.7%**	**9.0%**	**43.4%**

4.2 Qualitative Properties of Bio-oil

Each fraction of bio-oil had a distinct appearance that was consistent through all of the fast pyrolysis trials. Figure 22 shows samples of bio-oil produced from oak. The first and second fractions of bio-oil (SF1 and SF2) behaved and looked similar. These fractions of bio-oil were collected as a liquid, and as the bio-oil cooled, it transitioned into a solid. The solid bio-oil from SF1 and SF2 became like thick molasses upon reheating to approximately 60^{o}C and a pourable liquid at 75^{o}C. These first two fractions also had a sweet, barbeque smell.

The third fraction (SF3) of bio-oil had a consistency similar to maple syrup. The bio-oil in this fraction was designed to be the final condensation step before water began to condense. SF3 appeared to be a black bio-oil until it was spread thin. Once spread thin,

SF3 appeared to have a red tint. The red tint of this fraction is due to the compounds that were collected; specifically the multiple phenolic compounds found in this fraction.

SF4, which was an ESP fraction, had a similar consistency to SF3. The bio-oil was pourable with a consistency similar to that of maple syrup. The color of the fourth fraction of bio-oil appeared to be pitch black, even when spread thin. The dark black coloring can be attributed to the nature of the aerosols that were contained in this fraction. Aerosols contain a wide array of compounds, including lignin derived oligomers. These lignin derived oligomers are typically found to be very dark and black in color.

The last fraction (SF5) was a very watery, thin fraction. The liquid collected in this fraction was mainly water. The high water content produced a liquid that had a consistency that was similar to water. Depending on the amount of water that was collected, the color of this fraction varied. Typically SF5 was clear with a red tint. If the ESPs were not operating correctly, black oily droplets could be seen floating on the top of this fraction. SF5 had an overpowering acidic smell.

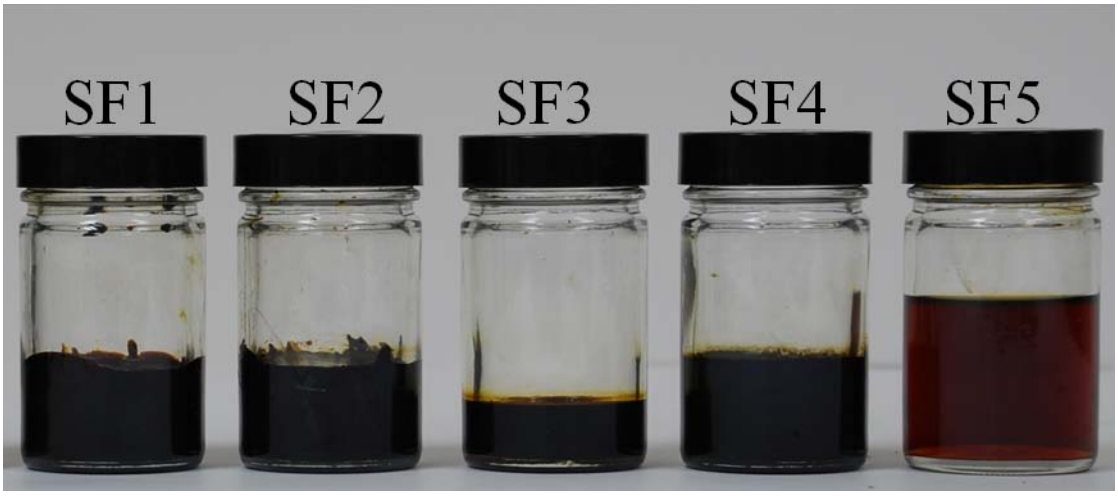

Figure 22 Bio-oil Samples from Oak

4.3 Moisture Content

One of the primary goals of the fractionating bio-oil collection system is to collect bio-oil fractions with low amounts of water. This will have multiple effects on the quality and composition of the bio-oil. Removing the water from the bio-oil creates a viscous bio-oil that is more difficult to pump. Alternatively, the presence of water in a liquid reduces the higher heating value of it. This is due to the need to vaporize the water when combusting the bio-oil. Typical whole bio-oil has a moisture content of around 25%.[2]

The moisture content of the bio-oil fractions from all of the fast pyrolysis trials was completed by using a Karl-Fischer Titrator. The average moisture content for each of the fractions and biomasses is shown in Figure 23. The different biomasses gave visually significantly different moisture contents, but the trend was the same for all three biomasses.

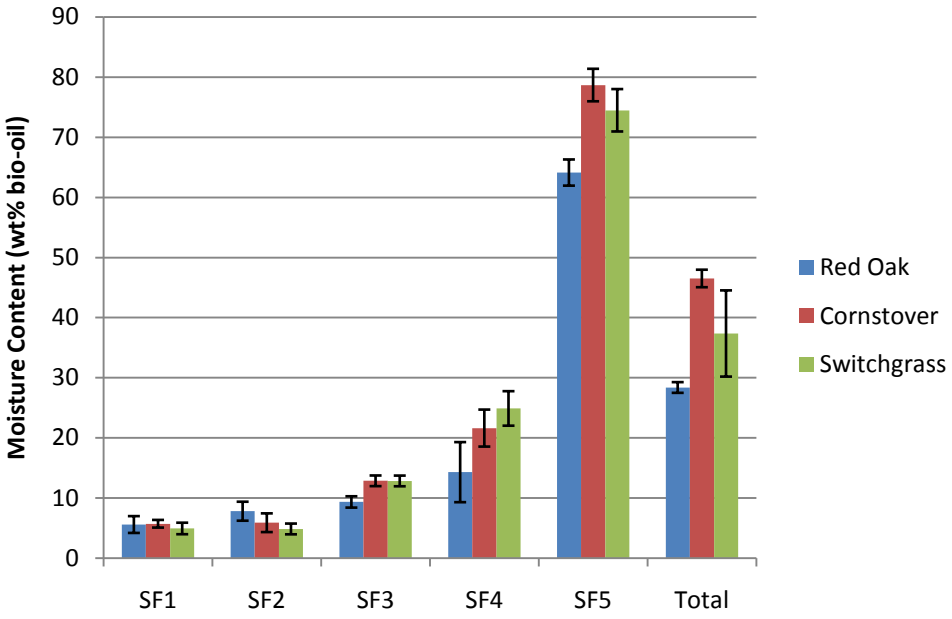

Figure 23 Average Moisture Content in Bio-oil Fractions

The general trend in the experiments was increasing moisture content with decreasing condenser temperatures. In all of the tests, SF1 and SF2 both had significantly less moisture than the other fractions. The bio-oil collection system was designed to collect little to no water in the first two fractions of bio-oil. The presence of water in the upstream fractions (SF1 and SF2) was not expected, but can be explained:

- Water could condense on the bio-oil that had already been collected in the bottle or on the bottle walls if they were cooler than the dew point of water.
- Water could be produced through reactions that occur while the bio-oil is cooling.
- Water molecules could bond with larger polar molecules through hydrogen bonding.

As the bio-oil was gathered in SF3 and SF4, more moisture was condensed and collected in the bio-oil. This occurred even though the wall temperature set-point for SF3 was theoretically higher than the dew point of water. There are multiple explanations for this occurrence. The most likely explanation for the moisture content in fractions 3 and 4 is a change in water vapor pressure. The design vapor pressure was based on a theoretical combination of bio-oil constituents. If the bio-oil composition had changed due to secondary reactions or differing biomass, the vapor pressure of water would have changed as well. The dew point of water increases with the concentration of water in the product stream. This would cause water to begin to condense even though the condenser wall set-point was thought to be greater than the dew point of water.

The last fraction of bio-oil (SF5) was mainly water. The primary goal of this fraction was to collect the water and acid found in the bio-oil. The results show that this was partially accomplished. In each test, a majority of the water was collected in the SF5.

Even though there is a trend of increasing moisture content as the bio-oil progresses from SF1 to SF5, the different biomasses have noticeably different moisture contents. Red oak typically had lower moisture concentration for each of the fractions when compared to

the other two biomasses. Cornstover and switchgrass typically had higher moisture contents overall. Other than SF5, each fraction had less water than typical bio-oil.

Bio-oil was collected in the separate fractions in different ratios depending on the biomass that was being processed. There are many ways to compare the moisture content, but comparing them on a basis of grams of water per gram of bio-oil collected places each biomass on equal footing. This analysis is used throughout this chapter to compare the properties of the bio-oil produced from different biomasses. Figure 24 displays the % moisture contained in the bio-oil.

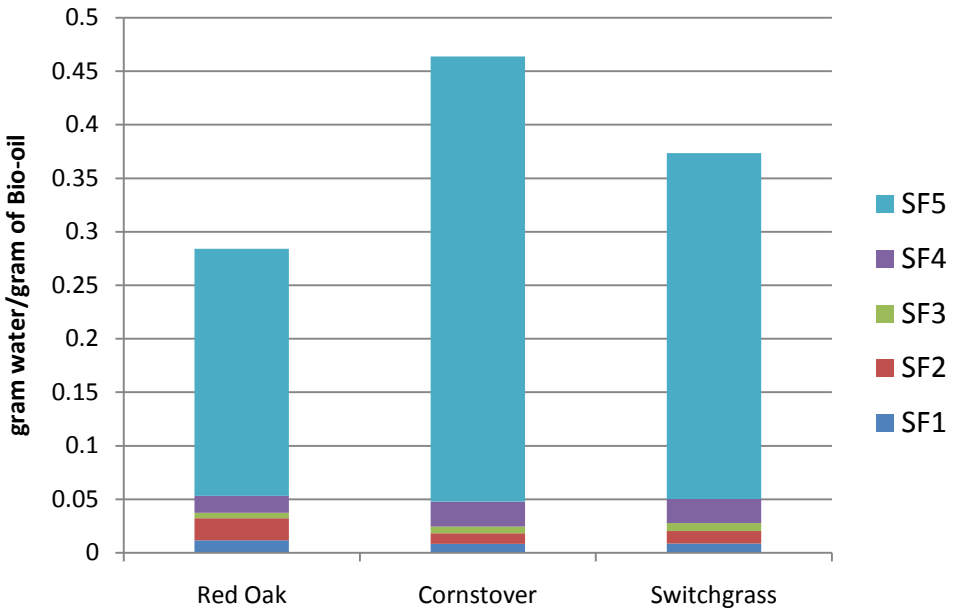

Figure 24 Comparison of Moisture Content by Biomass (Wet Basis)

This comparison shows that more water was produced from cornstover than from the other two biomasses. This analysis also shows that the final fraction of bio-oil consistently collected over 80% of the water that was collected from the fast pyrolysis process, while cornstover and switchgrass collected virtually the same ratio of water to biomass in the first four fractions. This indicates that the bio-oil collection system

fractionated these early fractions in a similar method during these tests. Red oak though collected large amounts of water, compared to the other biomasses, in the first two fractions. A large majority of the water was pushed to the last condenser while the first four condensers collected less than 15% of the water.

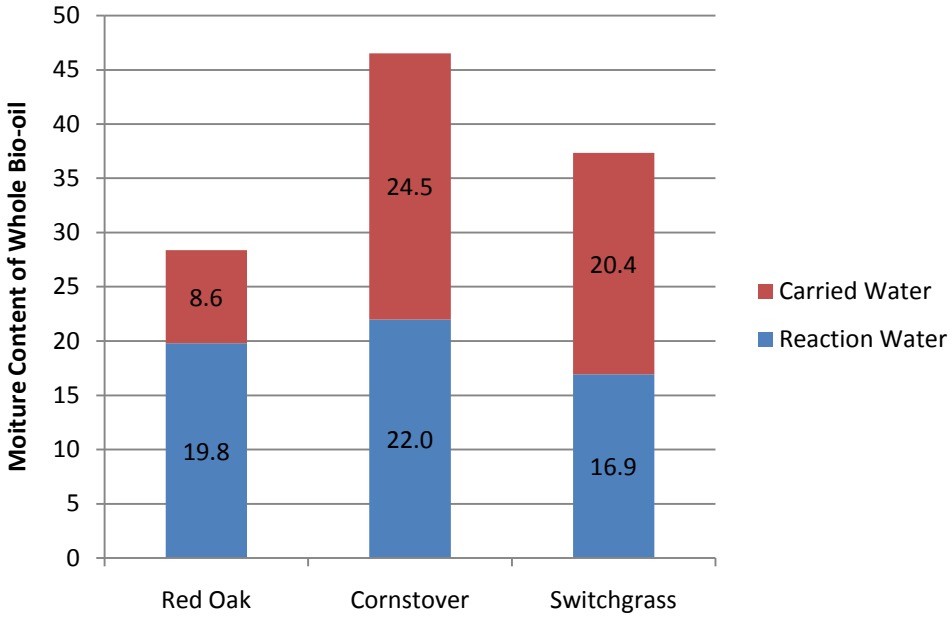

Figure 25 Comparison of Carried and Reaction Water in Whole Bio-oil

When comparing the moisture content of bio-oil, it is helpful to separate the water into carried and reaction water. The carried water is water that entered the system as trapped moisture in the biomass. The reaction water is water that was generated as a byproduct of the multitude of reactions that occur during fast pyrolysis. Figure 25 shows the difference between the carried and reaction water from each biomass. This figure illustrates that the carried water was not the most significant contributor to moisture found in the bio-oil. Rather, the moisture found in the bio-oil was generated mainly from the reactions that occurred during the fast pyrolysis process. Through this analysis it is shown that cornstover produces the largest amount of water during the process. The increased production of water indicates the presence of secondary reactions which are catalyzed by ash and char. These secondary reactions reduce the overall production of

bio-oil and increase the moisture content, char production and non-condensable gas production of the process.

4.4 Higher Heating Value

The higher heating value, which was defined earlier in the term definitions, is a key property of bio-oil. This value, which is determined with a bomb calorimeter, is an indication of the amount of energy that could be utilized when the bio-oil is combusted. Conventional fuel oils have heating values that are typically between 42-44 MJ/kg while traditional bio-oil only has heating values around 17 MJ/kg (wet basis).[38] The analysis of the bio-oil was completed and is presented on a wet basis unless otherwise noted.

The average heating values of the individual fractions from each biomass are shown in Figure 26. The average HHV for each biomass is also given on a mass averaged basis. The results from the individual biomasses varied, but the overall trend of the higher heating values was the same for all biomasses. As the collection temperature lowered, the higher heating value of the bio-oil lowered as well. This corresponds to the amount of water that was collected in each of the bio-oil fractions. Energy is required to vaporize the water in bio-oil, thus the energy for vaporization lowers the total energy content of the bio-oil. This also explains the lower overall energy contents of the cornstover and switchgrass bio-oils which had higher moisture contents than the red oak bio-oil.

The total energy content of the bio-oil that was produced from the multiple biomasses is also presented in Figure 26 and Appendix C. The HHV for the total red oak bio-oil was determined to be 17.3 MJ/kg. The mass average heating value was determined by multiplying the HHV for each fraction with the mass of bio-oil collected for each fraction. This value was then divided by the total mass collected to produce the total higher heating value. Based on this method, the switchgrass bio-oil had an HHV of 16.2 MJ/kg and the cornstover bio-oil had an HHV of 17.7 MJ/kg. These HHVs are lower than the typical HHV that has been previously presented in the literature.[38] These lower

energy contents can be attributed to the higher moisture content and lower overall yield that was collected for these two biomasses. The lower yield and higher moisture content could be due to secondary reactions that break the larger bio-oil molecules into smaller organic molecules. These secondary reactions produce more char, NCG and low molecular weight compounds, including water.

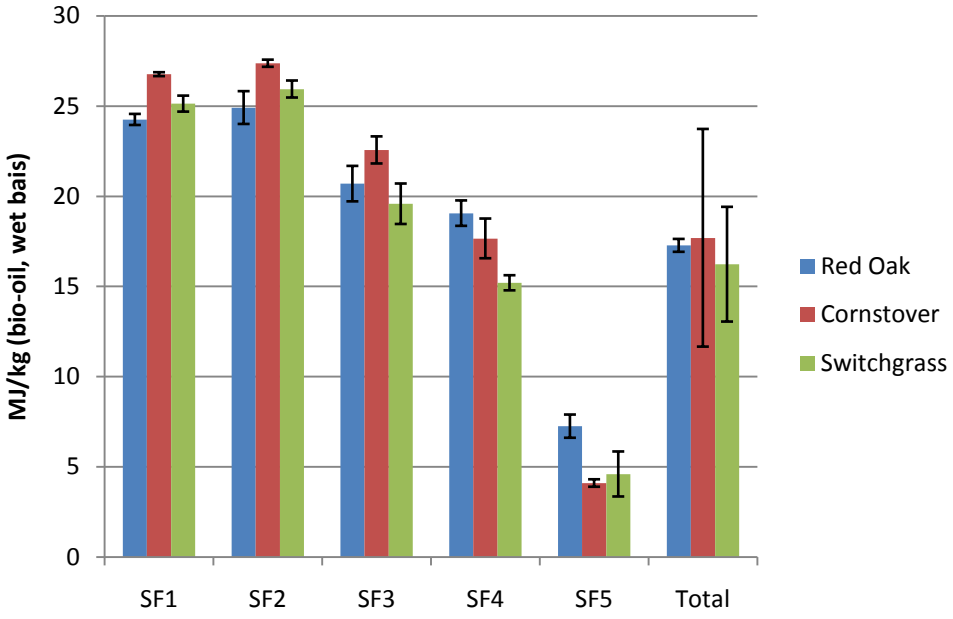

Figure 26 Higher Heating Value of Bio-oil Fractions (Wet Basis)

The energy content of the individual fractions of bio-oil range from over 25 MJ/kg to less than 10 MJ/kg. The highest energy contents were consistently found in the first two condensers. Complete analysis can be seen in Appendix C. The first two fractions contain 67.6% of the total energy for red oak. This compares to 62.5% for cornstover and 65.38% for switchgrass. The final fraction of bio-oil contains the lowest HHV of any of the bio-oil fractions. The final fraction (SF5) of red oak bio-oil has a higher heating value of 7.3 MJ/kg. Similarly, SF5 for switchgrass and cornstover had HHVs of 4.6 MJ/kg and 4.1 MJ/kg. The differences in heating values for SF5 can be correlated to the moisture content. Cornstover bio-oil had higher moisture content in SF5 than

switchgrass, which had higher moisture content than red oak. As the moisture content increased, the energy content of the last fraction decreased.

Due to differences in bio-oil yields, it is helpful to compare the energy content on a level base. Figure 27 presents the heating value of the mass averaged bio-oil (in MJ/kg of bio-oil), separated into individual fractions. Comparing the heating value on a whole bio-oil basis provides an equal basis to compare the bio-oils produced from different biomasses. This graphic illustrates that red oak was the best biomass that was tested for the conversion of biomass to a liquid energy carrier. For the bio-oil that was produced and tested, red oak bio-oil contained 17.5 MJ/kg of biomass reacted. This compares to biomass energy values that are reported between 15-19 MJ/kg.[49] Cornstover and switchgrass each produced 13.7 and 15.2 MJ/kg of biomass fed respectively.

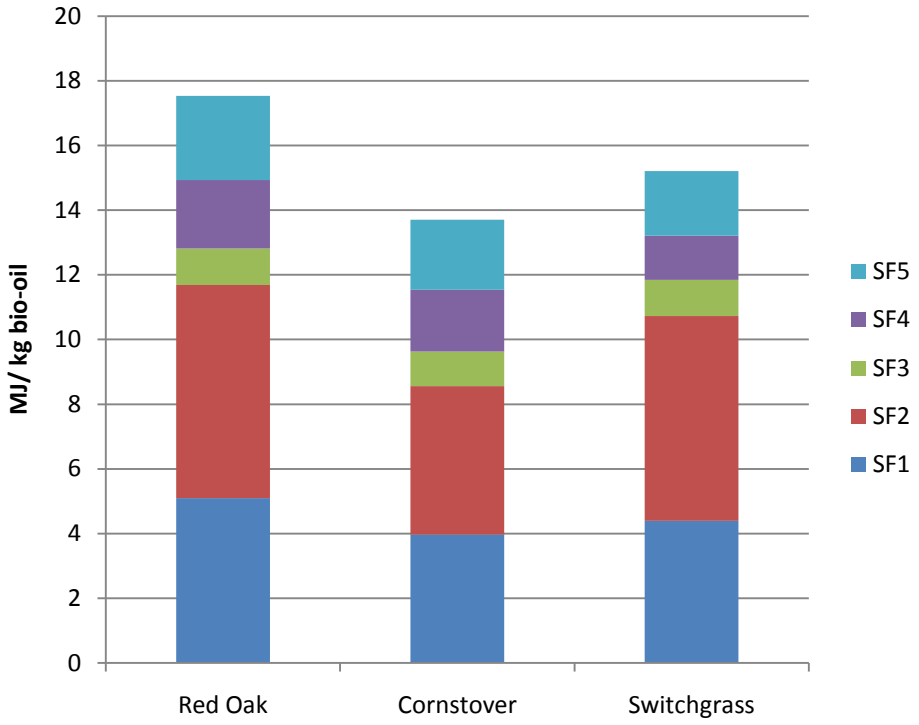

Figure 27 Heating Value of Bio-oil by Biomass (Wet Basis)

4.5 MAN

The modified acid number (MAN), as defined in Section 1.2, is the amount of KOH in mg that is required to neutralize the organic (carboxylic) acids in a gram of sample liquid. This method of determining acid content of bio-oil is more quantitative than pH. pH is a qualitative measurement that can be used to compare the severity of acid content, but not the actual amount of acids present. Typical pH measurements for bio-oil are reported to be 2.5.[2]

The modified acid number for the separate fractions of bio-oil is shown in Figure 28. This figure contains the average modified acid numbers for each fraction of bio-oil for each biomass that was tested. A mass averaged overall MAN is also shown in this figure. This figure also denotes the standard deviation for each value presented as error bars.

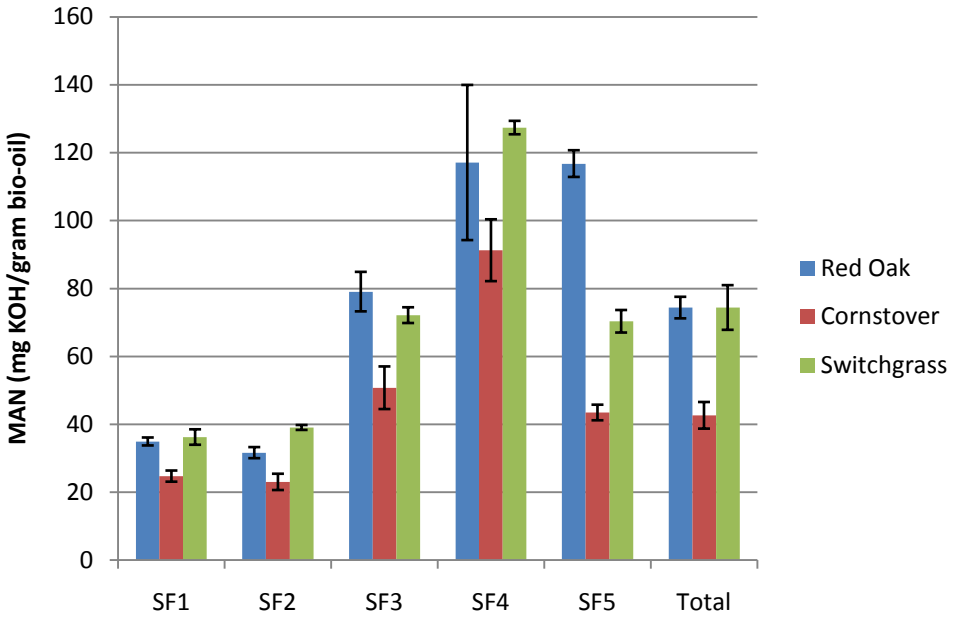

Figure 28 Modified acid number of Bio-oil Fractions (Wet Basis)

The MAN for each fraction differed greatly both between fractions and between biomasses. There was an overall trend that can be seen for each fraction. Stage fractions

1 and 2 had the lowest MANs. These values were both consistently less than 40 mg KOH/gram of bio-oil. The fraction with the highest MAN was very dependent on the biomass. Cornstover and switchgrass behaved similarly to each other, although cornstover bio-oil had a noticeably lower MAN than bio-oil produced from switchgrass. The first two fractions of bio-oil from both cornstover and switchgrass had similar MANs followed by a higher MAN in the third fraction. The fourth fraction of bio-oil for these biomasses had the highest MAN of any fraction from the respective biomass. The fourth fraction was ESP fraction that had cooled to approximately 75^{o}C before being collected.

The final fraction of bio-oil had a lower MAN than the fourth fraction, but, as can be seen in Figure 29, over half of the total acid that was found in the bio-oil was contained in this fraction. Cornstover, which had lowest MAN for stage fraction 5 (43.5 mg KOH/ gram of bio-oil) also had the highest average moisture content of any fraction (78.7 wt%). The high concentration of water present in the final fraction dilutes the acids that are present. This allows for a small MAN but a large amount of collected acid when compared to the other fractions on a wet basis.

Bio-oil produced from red oak had the highest overall MAN. SF4 and SF5 each had MANs that averaged 117.1 and 116.8 mg KOH/gram of bio-oil respectively. These MANs were significantly higher than the other three fractions which averaged 34.9, 31.6 and 79.1 mg KOH/gram of bio-oil. This is an indication that the bio-oil collection system is successfully separating a significant portion of the acids from the rest of the bio-oil. Another indication can be seen in Figure 29. This figure breaks the MAN into biomass types and presents the MAN as mg KOH/gram of bio-oil produced. This figure shows that approximately 56% of the total acid that is found in the bio-oil is contained in the final fraction of bio-oil from red oak. This figure also shows that cornstover produced the lowest amount of total acid but still collected about 54% of that acid in the final fraction. The lower acid content in cornstover could be due to the fact that cornstover typically has a lower concentration of hemicelluloses than either switchgrass or red oak

as shown in Table 5. By collecting over half of the acid in the final fraction of bio-oil, this system is lowering the acid content of the other four fractions.

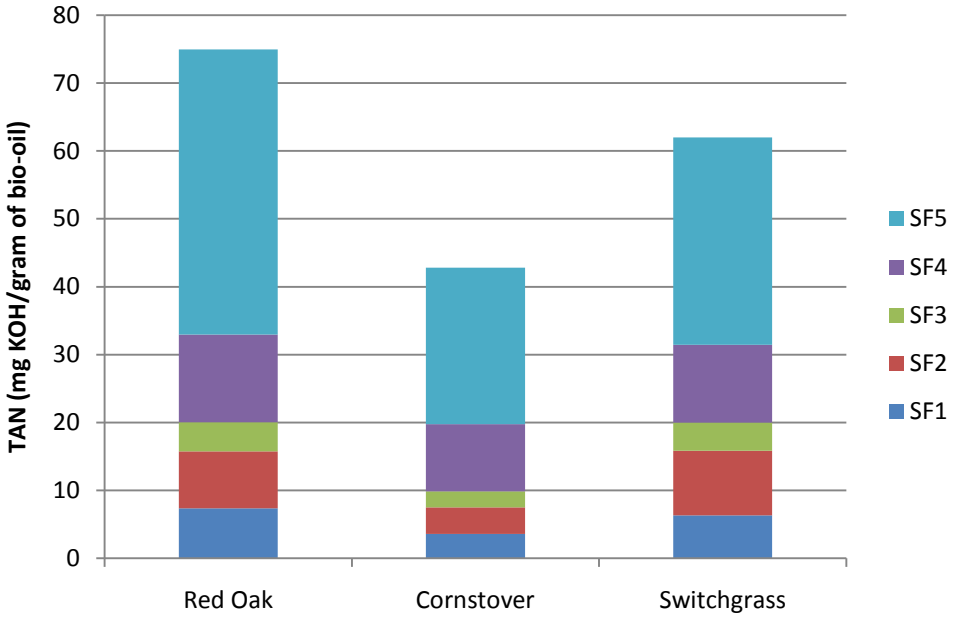

Figure 29 Mass Averaged MAN by Biomass in a mg KOH/g whole bio-oil

The modified acid number takes into account only carboxylic acids, although some of the acidic compounds that are detected are non-conventional carboxylic acids. These other compounds include phenolic compounds that contain a carboxyl group. It is likely that the modified acid number that was measured for SF1 and SF2 consists of many "acidic tars" (phenolic compounds with acidic tendancies). Further indication of the effect of the fractionation technology can be shown through the acetic acid content of the bio-oil. This can be seen in Section 4.7 Chemical Analysis.

4.6 Elemental Analysis

The elemental analysis of each bio-oil fraction was completed in triplicate and the results are presented and discussed below. All of the elemental analysis is presented on a moisture free basis. Full results can be seen in Appendix C.

Carbon contents (dry basis) of the bio-oil fractions are shown in Figure 30. This figure illustrates the significant difference between the first two stage fractions (SF1 and SF2) and the final stage fraction (SF5). The first two fractions have carbon contents that exceed 60%, with the bio-oil from cornstover exceeding 65%. Meanwhile, the final fraction of bio-oil has carbon contents that are less than 45% by weight on a dry basis.

Typical wood-derived bio-oil contains between 54 and 58% carbon on a dry basis.[9] The mass averaged bio-oil contained carbon contents that ranged from 51.5% to 58.7% which falls into the general range of carbon for whole bio-oil. The differences between the fractions of bio-oil and the typical carbon contents are significant. These differences indicate that more carbon is being collected in the first two fractions (on a dry basis) than typical bio-oil.

A simple explanation for the differences between the fractions concerns the size of organic molecules that are present in the individual bio-oil fractions. Carbon has a molecular weight of 12 grams per mole which is significantly larger than that of hydrogen but slightly less than the molecular weight of oxygen. Large molecules typically have a higher carbon to oxygen and carbon to hydrogen ratio than smaller molecules. This explains why the concentration of carbon is higher in the first two fractions where there are large concentrations of high molecular weight compounds than in the final fraction where there are mainly low molecular weight compounds.

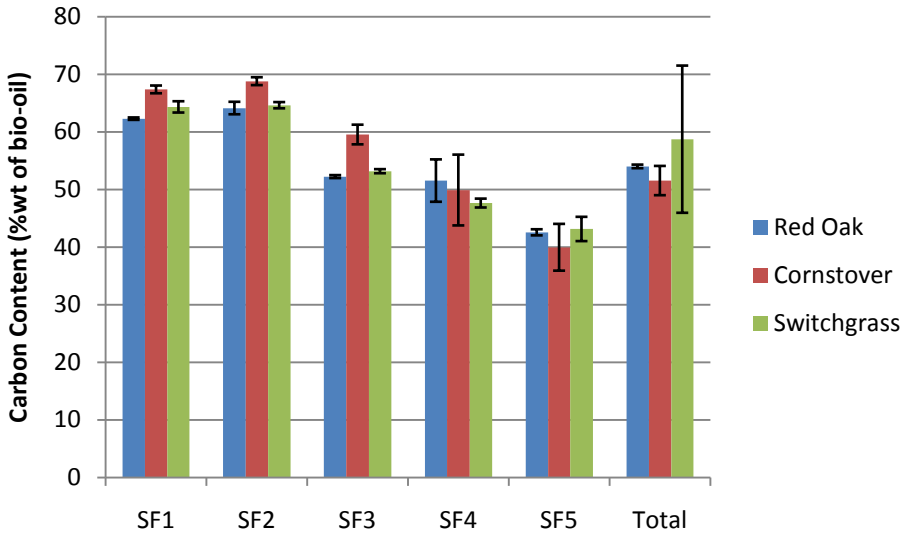

Figure 30 Carbon Content of Bio-oil Fractions (Dry Basis)

The hydrogen content of the bio-oil is shown in Figure 31. This figure illustrates that the hydrogen content (on a dry basis) is relatively constant as it progresses from the first fraction to the fourth fraction. Meanwhile the final fraction of bio-oil contained significantly less hydrogen than the other four fractions. Typical bio-oil contains between 5.5 and 7% of hydrogen by weight.[9] Based on this analysis, it appears that the hydrogen content of the individual fractions of bio-oil is similar to the average concentration of hydrogen found in other bio-oil. This could be due to the high amount of water that was produced during the fast pyrolysis process. This would deprive the rest of the bio-oil from the available hydrogen.

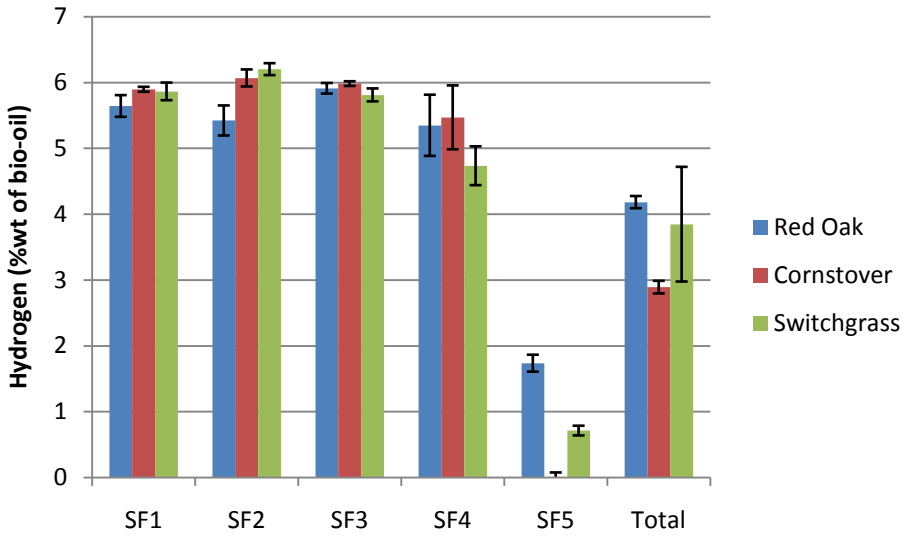

Figure 31 Hydrogen Content of Bio-oil Fractions (Dry Basis)

Oxygen content is a very important property of bio-oil due to its negative effect on heating value. Figure 32 illustrates the differences in oxygen content (on a dry basis) between the separate stage fractions. The oxygen content of SF1 and SF2 for each biomass was similar. Meanwhile, the oxygen content (on a dry basis) is higher in SF3 and SF4 than in SF1 and SF2. Typical bio-oil has an oxygen content that ranges between 35 and 40% by weight.[9] The oxygen content of both the bio-oil fractions and the whole bio-oil is lower than the typical bio-oil that is reported in the literature. This, similar to hydrogen, could be due to the higher amount of water that was produced through the fast pyrolysis reactions.

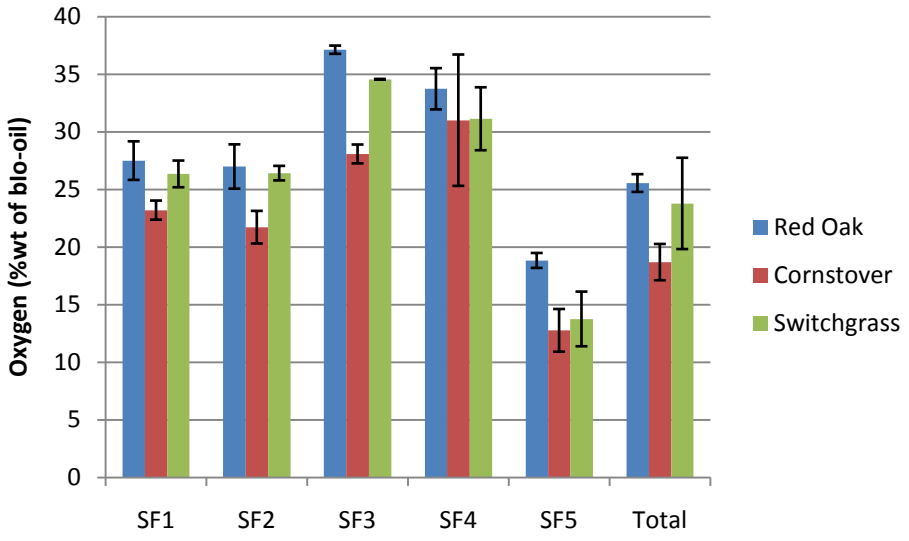

Figure 32 Oxygen Content of Bio-oil Fractions (Dry Basis)

The presence of nitrogen and sulfur in bio-oil is viewed as a negative occurrence. Nitrogen and sulfur produce NOx and SOx when combusted in the bio-oil. NOx and SOx are pollutants that are heavily monitored and controlled in many industrial situations. Figure 34 and Figure 35 illustrate the nitrogen and sulfur content of the individual fractions of bio-oil. Nitrogen content decreased as the bio-oil proceeded from the first stage fraction to the last. Nitrogen compounds that have been found in bio-oil include both amines and pyridines.[50] The amines typically have low boiling points while the pyridines have boiling points that exceed 115°C. Like phenols, pyridines have varying boiling points depending on the degree of substitution found on the aromatic ring. The structure of pyridine can be seen in Figure 33. The presence of pyridines would explain the presence of large concentrations of nitrogen in the first two fractions of bio-oil.

Both nitrogen and sulfur contents are strongly dependant on the initial nitrogen and sulfur contents of the biomass. Red oak contains a smaller amount of nitrogen when compared to switchgrass and cornstover. The cornstover contains the largest amount of nitrogen, which can be seen in both Table 6 and Figure 34.

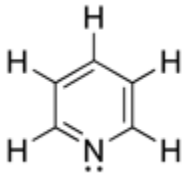

Figure 33 Pyridine Molecule

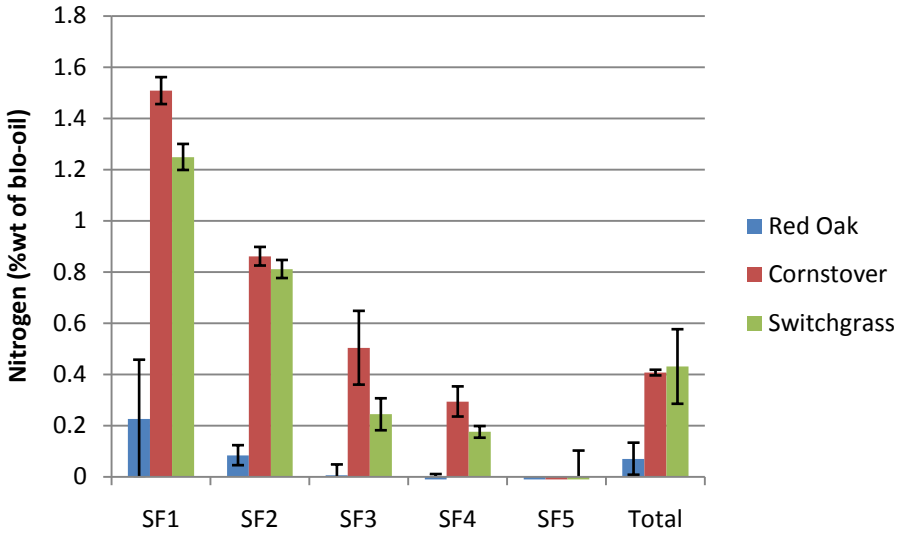

Figure 34 Nitrogen Content of Bio-oil Fractions (Dry Basis)

The sulfur content of the bio-oil was measured on a separate instrument than the carbon, hydrogen and nitrogen. The results from this analysis can be seen in Figure 35. Sulfur content, much like nitrogen content, is strongly dependant on the original sulfur content of the biomass. It is evident, based on Figure 35, that the sulfur is carried through the system as a medium weight compound. The highest concentrations of sulfur were found in the third and fourth fractions. Based on the chemical analysis, these two fractions consist of high concentrations of medium weight compounds, including furans and phenolics. Cornstover and switchgrass produced bio-oil with the highest concentrations of sulfur.

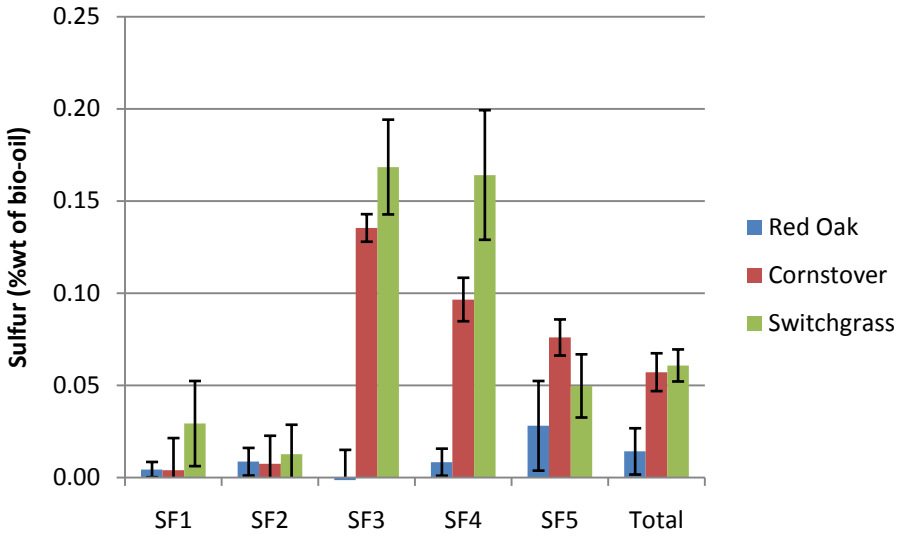

Figure 35 Sulfur Content of Bio-oil Fractions (Dry Basis)

The ash content of the bio-oil was determined with a thermal gravimetric analyzer (TGA). The results for this analysis are illustrated in Figure 36. According to this analysis, the largest concentration of ash content is found in the fourth fraction of bio-oil. This fraction of bio-oil is from an ESP that removes aerosols, which are formed by one of two mechanisms. First, the aerosol could have been produced in the fast pyrolysis reactor but was too small of an aerosol to be removed in the first ESP. Some aerosols contain particulate matter that is carried through the system. During the second pathway, liquid that has been condensed could be sheared into liquid droplets as it is dropping from the condenser tubes to the collection bottle. These aerosol droplets would be pure liquid with little to no particulate matter. The most logical explanation for the presence of large quantities of ash in SF4 would be the presence of solid particulate that is caught in small aerosol droplets. Based on the analysis that was completed for red oak, cornstover and switchgrass, 28%, 47% and 56% of the ash was collected in SF4 for each of the respective fractions.

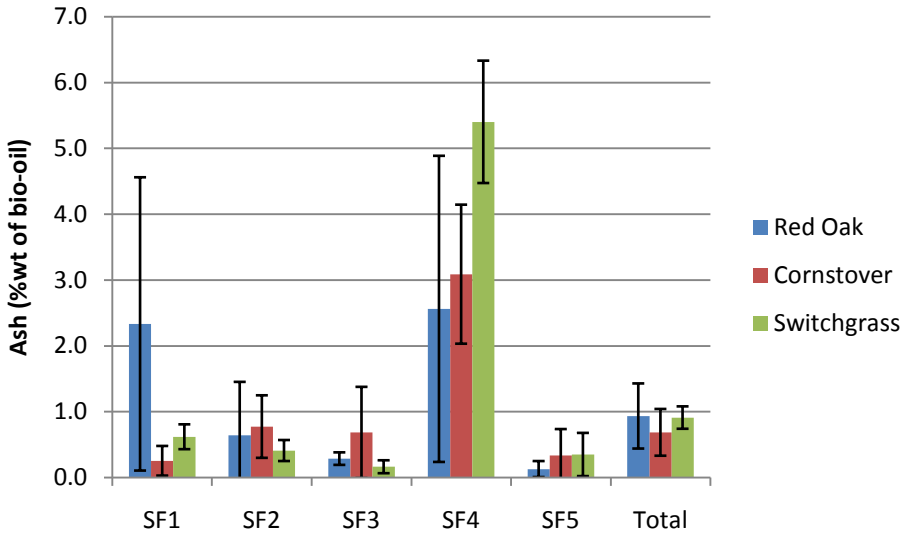

Figure 36 Ash Content of Bio-oil Fractions (Dry Basis)

4.7 Chemical Analysis

4.7.1 Introduction

The chemical analysis of the bio-oil was completed for each fraction. This data was compiled and used to create Figure 37, Figure 38 and Figure 39. These results are based on a mass-averaged analysis. This analysis takes into account the concentration of a component found in a fraction and the amount of bio-oil that was produced in that fraction. This section provides a detailed breakdown of the chemical analysis of the bio-oil. All weight percents presented in this section are given on a wet basis unless otherwise denoted.

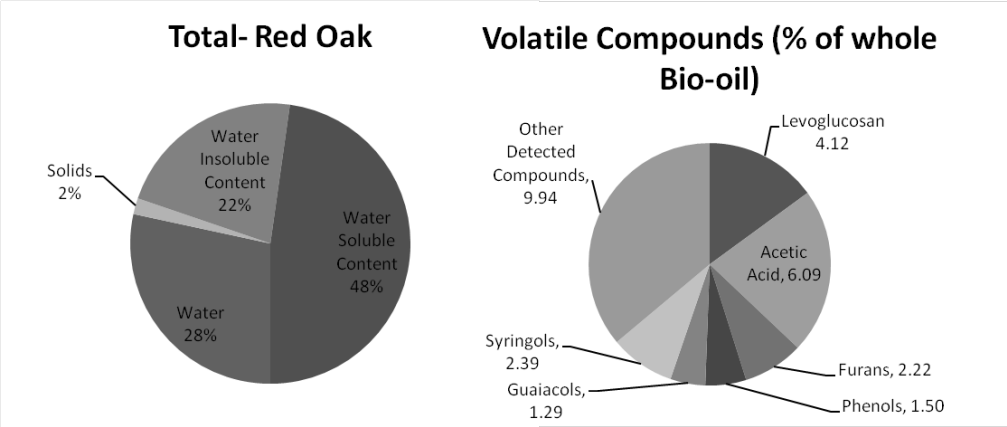

Figure 37 Chemical Analysis of Red Oak obtained through GC/MS and GC/FID

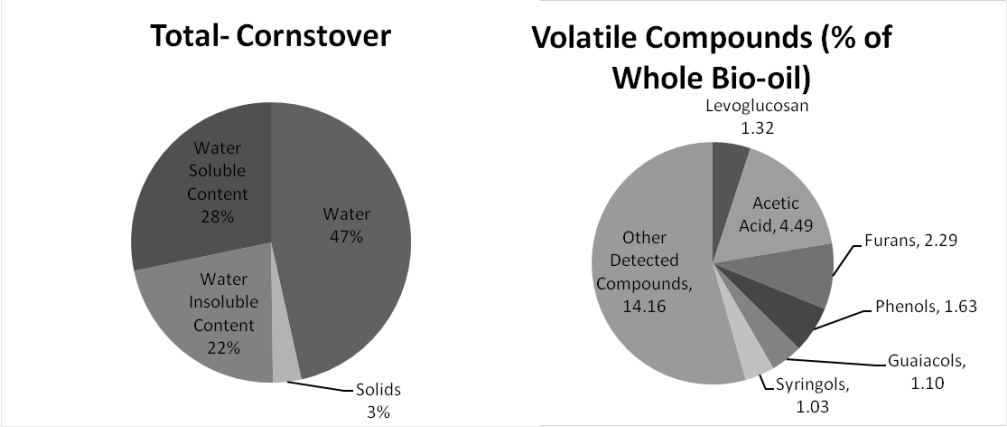

Figure 38 Bio-oil Composition Cornstover obtained through GC/MS and GC/FID

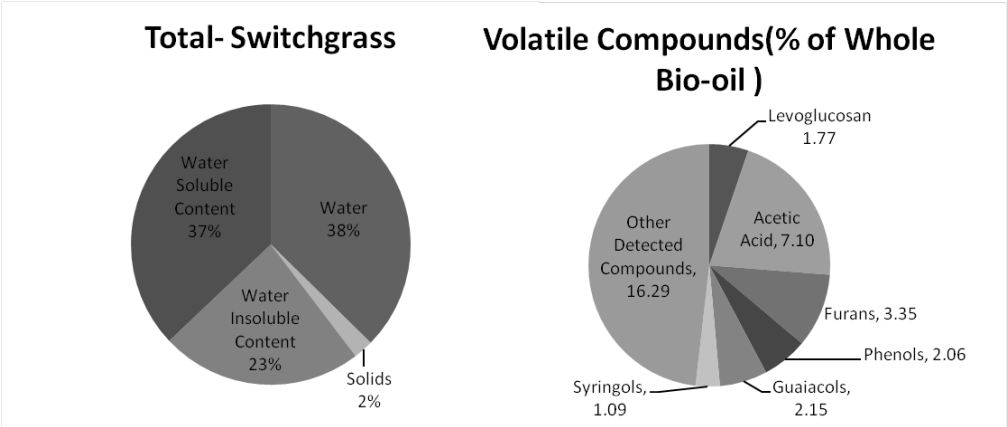

Figure 39 Bio-oil Composition Switchgrass obtained through GC/MS and GC/FID

4.7.2 Levoglucosan

The concentration of levoglucosan (1,6-Anhydro-α-D-glucopyranose) was determined with a GC/MS. This anhydrosugar has long been a compound of interest in fast pyrolysis bio-oil. Typical bio-oil contains between 3 and 4.5% levoglucosan.[22] The concentration of levoglucosan in each fraction of bio-oil can be seen in Figure 40. This figure illustrates the degree of fractionation of levoglucosan. This figure clearly illustrates that the first two fractions (SF1 and SF2) of bio-oil contain the highest concentrations of levoglucosan. The final three fractions of bio-oil each have very low concentrations of levoglucosan. In fact, levoglucosan was not detected in the final fraction of bio-oil produced from cornstover or switchgrass.

Red oak produced the highest concentrations of levoglucosan in each fraction. The highest overall concentration of levoglucosan detected was in the first fraction (SF1) of red oak bio-oil. This fraction had 10% (by weight) levoglucosan.

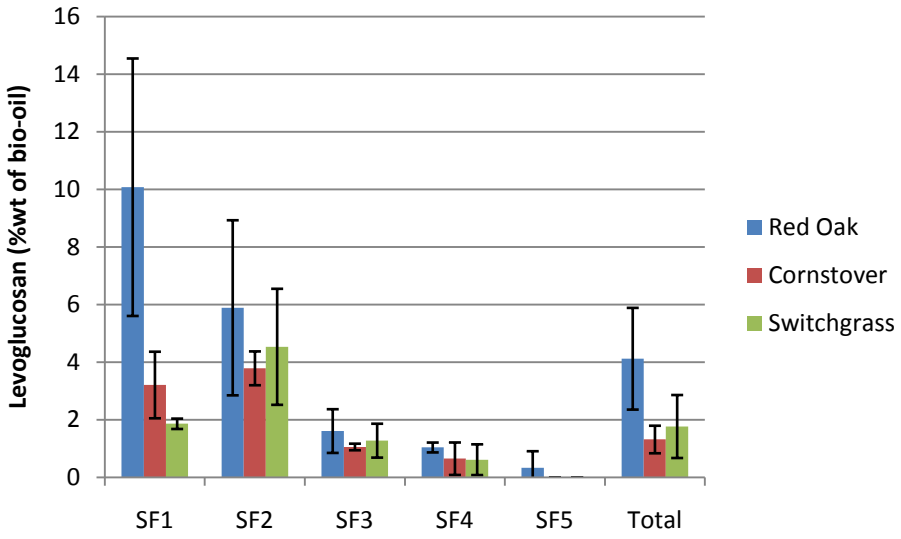

Figure 40 Levoglucosan Content of Bio-oil Fractions (Wet Basis)

An interesting observation can be made concerning the presence of levoglucosan in the second fraction. The initial hypothesis concerning levoglucosan was that it exited the reactor as a vapor. The presence of levoglucosan in the second fraction indicates that this anhydrosugar exits the reactor as an aerosol as well. This is most apparent in the fractions of bio-oil generated from switchgrass. The concentration of levoglucosan in the ESP fraction (SF2) is higher than the concentration in the condenser fraction (SF1). This also occurs in the same fractions of cornstover bio-oil. The ESP fraction (SF2) has a significant concentration of levoglucosan, but it is not higher than the detected concentration that was found in the first fraction.

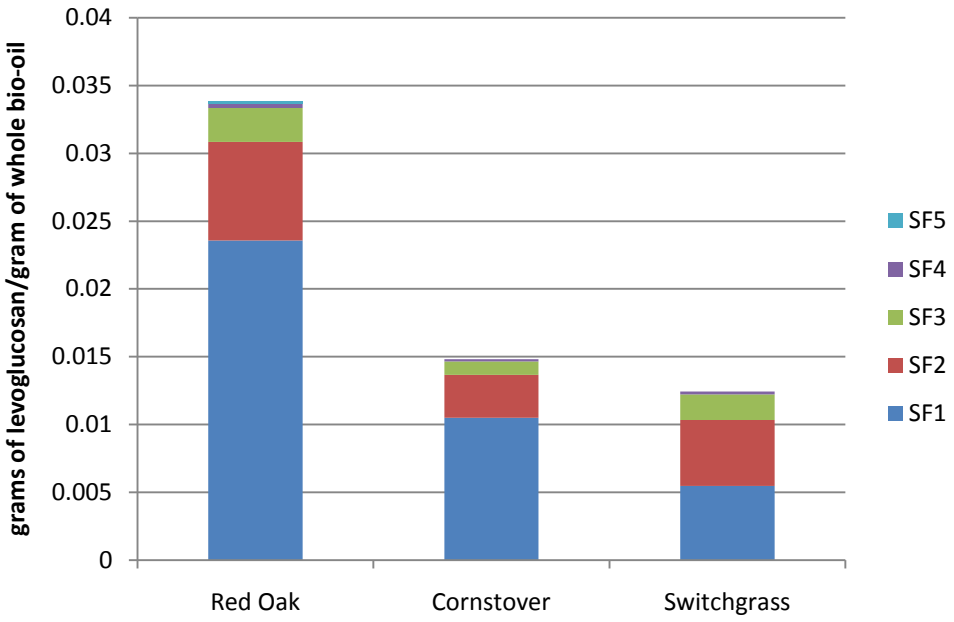

Figure 41 Mass Averaged Levoglucosan Content by Biomass (Dry Basis)

When comparing the bio-oil created from the different biomasses, it is helpful to compare each on the same basis. For levoglucosan production, Figure 41 compares each biomass on a gram of levoglucosan per gram of whole bio-oil collected basis. This method illustrates that red oak produces a significantly higher amount of levoglucosan than either cornstover or switchgrass. These differences in levoglucosan production correlate to the differences in cellulose in the different biomasses. This figure also illustrates the fact that

the vast majority (over 90% for each biomass) of levoglucosan is collected in the first two fractions.

The significant differences in total levoglucosan produced are most likely due to ash content in the biomass. It has been shown in the literature that ach has a negative effect on the pyrolysis of cellulose into levoglucosan and other valuable organic molecules.[24] Analysis of the biomass has shown that both cornstover and switchgrass have significant amounts of ash. This ash has reduced the amount of levoglucosan that was produced from these two biomasses, as can be seen in Figure 41.

4.7.3 Acetic Acid

Acetic acid content was measured with a gas chromatograph-flame ionization detector (GC/FID). The bio-oil was "washed" with water to extract the water soluble compounds. The water mixtures were then analyzed on the GC/FID to determine the concentrations of the different water soluble compounds. Figure 42 presents the results for acetic acid. This chart also contains the standard deviations of the samples.

Figure 42 illustrates that the acetic acid content of the bio-oil differs depending on the fraction that was tested. The first two fractions (SF1 and SF2) consistently had the lowest concentration of acetic acid. Contrary to expectations, the fourth fraction (SF4) always contained the highest concentration of acetic acid. The overall goal of the system was to collect the vast majority of the acetic acid in the final fraction with the first four fractions having minimal acid content. Even though SF5 is meant to collect the majority of the acids present in the bio-oil, SF5 had lower concentrations than two of the other fractions. This can be attributed to the high volume of liquid collected and the large concentration of water present in this fraction.

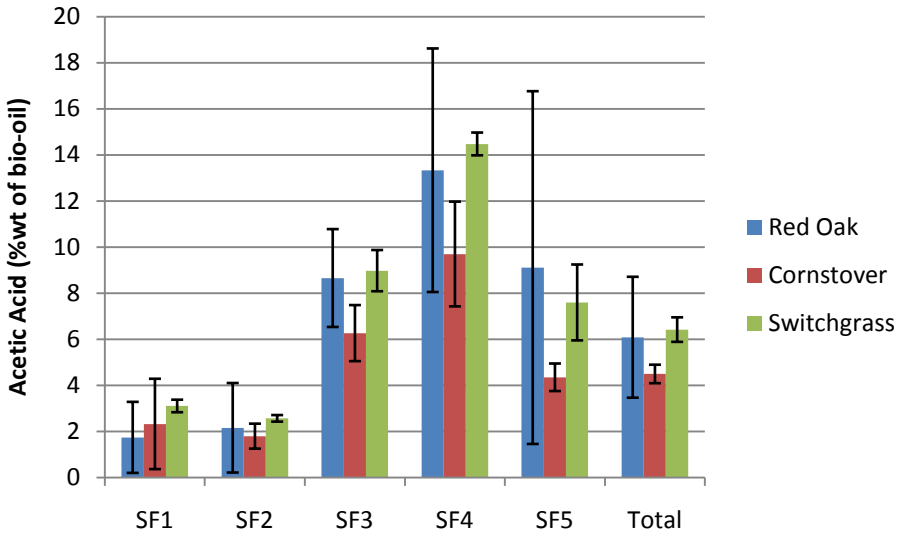

Figure 42 Acetic Acid Content of Bio-oil Fractions (Wet Basis)

Acetic acid concentrations have been reported in the literature between 2.5 and 4.7%.[22] SF1 and 2 both had acetic acid concentrations that are lower than the reported values. Otherwise, the other fractions all had higher acetic acid concentrations than the reported values. The mass averaged total also had a higher concentration. This indicates that secondary reactions are breaking larger molecules down into smaller compounds, which include acetic acid.

One possibility for the large concentration of acetic acid in stage fraction 4 could be that condensation occurred while the aerosols were collected. The presence of aerosols increases the surface area available for condensation. The extra residence time in the ESP could have allowed for the acetic acid to collect on the aerosols because of hydrogen bonding with other polar compounds. Acetic acid is hydrophilic which would allow it to bond to water. As was shown in Section 4.3 Moisture Content, SF4 had moisture contents that range from 14% to 25%.

Even though SF4 contains the largest concentration of acetic acid, it does not contain the highest amount. When the acetic acid content of each fraction is compared by

investigating the total amount produced, it is easy to see that the final fraction contains the highest total amount of acetic acid. Figure 43 compares the acetic acid content on a basis of grams of acetic acid per gram of total bio-oil collected. This graph shows that the final fraction of bio-oil has the highest total mass of acetic acid. For each of the biomasses tested, SF5 contained over 54% of the total acetic acid produced in the bio-oil because of the large volume of bio-oil collected in this fraction. This indicates that the bio-oil collection system has the capability to collect a majority of the acetic acid in a single fraction.

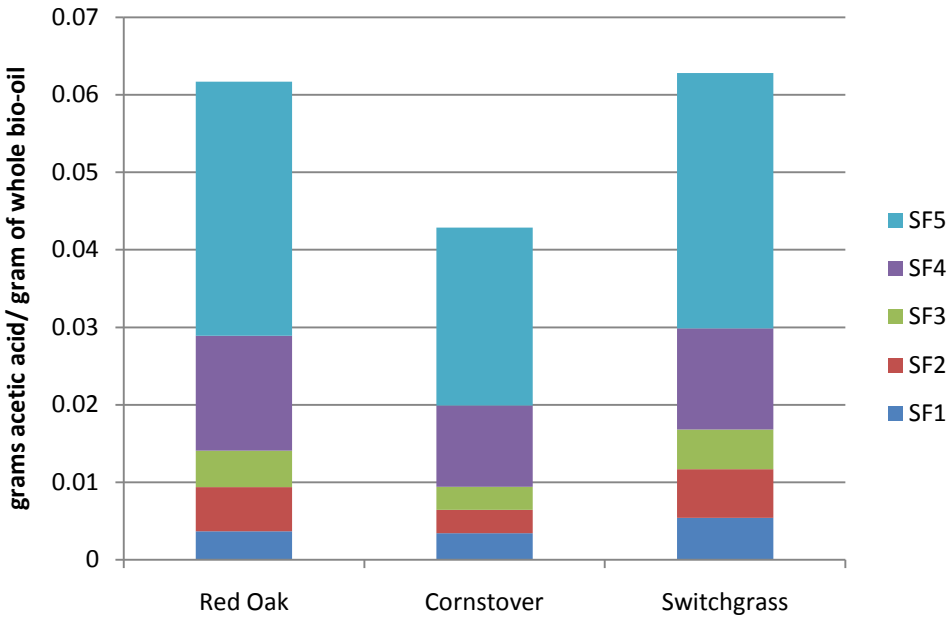

Figure 43 Mass Averaged Acetic Acid Content by Biomass (Dry Basis)

The uncertainty of acetic acid concentration can be partially attributed to the methods used to test for acetic acid. The test method includes a water extraction to collect all water soluble compounds. This process is based on vigorously mixing water and bio-oil. This action is performed with a group of equipment that includes vortex mixers and a sonicator. If the samples were not mixed exactly the same, there is a possibility that different degrees of extraction could be achieved. This could cause significant differences in acetic acid concentration.

4.7.4 Furans

The concentration of furans was determined with both the GC/MS and GC/FID. For this study, the compounds that are considered furans can be found in Section 3.4 Test Methods. Figure 44 illustrates the wt% of furans in each fraction as well as the mass averaged total concentration of furans in the bio-oil.

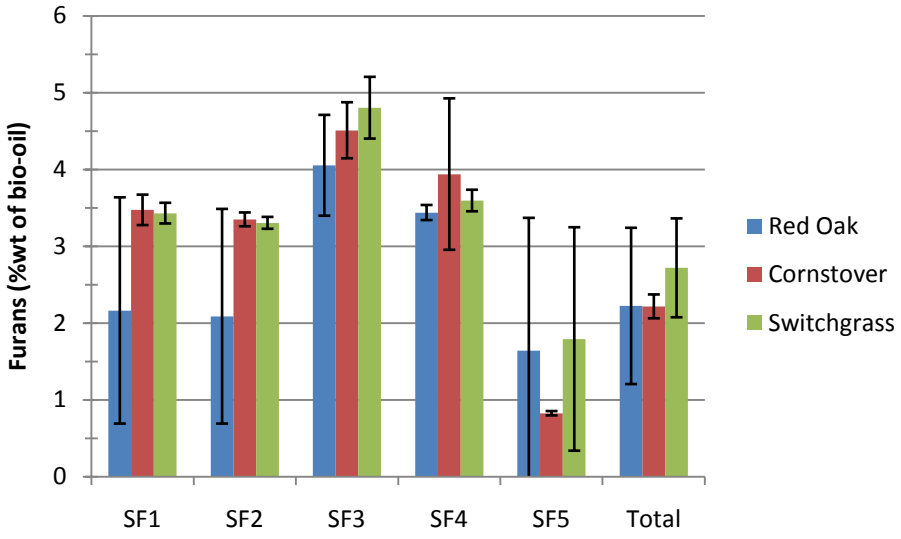

Figure 44 Concentration of Furans in Bio-oil Fractions (Wet Basis)

This graph illustrates that the highest concentration of furans can be found in the third fraction (SF3). The last fraction (SF5) of bio-oil consistently had the lowest concentration of furans. According to the analysis that was performed, furans condensed or were collected as both vapors and aerosols at many different temperatures. The compounds that are grouped under the description have a large range of boiling points and molecular weights.

Bio-oil has been reported to have furan concentrations between 1 and 1.5%. The fractions of bio-oil each have higher concentrations of furans that are higher than the reported furan content. This leads to an overall, mass averaged, furan content of over 2% for each of the biomasses.

Figure 45 presents the furan content on a gram of furans per gram of total collected bio-oil basis. This analysis helps to distinguish the total amount of furans that were produced from each biomass. This analysis can also provide insight into how much each fraction contributes to the total furan content. The analysis indicates that switchgrass produces the highest total amount of furans. The GC/MS analysis also illustrates that, even with the low concentrations of furans present in the last fraction (SF5), it still contributes to a large portion of the total furan content. The first two fractions, though, contain the highest overall amounts of furans. This could be attributed to the high boiling point of the larger furan compounds. This figure also illustrates that even though cornstover bio-oil contains a larger concentration of furans in many of the fractions, cornstover and red oak produced very similar total amounts of furans.

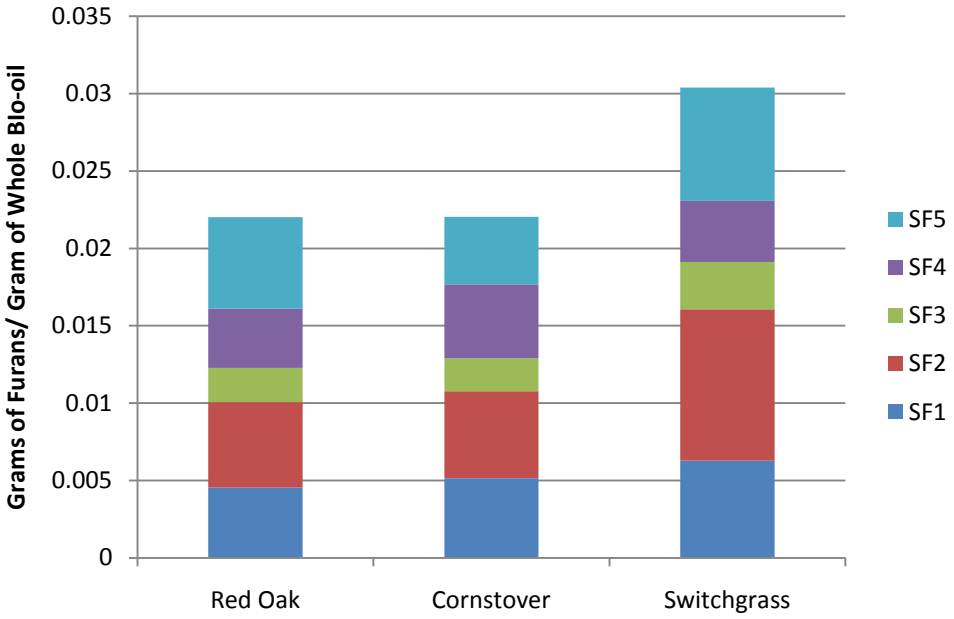

Figure 45 Mass Averaged Furan Content by Biomass (Dry Basis)

4.7.5 Phenols

The total concentration of phenolic compounds was determined using a gas chromatograph/mass spectrometer (GC/MS) according to the methods discussed in Section 3.4 Test Methods. Figure 46 denotes the overall concentration of phenolic compounds for each fraction of bio-oil.

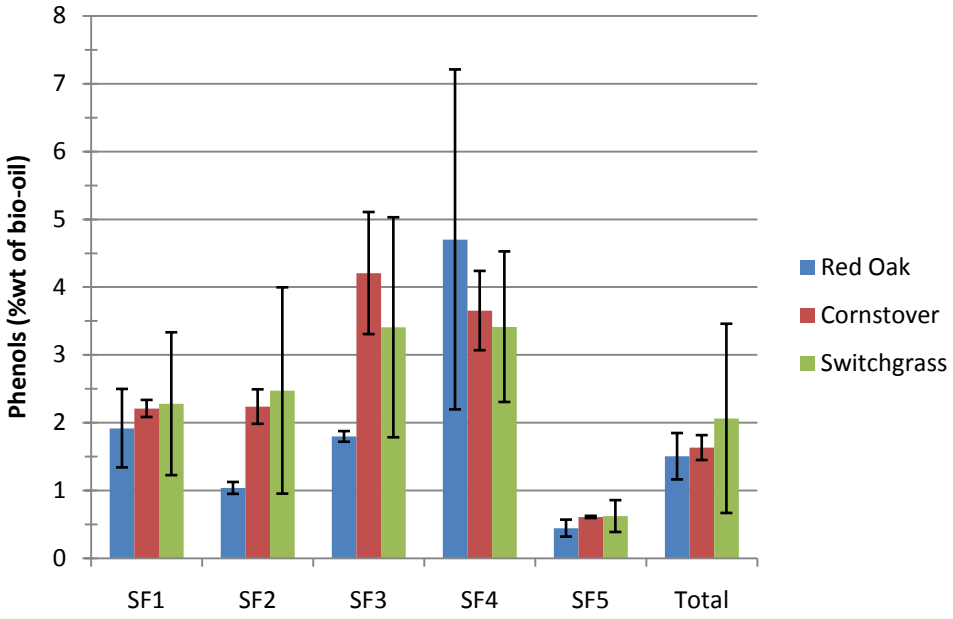

Figure 46 Phenolic Concentration in Bio-oil Fractions (Wet Basis)

Depending on the biomass, the highest concentration was found in different fractions. For red oak, the highest concentration was found in the fourth fraction (SF4). For cornstover and switchgrass though, the highest concentrations of phenolics could be found in the third and fourth fractions (SF 3 and 4). Branca et.al[22] report phenol concentrations between .4 and .8 % for whole bio-oil. The GC/MS analysis indicates that the fractionated bio-oil has a much higher concentration of phenols. Even SF5, which has the lowest concentration of phenolic compounds, has a similar concentration to the typical bio-oil.

The bio-collection system was designed to collect the majority of phenolics in the third fraction. The presence of phenolics in significant quantities in the first two fractions, though, can be explained. The system was designed using phenol as the model compound. Except for phenol, all of the compounds in the phenol group (Table 2) are substituted phenolics with boiling points higher than that of un-substituted phenol. Phenol is one of the extremes and not an average compound that could act as a true representative of the phenol group. Further improvements to the design of the bio-oil collection system will have to take into account the differences between the many types of phenols that are present in bio-oil.

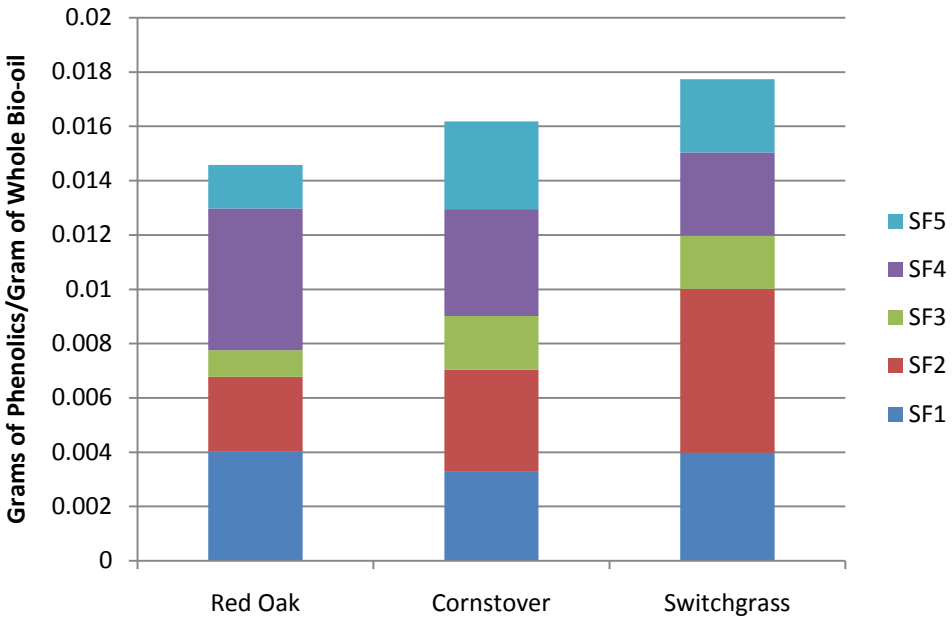

Figure 47 Mass Averaged Phenolic Content by Biomass (Dry Basis)

When comparing the phenolics in the bio-oil, it is beneficial to compare the amount produced on a gram of total bio-oil collected basis. Figure 47 contains this comparison. This figure illustrates that switchgrass produces the largest quantity of phenolic compounds. This figure also illustrates that nearly 60% of the total phenolics produced are found in the first three fractions. Based on this analysis, there does not appear to be

much difference between the total mass of phenolic compounds produced from the different biomasses.

4.7.6 Guaiacols

The analysis of the bio-oil to determine the amount of guaiacols present was completed with a gas chromatograph/mass spectrometer (GC/MS). This analysis provides insight into the structural differences for the lignin of different biomasses. Guaiacol, which is a substituted phenol with a methoxy group attached, is produced from lignin. Depending on the structure of the lignin and the substitutions occurring on the aromatic rings within the lignin, different amounts of phenols, guaiacols and syringols can be produced.

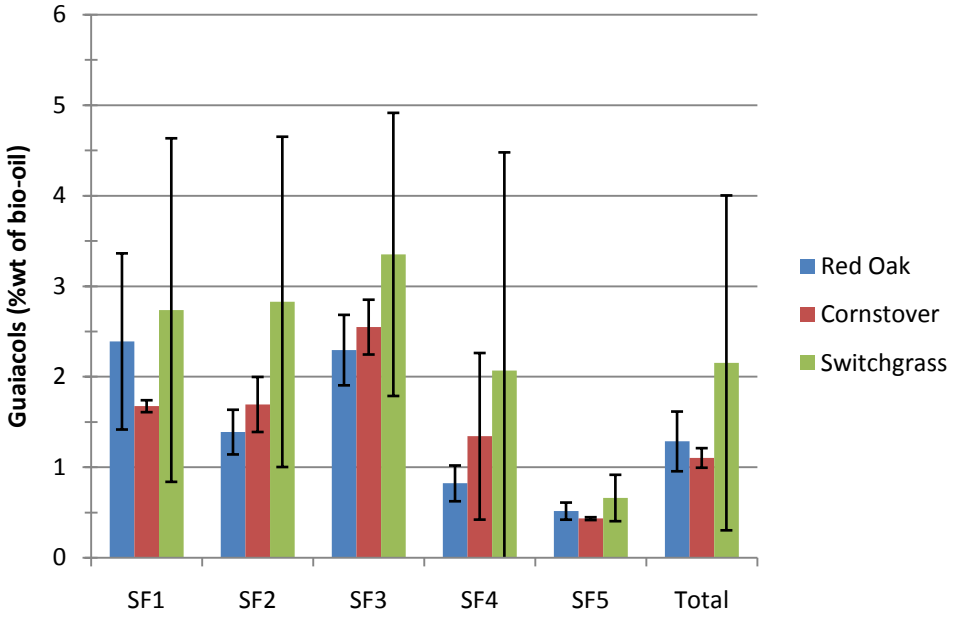

Figure 48 Concentration of Guaiacols in Bio-oil Fractions (Wet Basis)

Figure 48 illustrates the concentration of guaiacols within each fraction of bio-oil. An interesting occurrence is observed in the concentrations of guaiacols in the red oak bio-oil. The first and third fractions, both vapor condensers, each had higher concentrations

of guaiacols than the second fraction, an ESP. This indicates that a large portion of the guaiacols produced from red oak are exiting the reactor as vapors, rather than aerosols. Bio-oil has been reported to have between 3 and 6% guaiacols by weight.[22]

For both switchgrass and cornstover, Figure 48 illustrates that the largest concentration of guaiacols are collected in the third fraction. For all of the biomasses, the fourth and fifth fractions of bio-oil contained the lowest concentrations of guaiacols. The reported values, for whole bio-oil, are higher than the measured concentrations that were produced for this study. This could be due to the biomass used to determine the reported values. Guaiacols are produced from the lignin and the structure of the lignin dictates the percentage of guaiacols that can be produced. Differences in the pyrolysis of the lignin could affect the percentage of measured guaiacols as well.

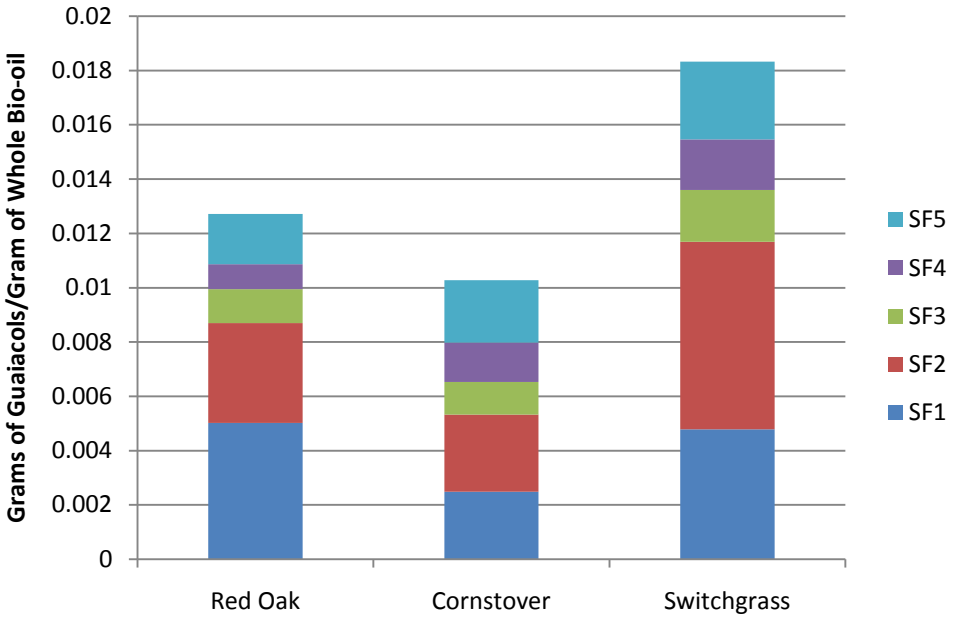

Figure 49 Mass Averaged Content of Guaiacols by Biomass (Dry Basis)

To determine which biomass produced the highest amount of guaiacols, the guaiacol content for each biomass was compared on a gram of guaiacols produced per gram of total bio-oil collected basis. The results of this analysis can be seen in Figure 49. This

figure clearly illustrates that switchgrass produced the largest amount of guaiacols. It also illustrates that the first two fractions of bio-oil contain the majority of the guaiacols. This occurs in red oak even though the second fraction had a lower concentration than the first and third fractions. This can occur because the third fraction produced significantly less bio-oil than the second fraction.

4.7.7 Syringols

Syringols, much like guaiacols, are indicators for lignin derivatives. Syringols are a substituted phenol with two methoxy groups attached to the aromatic ring rather than the single methoxy group found on guaiacols. The concentration of these compounds was determined through GC/MS analysis and the results are shown in Figure 50.

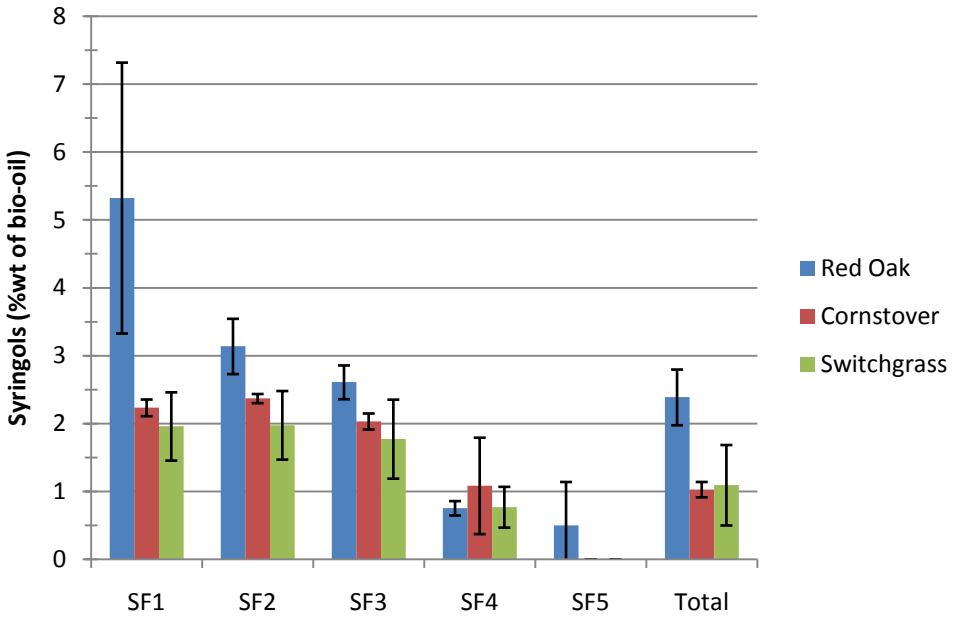

Figure 50 Concentration of Syringols in Bio-oil Fractions (Wet Basis)

This figure clearly illustrates that the first fraction from red oak had the highest concentration of syringols. From the results that were gathered for this study, red oak appeared to produce the largest concentrations in each of the fractions collected. This

indicates that hard wood lignin contains a larger percentage of aromatic rings with two methoxy groups when compared to cornstover or switchgrass. The general trend for syringol collection was similar to that of other compounds. As the collection temperature decreased, the amount of syringols collected also decreased. Branca et al.[22] report syringol concentrations between .3 and 2%. Much like phenol and guaiacol, the difference between reported values and the measured values could be a matter of biomass or pyrolysis conditions.

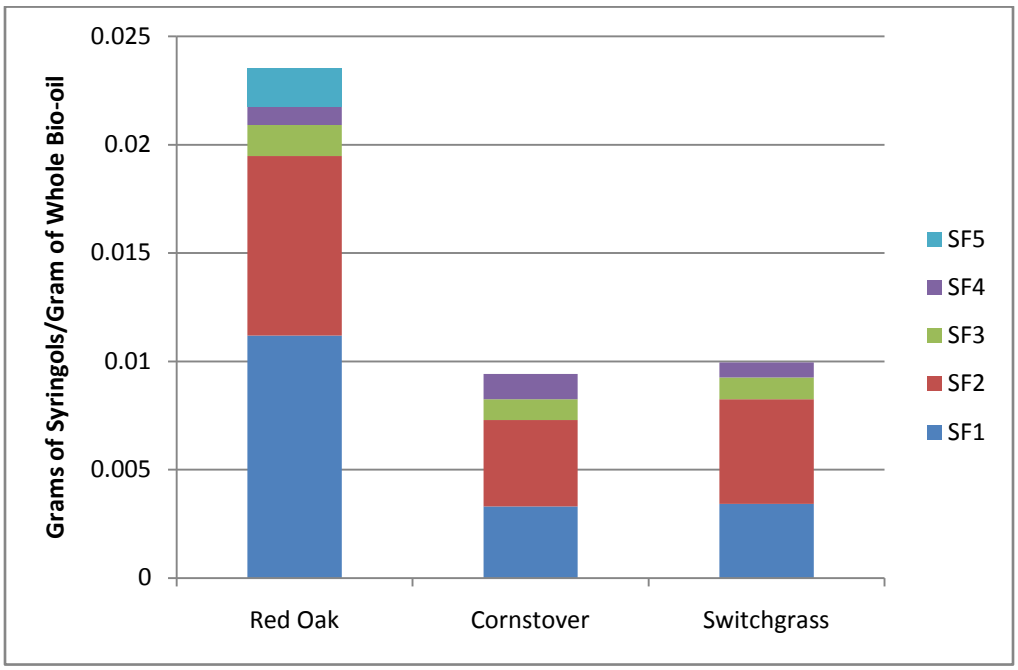

Figure 51 Mass Averaged Content of Syringols by Biomass (Dry Basis)

To compare the total amounts of syringols produced, the syringol content from each biomass was evaluated. The results from this evaluation are shown in Figure 51. This figure clearly illustrates that red oak produces the largest amount of syringols when compared to switchgrass and cornstover. It has been shown in literature that different biomasses have unique lignin structures.[22, 51] These unique lignin structures can lead to distinct distributions of phenolic compounds like syringols. This figure also illustrates that almost all of the syringols are collected in the first and second fractions. Syringols, which are highly substituted, have high boiling points which allow them to be collected

in the first two fractions. These two fractions contained over 77% of the syringols for each biomass that was reacted.

4.8 Water Insoluble Content

The quantification of the water insoluble compounds that are found in bio-oil can be an indication of many different attributes that affect bio-oil quality. A majority of water insoluble compounds are products of the lignin that can be found in the original biomass. These compounds in the bio-oil are referred to as pyrolytic lignin. Most water insoluble compounds are also very large in molecular weight and structure. The largest compounds were found in the first condenser and in the ESPs. Oasmaa et al. report water insoluble content between 15 and 20%.[52]

When comparing the fractions of bio-oil in Figure 52, it can be seen that SF 1 and 2 both have high percentages of water insoluble material. The first fraction had the highest percentage of water insoluble components for both cornstover (69.6%) and switchgrass (61.1%). For red oak, the average percentage of water insoluble material was higher in the second fraction (50.2%) when compared to all other fractions of red oak bio-oil. These values are well over other reported water insoluble contents that can be found in the literature. SF 3, 4 and 5 each had significantly lower percentages of water insoluble content. SF 2 and 3 had water insoluble contents that were in the range of typical bio-oil. SF 1 was designed to collect high molecular weight compounds that are in the vapor phase, while SF 2 was designed to collect the compounds that are in the liquid aerosol phase. These liquid aerosols are naturally large molecular weight compounds.

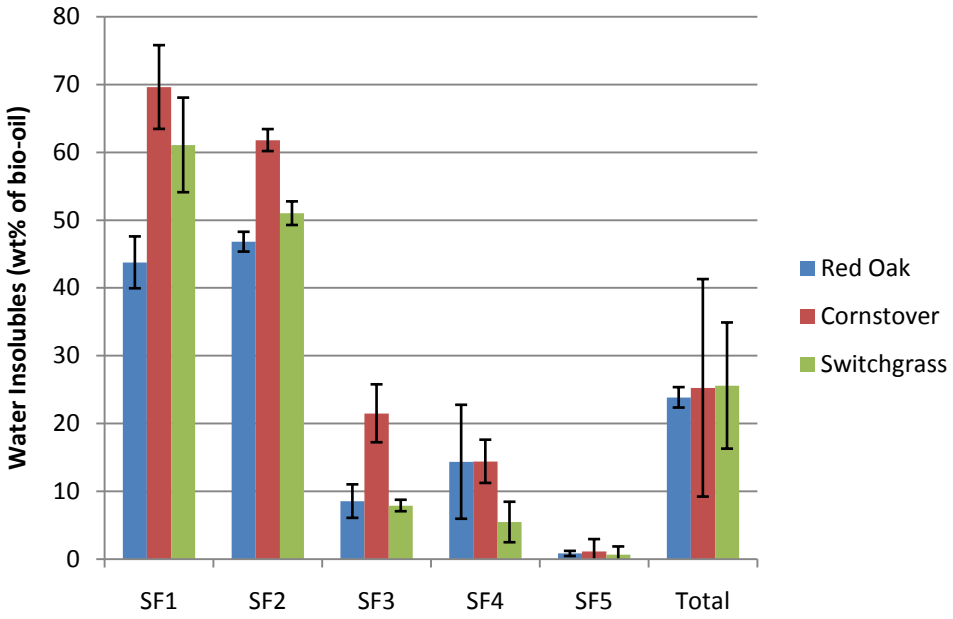

Figure 52 Water Insolubles Concentration of Bio-oil Fractions (Wet Basis)

Mohan states that oligomeric species of bio-oil, which are lignin derivatives, are "blown apart" during the rapid vaporization of water in the biomass particles[9] to generate aerosols. Similarly, Ba et al. states that the water insoluble portion of bio-oil consists of lignin derived compounds.[34] Aerosol collection in the second fraction has led to high percentages of water insoluble material in this fraction. These water insolubles are presumed to be lignin derived oligomeric aerosols. The large oligomeric aerosols have high molecular weights and high boiling points allowing them to exist in the liquid phase even in high temperature environments. High water insoluble contents in the first condenser (SF1) are due to either the vaporization of a portion of the aerosols into the vapor phase or the impaction of aerosols on the walls of the first condenser. While vaporization of these compounds is possible, it is more likely that aerosols were collected in this fraction with the desired vapors. There are a number of mechanisms that could be cause of the collection of aerosol droplets in this condenser. The aerosols could have impacted on the condenser walls through either vigorous mixing or thermophoretic forces. Even though the condenser was designed as a laminar flow condenser, there could have been a disturbance in the flow that forced it to become turbulent, thus causing

the aerosol droplets to impact the wall. This disturbance could be anything from the transition from the pipe to the tubes to a build-up of bio-oil on the condenser tube walls. Either of these causes are likely to have caused turbulent flow through this condenser. Another likely possibility is that the assumptions for flow properties were not correct based on the assumed mixture of compounds in the flow. Thermophoretic forces are caused temperature differences between a solid and a fluid. The forces draw particles from the warm fluid to a cooler surface. In the case of the first condenser, the hot gases could be affected by the cooler surface on the condenser tube walls. More than likely, the aerosols were forced to the walls by turbulent flow in the condenser tubes.

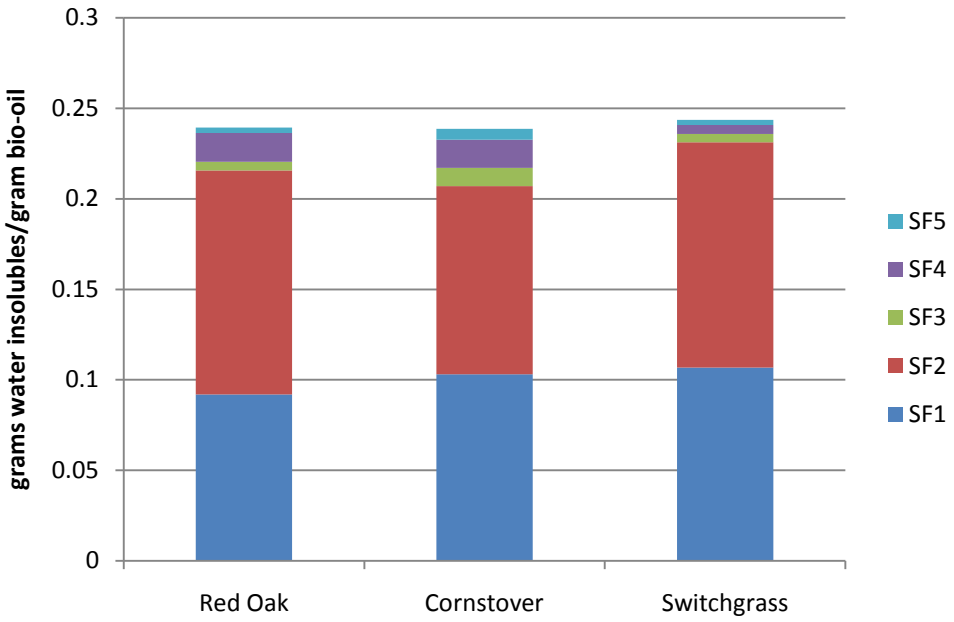

Figure 53 Water Insolubles by Biomass (Dry Basis)

To compare the different biomasses, the water insolubles were averaged by the mass of bio-oil collected which can then be translated into grams of water insoluble components per gram of bio-oil collected in the bio-oil collection system. The results can be seen in Figure 53. This chart illustrates that red oak produced the largest total amount of water insoluble content while cornstover and switchgrass produced slightly less. The water

insoluble content differences are consistent with the typical lignin contents of the selected biomases. It also can illustrate the fact that the vast majority of water insoluble components, which are found in the bio-oil, are found in the first two fractions. The other three fractions contain less than 25% of the total water insoluble components.

The total mass of water insoluble components found in the bio-oil from individual biomasses was found to be analogous to the amount of lignin that was in each biomass. Red oak, which had 20% lignin by weight, produced the highest amount of water insoluble components (0.14 grams of water insoluble components per gram of biomass). Cornstover and switchgrass, which typically contain 19% and 18% lignin by weight respectively, produced similar amounts of water insoluble components (.1340 and .1309 grams of water insoluble components per gram of biomass comparatively). According to this analysis and the assumption that all of the water insoluble components are derived from lignin, each of the biomass produced the water insoluble components in the same ratios. This can be seen in Table 9. The rest of the lignin contributes the phenols, guaiacols and syringols as well as other organic compounds.

Table 9 Comparison of Water Insolubles and Lignin

	Red Oak	Cornstover	Switchgrass
% of water insolubles from biomass	14.05	13.40	13.09
% wt of lignin	20	19	18
Grams water insolubles/gram of lignin	0.70	0.71	0.73

4.9 Solids Content

The solids content of the bio-oil was determined by following the procedures discussed earlier in the methods section, Section 3.4.3 Bio-oil Analysis. The results from this

analysis are shown in Figure 54. This figure illustrates the difference in solids content in each of the fractions of bio-oil produced from the three selected biomasses.

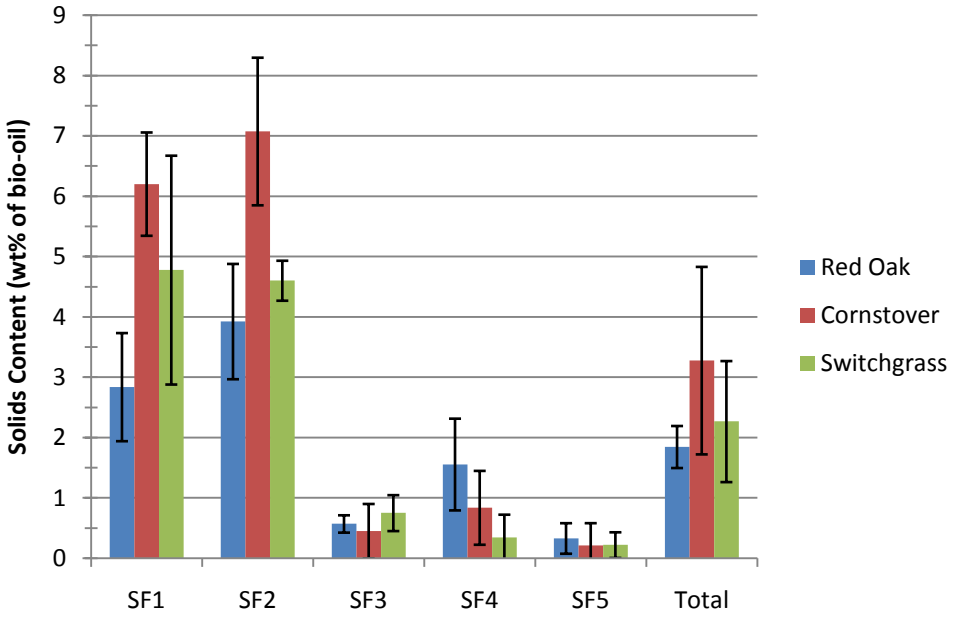

Figure 54 Solids Content in Bio-oil Fractions (Wet Basis)

The calculated solids content indicates that the first two fractions of bio-oil contained the highest percentage of solids. Each of the final three fractions (SF 3,4,5) contained significantly less solid particulate when compared to the first two fractions (SF1 and SF2). Based on the solids content of each fraction, there does not appear to be any noticeable trends in solids content. Bridgwater reports that typical bio-oil contains around 0.2% solids but 3% is also encountered often as well.[2, 38] The bio-oil that was produced for this study contained more solids than typical bio-oil, but this was due to inefficient solids removal.

Further investigation of the solids content of each fraction indicates that there was a substantial amount of solids collected in SF1. This fraction, which was theoretically operated in a laminar flow regime, should not have collected many solids. There are multiple mechanism that could be the cause of this collection. The most obvious would

be that the condenser was in fact not operating in a laminar flow regime, thus causing vigorous mixing at the cooling surface. This mixing would allow solids and aerosols to be collected at the wall through impaction. Secondly, the residue that was collected as solids could be condensed organic residues that were too large to pass through the filters that were used for the analysis. Finally, the solids could have been forced to the condenser wall through thermophoretic forces caused by the heat gradient that exists between the hot vapors and the cool condenser wall. This temperature gradient could have been large enough to cause both solids and aerosols to travel towards the walls allowing them to be collected. The full explanation of the high solids content of SF1 is more than likely a combination of the three reasons. There was a large temperature gradient present within the condenser tubes and any disruption in the flow through the condenser tubes could have cause the boundary layer in the flow to become turbulent.

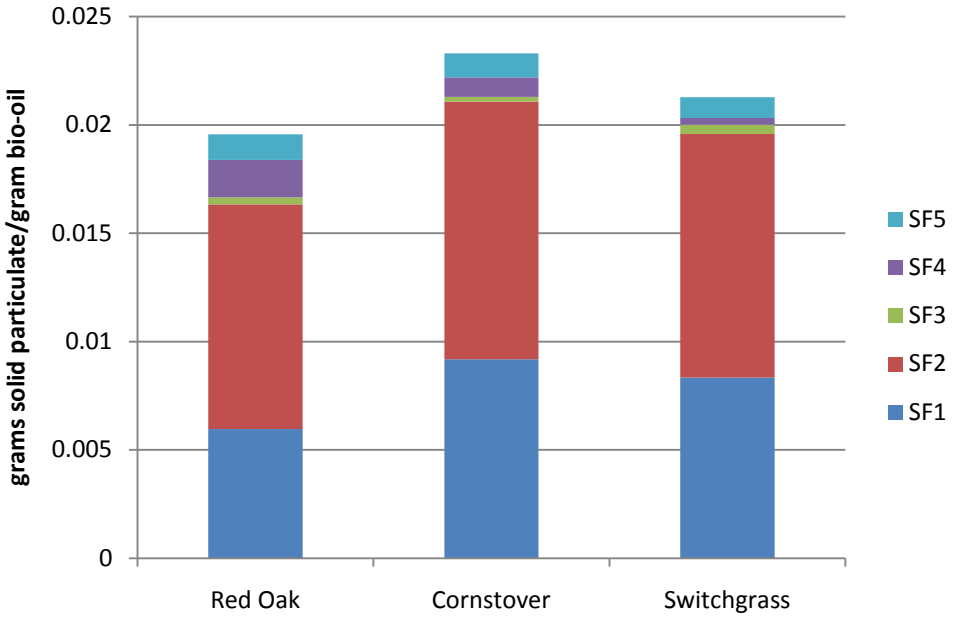

Figure 55 Solids Content by Biomass (Dry Basis)

To further analyze the amount of solids content that was found in the bio-oil, the total percentage of solid particulate collected in the bio-oil. This analysis is shown in Figure

55. This figure illustrates the fact that the vast majority of solid particulate is collected in the first two fractions of bio-oil (SF1 and SF2). This analysis also shows that cornstover produced the largest amount of solid particulate in the bio-oil. In the same manner, the figure denotes that switchgrass and red oak produced similar amounts of solid particulate on a dry biomass basis.

Due to the fact that the different biomasses produced different amounts of char, a comparison of the particulate efficiency would provide more insight into the operation of the fast pyrolysis system. Table 10 shows that the efficiency of the gas cyclones ranged between 95.3% and 96.3%. This table shows how much of the solids produced from each biomass were collected in both the bio-oil and the cyclones. By comparing the amount collected in the cyclones to the total amount of solids produced, collection efficiency was determined. Red oak, which had the highest solids content in the bio-oil, had the lowest cyclone efficiency. As expected, switchgrass, which had the lowest solids content, had the highest cyclone efficiency.

Table 10 Cyclone Efficiency

	Red Oak	Cornstover	Switchgrass
Solids in Bio-oil (wt% of Biomass)	1.11%	1.15%	1.01%
Char Collected in Cyclones (% of Biomass)	22.28%	28.77%	26.17%
Percentage Total Solids Produced in Bio-oil	4.73%	3.84%	3.71%
Cyclone Efficiency	95.27%	96.16%	96.29%

4.10 Viscosity

Viscosity measurements were conducted at two different temperatures. These temperatures were dependant on the stage fraction. For the first two stage fractions (SF1 and SF2), the viscosity was measured at 60^{o}C in accordance to ASTM D2170.[47] This standard provides the method of measuring the kinematic viscosity of asphalts. The other

three fractions (SF3, SF4 and SF5) were each analyzed at 40°C in accordance to ASTM D445.[45]

The kinematic viscosity for the first two fractions of bio-oil is shown in Figure 56. These viscosities were measured at 60°C in accordance with ASTM standard D2170. This standard is commonly used to determine the viscosity of liquid asphalts. This method was used because of the increased viscosity of the first two fractions of bio-oil.

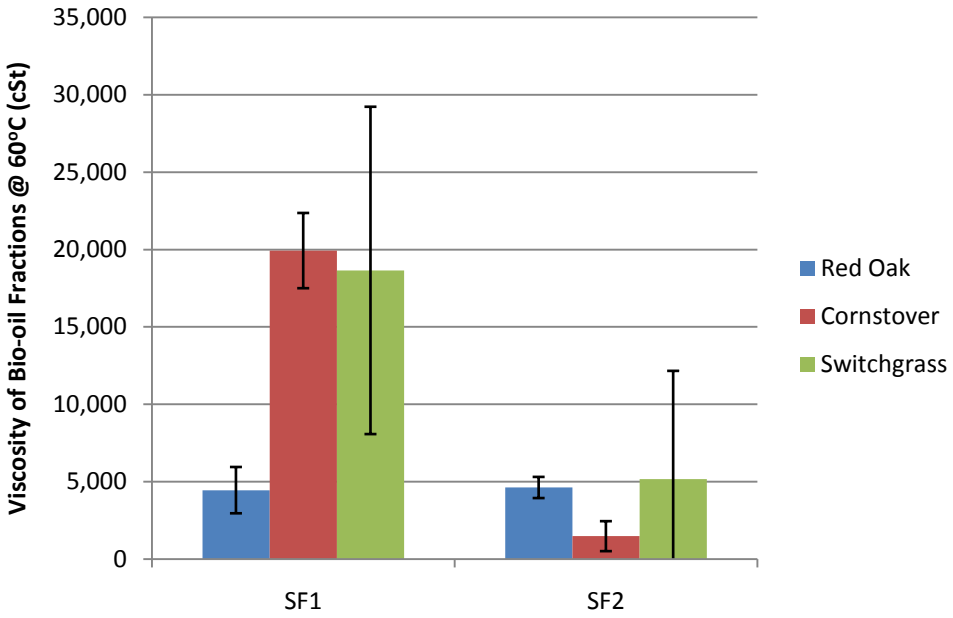

Figure 56 Kinematic Viscosity of Bio-oil Fractions Measured @ 60°C (ASTM D2170)

The data indicates that for cornstover and switchgrass, the first fraction of bio-oil (SF1) had a significantly higher viscosity when compared to the second fraction (SF2). The viscosities of the first two fractions are similar in magnitude. The switchgrass bio-oil had the largest standard deviation indicating that the viscosity was not consistent from test to test. This is illustrated through the error bars shown in Figure 56. These error bars are based on the standard deviation between the three tests that were performed on switchgrass. Once again, switchgrass had large variances in water insoluble content in

the first two fractions of bio-oil. This can be seen in Figure 52. This large variance could be a factor in the large variance seen in the viscosity of these bio-oil fractions.

The average kinematic viscosities for the final three fractions are shown in Figure 57. The graph illustrates the varying viscosities that can be found in the different fractions. The viscosity of these three fractions is heavily dependent on the moisture content of the bio-oil. The kinematic viscosity of the final fraction of bio-oil (SF5) was consistently measured around 1 cSt. This fraction consisted of more than 60% water, which has a viscosity of 0.658 cSt at 40°C. SF 3 and 4 had a large amount of variance. This variance could be associated with the biomass and the constituents that were collected, as well as the moisture content. The large variance could be due to the variance that is found in the water insoluble content. Water insolubles, which are large molecules, could have a significant effect on the viscosity of the bio-oil.

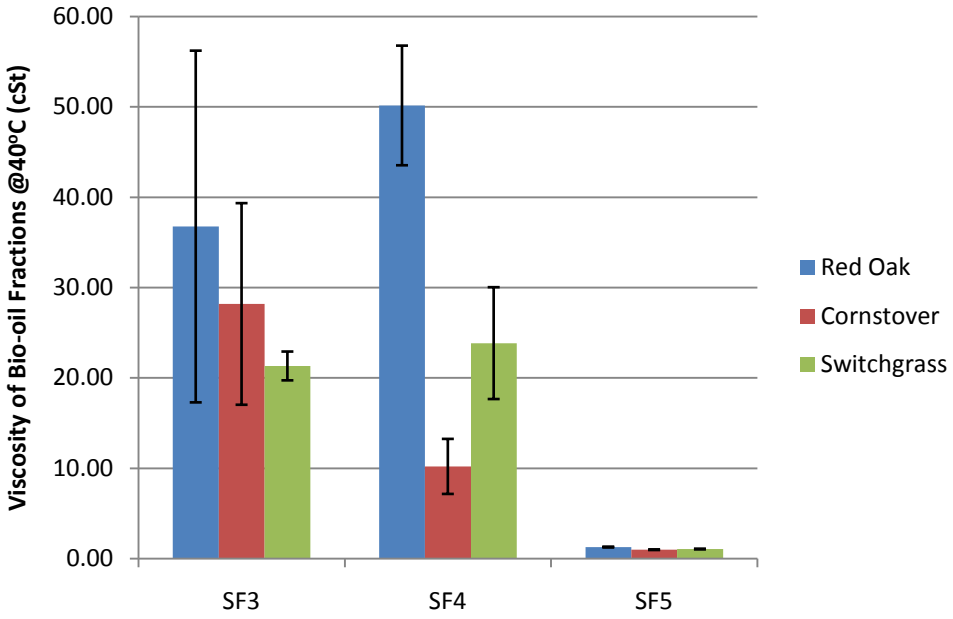

Figure 57 Kinematic Viscosity of Bio-oil Fractions Measured @ 40°C (ASTM D445)

4.11 Discussion of Differences Between Whole Bio-oil and Fractionated Bio-oil

The comparison of whole bio-oil to fractionated bio-oil has revealed many differences between the two. These comparisons have been presented throughout Chapter 4. This section will include discussion into a comparison of the overall fractions and the mass averaged whole bio-oil that was presented before. Figure 58 illustrates the breakdown of the bio-oil produced from red oak. In the same manner, Figure 59 presents the breakdown of the bio-oil produced from cornstover and Figure 60 presents the breakdown of the bio-oil produced from switchgrass.

There are many properties that are improved through fractionation. One of the properties that have seen the most improvement is the moisture content of the fractionated bio-oil. Other than the last fraction from each biomass, all of the fractions have significantly less moisture than the whole bio-oil. This reduction in moisture content can be attributed to the elevated temperatures on the cooling surfaces that are found within the bio-oil collection system. These elevated temperatures have the ability to slow down and even prevent the condensation of water. This has led to higher energy contents and larger concentrations of valuable compounds. One of the drawbacks to the lower moisture contents would be the increased viscosity of the bio-oil. The first two fractions of bio-oil from each biomass are considered semi-solids that become flowable when reheated to above 60^{o}C. The increase in viscosity will lead to problems with materials handling (mainly associated with pumping). This can be overcome, though, by working with these fractions while they are warm.

Another property that has seen significant improvement is the water insoluble content. This property is a measure of the oligomer content in each fraction. These oligomers are mainly lignin derivatives and have large molecular weights. Many hope that these oligomers can act as building blocks for other chemical processes.[53] The whole bio-oil for each biomass contains less than 30% water insoluble content. This compares to the

first and second fractions of the bio-oil that each can contain over 60% water insoluble content depending on the biomass.

One main drawback to water insoluble content, which contains large molecular weight compounds, is found when a distillation is performed on the bio-oil. The larger compounds that are considered the water insolubles can polymerize when heated to moderate temperatures or even coke when heated to extreme temperatures. This creates difficulties when attempting to separate the lighter compounds from the bio-oil. The final fraction of bio-oil for each biomass contains less than 1% water insoluble content. This would allow for simple distillation to be attempted without any problems occurring with sludge (polymerization) due to the lack of non-volatile material.[54]

Two of the compounds that were used as model compounds for the design include acetic acid and levoglucosan. The levoglucosan represents anhydrosugars, which are direct products of the pyrolysis of cellulose. It was hypothesized that this compound could be collected entirely in the first fraction. This hypothesis was made with the assumption that the levoglucosan exited the reactor as a vapor. According to the results, a significant majority of the levoglucosan was collected in the first two fractions (SF1 and SF2). The fact that there was levoglucosan found in the second fraction indicates that the levoglucosan exited the reactor as both a vapor and an aerosol. Based on where the levoglucosan was collected, the fractionated bio-oil collection system was capable of collecting levoglucosan in the early fractions.

Acetic acid is produced from each of the main components in biomass with the majority being formed from hemicelluloses.[9, 22, 24] According to the graph shown in Figure 17, the dew point of acetic acid is below 0^{o}C, yet acetic acid is still detected in each fraction. Only the first and second fractions contained a lower concentration than the whole bio-oil. The presence of acetic acid in bio-oil fractions that theoretically should not contain acetic acid has a couple possible explanations. First, acetic acid is considered hydrophilic. This indicates that acetic acid can “bond” with or dissolve in water and

other polar compounds. This would allow acetic acid, which is present in the vapor phase, to attach to polar compounds through hydrogen bonding. When the bio-oil is then mixed in water, the acetic acid would be attracted more to the water than the other compound, thus releasing it into the water to be analyzed. Another plausible explanation considers the fact that there are likely carboxyl groups that are attached to larger compounds. These larger compounds include phenols and other compounds that have been produced from lignin. When these large compounds, are mixed with the warm water that was utilized to extract the water soluble compounds, the carboxyl groups could be extracted from the bio-oil. This removal of carboxyl groups could result in a false reading of acetic acid from the GC/FID.

One aspect of the bio-oil that is hampered by the fractionation is the solids. The overall bio-oil contained normal amounts of solids, but due to the nature of the bio-oil collection system, the solids content was concentrated into the first two fractions. The ESP fraction (SF2) typically had a larger percentage due to the fact that the solids are collected through the electrostatic forces present in the ESP. The higher solids content can lead to instabilities and problems with combustion and filtration.[38] The other fractions have much lower solids content when compared to the overall solids content of the whole bio-oil.

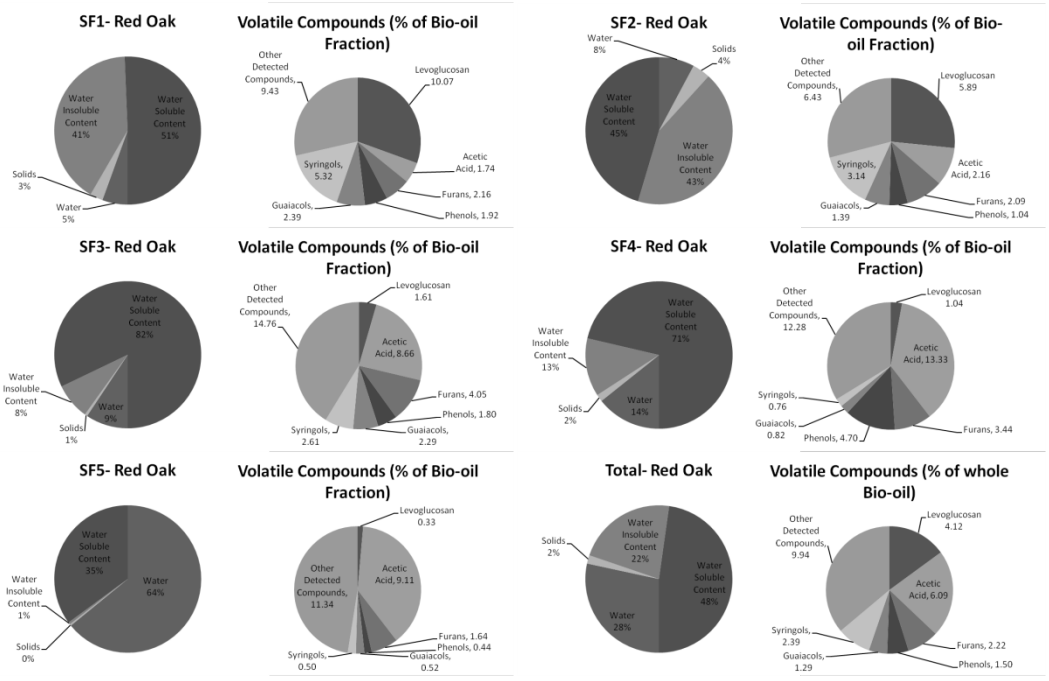

Figure 58 Red Oak Bio-oil Oil Comparison

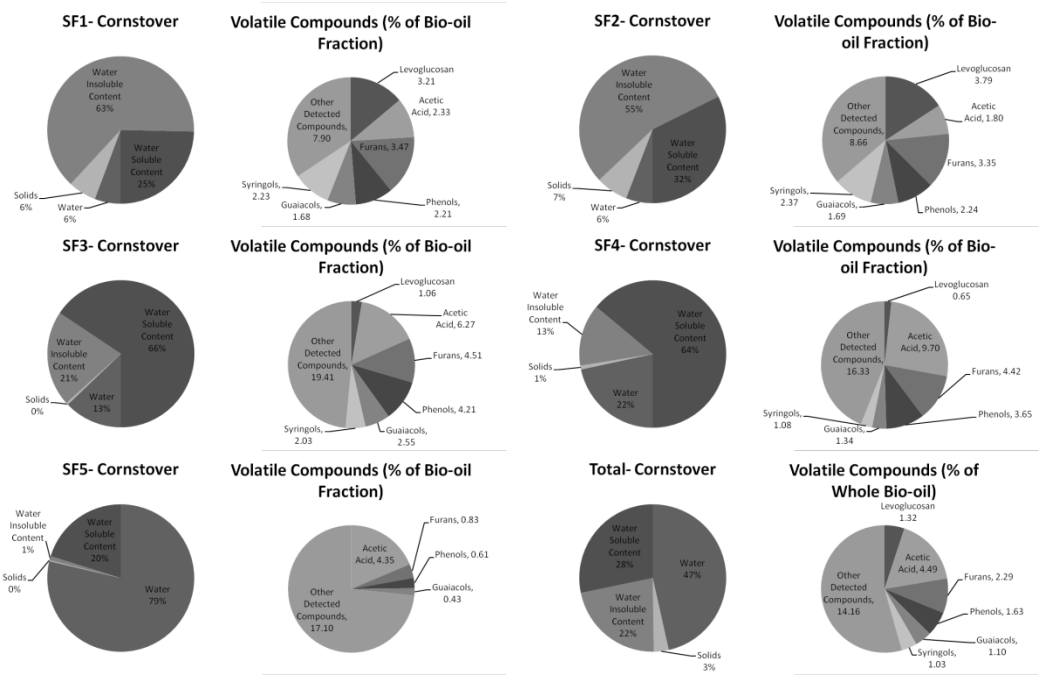

Figure 59 Cornstover Bio-oil Comparison

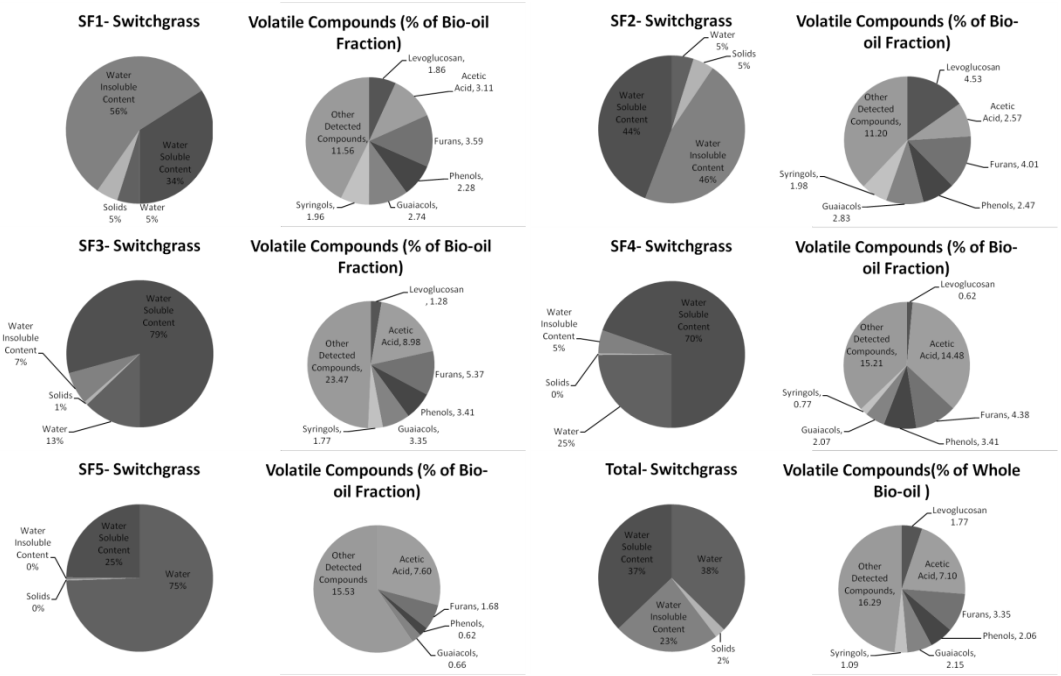

Figure 60 Switch Grass Bio-oil Comparison

4.12 MAN vs. Acetic Acid Concentration

The modified acid number is a measurement of the number of acidic compounds found within a sample of bio-oil. This value is encompassing of all carboxylic acids as well as mineral acids. These acids include acetic acid, formic acid and phenolic compounds with acidic tendencies. A comparison of the acetic acid concentration and modified acid number yielded a linear relationship. This relationship can be seen in Figure 61. This linear relationship demonstrates that the modified acid number is strongly related to the acetic acid content. It is also assumed that there are other acids present in the bio-oil even though acetic acid was the only acid quantified. Through further analysis and more testing, it could be determined that the acetic acid concentration could be approximated through the modified acid number titration rather than processing the water soluble portion of the bio-oil on the GC/FID. This relation could be used to quickly test the bio-oil for acetic acid.

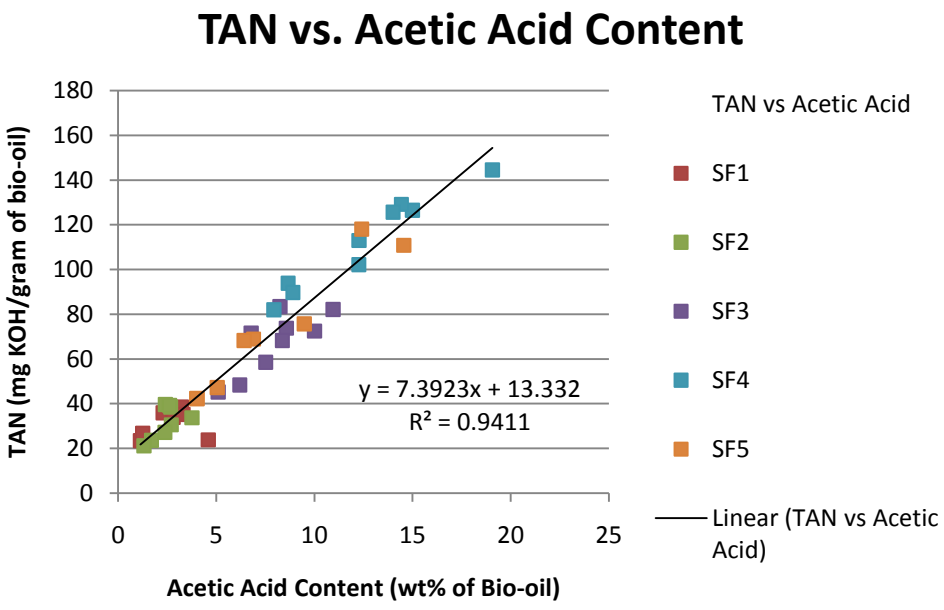

Figure 61 MAN vs. Acetic Acid of Fractionate Bio-oil (Wet Basis)

To determine how much of the modified acid number can be attributed to the acetic acid found in the bio-oil, a predicted modified acid number was based on only the acetic acid concentrations. The titration that is performed for MAN occurs on a 1:1 molar basis between KOH and carboxylic acid compounds. Equation 16 gives the equation that was used to determine the theoretical MAN. The concentration of acetic acid is transformed first into a partial molar ratio of moles of acetic acid per gram of bio-oil. The number of moles of acetic acid is equal to the number of moles of KOH that is required to neutralize the acid. The resultant partial molar concentration was then transformed into mg KOH/gram of bio-oil. The resultant value is the theoretical MAN due to acetic acid.

$$Predicted\ TAN = \frac{X\ gm\ Acetic\ Acid}{100\ gm\ Bio-oil} \times \frac{1 mole\ Acetic\ Acid}{50.05\ gm\ Acetic\ Acid} \times \frac{1\ mole\ KOH}{1\ mole\ Acetic\ Acid} \times \frac{56.1065\ gm\ KOH}{1\ mole\ KOH} \times \frac{1000\ mg\ KOH}{1\ gm\ KOH}$$

Equation 16

To compare the predicted MAN to the measured MAN, Figure 62, Figure 63 and Figure 64 were created. These figures illustrate the differences between the MANs for the individual fractions for each of the selected biomasses. The purpose of these three graphs is to illustrate the differences between not only the two MANs but also to illustrate the varying magnitudes of differences between the measured MAN and the predicted MAN.

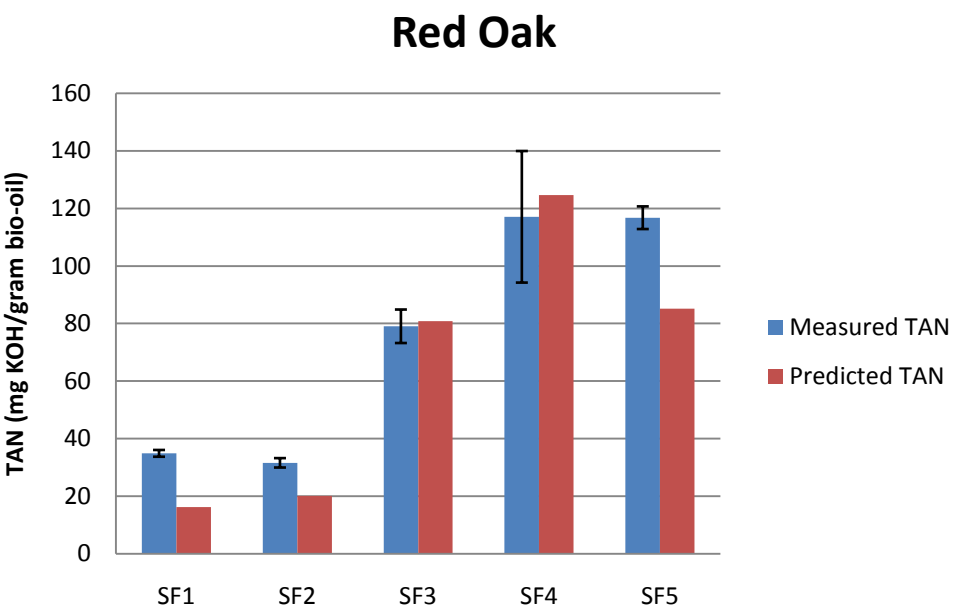

Figure 62 Red Oak Comparison of MAN (Wet Basis)

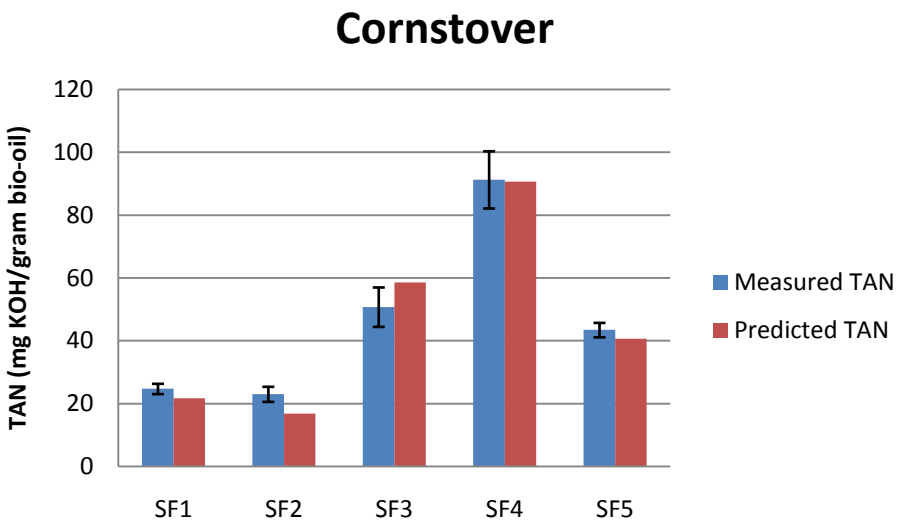

Figure 63 Cornstover Comparison of MAN (Wet Basis)

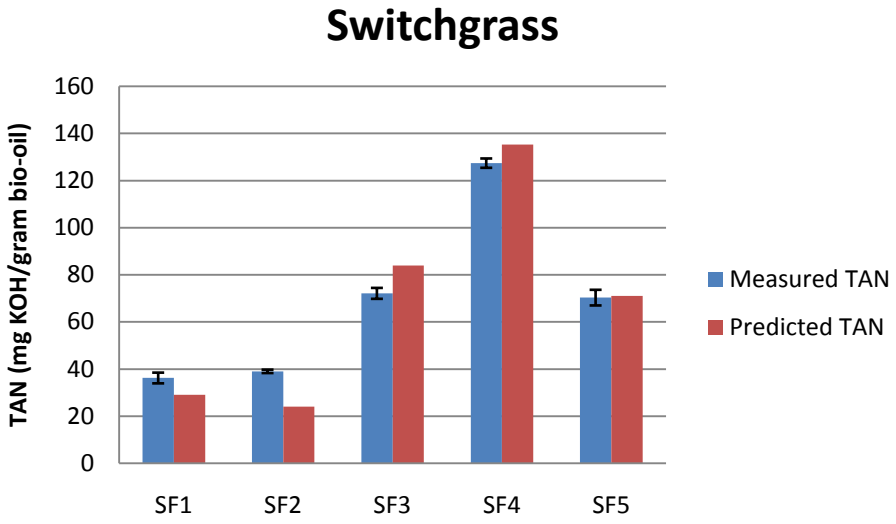

Figure 64 Switchgrass Comparison of MAN (Wet Basis)

For the first two fractions of bio-oil (SF1 and SF2), the measured MAN was consistently higher than the predicted MAN. This indicates that there are other acids present in these fractions that contribute to the MAN. This occurrence has been discussed before and it has been suggested that the presence of certain substituted phenolic compounds could result in an increased MAN.

A completely different situation was encountered for the final three fractions of bio-oil. These fractions had more variability and even included some fractions that had predicted MANs that were higher than the measured MAN. The higher predicted MAN could be a result of improper mixing of the samples or the uncertainty associated with the water extraction process that was used to determine the acetic acid content. The results for these three fractions suggest, though, that the majority of the acids that contribute to the MAN are acetic acid. The lack of other high molecular weight acids enables the MAN to become a pseudo measurement of acetic acid content.

This analysis works to enforce two different but equally important concepts. First, that both low molecular weight carboxylic acids and high molecular weight compounds

contribute to the modified acid number. The modified acid number is simplistically a count of the total number of moles of acid present in the bio-oil. Based on the acetic acid concentrations and the total number of moles of acetic acid produced, it is apparent that there are other acids that contribute to the MAN. Based on the fractions that have the highest percentage MAN that is not from acetic acid, it is assumed that one of the other acids that effects the MAN is large molecular weight phenolics that contain carbonxyl groups.

Secondly, in the last three fractions of bio-oil, the modified acid number perfectly correlates to the acetic acid concentration. In fact, based on the analysis shown above, the majority of the MAN is due to the acetic acid concentration in these three fractions. This analysis sheds light on the presence and type of acids that are present in the bio-oil. It also shows that the acetic acid and MAN are linearly related.

CHAPTER 5. SUMMARY AND CONCLUSIONS

From the analysis of the fractionated bio-oil, it is apparent that the fractionation of bio-oil can be achieved through the separation of vapors and aerosols to produce distinct fractions of bio-oil. This separation can be achieved through the selection of distinct operating conditions that dictate which compounds are collected. The practice of using "warm" heat transfer surfaces provides the ability to selectively condense bio-oil vapors. This process occurs because bio-oil is a complex combination of organic compounds that include anhydrosugars, phenolics, lignin derivatives, furans, alcohols, acids, water and many other organic compounds. Each of these groups of compounds has distinct properties; most importantly, boiling point and vapor pressure. The differences in boiling points allow the bio-oil to be condensed in many distinct fractions. By collecting the bio-oil vapors at different temperatures, the majority of the water and acetic acid can be collected in the final fraction (SF5), which was one of the main goals of this research.

The presence of aerosols in the product stream allows for the collection of an aerosol fraction that has distinct properties. This fraction (SF2) was collected in an isothermal ESP that actively collected the aerosols while the gas stream was still at an elevated temperature. This method prevented the collection of large amounts of water and acids in this fraction. These aerosols contained large concentrations of water insoluble content and other high molecular weight compounds. It is believed that these water insoluble compounds and oligomers are derivatives of lignin.

Higher Heating Value and Moisture Content

One of the bio-oil properties that were greatly improved with the fractionation process was the higher heating value (energy content) of the bio-oil fractions. Average bio-oil has an energy content of approximately 17 MJ/kg.[38] Meanwhile, the fractions of bio-oil that were produced through this bio-oil collection system had energy contents that ranged from 27.4 MJ/kg down to 4.1 MJ/kg. The higher heating value of the bio-oil was largely dependent on the fraction in which the bio-oil was collected and the original biomass.

The final fraction contained the lowest energy content, while the first three fractions where consistently over 20 MJ/kg. The energy content found in the final fraction of bio-oil can be attributed to the acids and other light hydrocarbons that are found in that fraction. If the first four fractions of bio-oil were to be combined to produce a "moisture free" bio-oil, this mixture would contain a higher heating value that is rarely seen in traditional bio-oil. For red oak, the combination of the first four fractions would result in 23.3 MJ/kg. For switchgrass and cornstover, heating values of 23.3 and 24.4 MJ/kg respectively were found for the combination of the first four fractions. These increased heating values could make bio-oil a suitable boiler fuel or home heating fuel.

The key contributing factor for the increased energy content in the combination of the first four fractions was the lower moisture content found in these fractions. In a similar fashion to the heating value, a comparison of the moisture content of a combination of the first four fractions yields moisture contents of 8.3%, 10.2%, and 8.9% for red oak, cornstover and switchgrass respectively. This low moisture content allows the energy content to be much higher than typical bio-oil which contains upwards of 25% moisture.[2]

While there is not a direct linear correlation between moisture content and higher heating value, there is a general trend. According to the analysis that was performed, as the moisture content increases, the higher heating value becomes lower and lower. This relationship is intuitive. The moisture content that is present in the bio-oil needs to be vaporized when the bio-oil is combusted. The enthalpy of vaporization of water robs some of the energy of combustion from the bio-oil.

Levoglucosan Production

The concentration of the GC/MS detectable compounds were significantly different based on the fraction of bio-oil and biomass that was being analyzed. The levoglucosan concentration was largely dependent on the cellulose concentration in the original biomass with the majority of the levoglucosan being collected in the first two fractions of

bio-oil. This indicated that the levoglucosan exited the reactor as both a vapor and an aerosol. In fact, in cornstover and switchgrass, more levoglucosan was collected as an aerosol than as a vapor. After full analysis, it is apparent that a combination of the first two fractions of red oak bio-oil would produce the highest concentration of levoglucosan and possibly other anyhydrosugars.

Lignin Derived Products

It is believed that the phenolics and the water insoluble content of the bio-oil are both products of the pyrolysis of lignin. According to the analysis of the phenols, guaiacols, syringols and water insoluble content, there appears to be other products that are produced from the lignin but these phenolic compounds and water insoluble components are more than likely produced from the lignin. The structure of lignin contains a large amount of aromatic rings that are the building blocks of phenolic compounds. In the same manner, the water insoluble content consists of many large molecular weight oligomers that could easily be produced from the lignin. Another possibility for the production of these large molecular weight compounds would be chains of five or six carbon sugars (depending on whether it is produced from cellulose or hemicellulose) that are longer than typical sugar monomers. A chain of this size could be large enough to be filtered out of the bio-oil during the water insoluble test.

The relative distribution of syringols and guaiacols provides some insight into the structure of lignin present in the different biomasses. The difference between guaiacols and syringols can be described as the degree of substitution found in each molecule. Guaiacols contain a single methoxy group, while syringols contain two methoxy groups in addition to the hydroxyl group that is in all phenolic compounds. The concentrations of the phenolics, syringols and guaiacols can lead to more information about the structure of the lignin, as well as the degree of substitution of the aromatic rings that are contained within the lignin structure.

Modified Acid Number vs. Acetic Acid Content

The results from this study have indicated that there is a direct and linear correlation between the acetic acid content of bio-oil and the total acid content of the specific bio-oil. Acetic acid is only one of many organic acids present in bio-oil that can be titrated during the MAN measurement, but it is the most prevalent acid present in bio-oil. The results have also shown that there are other acids present in the bio-oil, even though they are not quantified in the chemical analysis of the bio-oil. One of these acids could be 2-hydroxybenzoic acid, which should be considered an "acid tar." The presence of large molecular weight acids is the reason that there is a significant modified acid number for the fractions where acetic acid should not be collected.

Repeatability of Results

For some of the analysis, the repeatability of the results was not very high. This was seen for much of the bio-oil analysis. Some of the repeatability issues can stem from low concentrations or even differences in moisture content (which can have an effect on other properties). Below is a breakdown of the repeatability of each aspect of this study:

- Mass Balance – The mass balance saw little variability between tests. It appears that the collection of the bio-oil has a high degree of repeatability. For each biomass, the separate fractions produced repeatable percentages of bio-oil for each of the three tests.

- Moisture Content – The moisture content of each fraction was largely repeated for each test. Based on the analysis, the only fraction that had significant uncertainty was SF4. This fraction had uncertainty in other analysis as well. The other four fractions of bio-oil each had relatively high repeatability of water content.

- Higher Heating Value – The higher heating value for each fraction of bio-oil was determined to be a repeatable property. There was some uncertainty, but overall

each fraction of bio-oil from each biomass had similar higher heating values for each test.

- Modified Acid Number – For both SF3 and SF4, the MAN was not repeatable. This could be due to the uncertainties in the moisture content of these fractions. The other three fractions (SF 1, 2 and 5) each had repeatable total acid numbers.

- Elemental Analysis – The elemental analysis for the fractions of bio-oil was repeatable for carbon, hydrogen and oxygen. The ash, nitrogen and sulfur contents each had very large amounts of uncertainty. The sulfur and nitrogen each had very low concentrations in the fractions. This low concentration in each fraction makes even a small total change in concentration relatively large.

- Chemical Analysis- The chemical analysis for each fraction had a large amount of variability. The chemical analysis was performed by diluting the bio-oil in methanol at a 4% bio-oil to 96% methanol ratio. This creates a very dilute mixture where any uncertainties in measurements could lead to large discrepancies in concentrations.

- Water Insoluble Content – For each fraction of bio-oil, except SF2, the water insoluble content had a lot of variability. This could be due to differences in the way that the biomass was pyrolyzed or even differences in the mixing of the bio-oil and water. There are many proposed methods in the literature for the measurement of water insoluble content and the simple action of mixing the bio-oil/water mixture can cause discrepancies in the results.

- Solids Content – The solids content of the bio-oil fractions was largely uncertain. This could be due to different amounts of solids escaping the cyclone filters.

- Viscosity – The viscosity of the bio-oil was very variable. The variability could be largely due to variances in moisture content and water insoluble content for the different tests. Water will effectively lower the viscosity of the bio-oil while the water insoluble content should increase the viscosity. The variances in these two properties can greatly affect the viscosity of each sample.

Future Work

After analyzing the results from this research, it is apparent that there is much more work that can be done. First and foremost, the reactor system needs to be optimized with each biomass to determine the optimal conditions to collect the highest percentage of bio-oil. After this has been completed, it is recommended that the fractionating bio-oil collection system be operated at multiple operating conditions, varying the set-points to determine the effect that this has on the bio-oil properties and components. This research was completed by operating the system at a single set-point, but gaining knowledge concerning the effect that surface temperatures has on the collection of certain compounds could be useful.

Further analysis should be completed on the long term effects of the fractionating bio-oil collection system on the stability of the bio-oil. Accelerated tests have been completed, but aging the thick fractions at room temperature may produce differing results. The thick, almost solid fractions would react differently as at room temperature rather than as a liquid with more fluidity. Finally, more biomasses should be tested to see if there are any changes in bio-oil composition.

Fractionation vs. Whole Bio-oil

Before this research was started, the hope was that the fractionated bio-oil system would produce similar fractions for each biomass. Each of these fractions would just be produced in different ratios. After testing and analysis, it is apparent that each biomass

still produces a distinct bio-oil and that the same fraction of bio-oil is different depending on the biomass from which it was produced. This is because each biomass contains different amounts of cellulose, hemicellulose, lignin and ash. These differences lead to the production of different products.

The fractionated bio-oil collection system has shown that it is possible to actively fractionate bio-oil into distinct fractions during the bio-oil collection process. This fractionation process has the ability to produce distinct bio-oil fractions that have unique characteristics and properties. The first and second fractions of bio-oil that were collected were similar in properties and composition. Each of these fractions were high in levoglucosan and water insoluble content. These fractions were also low in water and acid content. The third and fourth fractions were each high in phenolic compounds and acetic acid, but had relatively low moisture contents. Compared to the other fractions, these two fractions did not contain a high amount of the bio-oil. The final fraction, which typically collected the largest amount of bio-oil, contained large amounts of water and large amounts of acetic acid. The concentration of acetic acid was not always the highest, but the overall mass of acetic acid produced was consistently the highest of any of the fractions.

In conclusion, the fractionation system produced fractionated bio-oil with improved qualities including water insoluble content, water content, acid content and, especially, heating value. This system was capable of producing fractionated bio-oil from all three biomasses that were tested (red oak, cornstover and switchgrass). This separation was achieved through the separation of vapors and aerosols and the selective condensation of the vapors.

APPENDIX A

Fluidized Bed Design Calculations

Reactor Dimension information

$r_{out} := \frac{6.625}{2}in$ $w_{thick} := .280in$

Green values are assumptions and blue sections are discussion

$r_{in} := r_{out} - w_{thick}$ $dia := 2 \cdot r_{in}$ $z := dia \cdot 2$

$A_{in} := 2r_{in} \cdot \pi \cdot z$ $A_{out} := 2r_{out} \cdot \pi \cdot z$ $A_{cs} := \frac{\pi}{4} \cdot dia^2$

$m_{biomass} := 8\frac{kg}{hr}$ $r_{heater} := r_{out} + 0.688in$

The reactor is designed using 6 inch standard pipe (Stainless Steel). The dimensions are shown above with the outer radius and the wall thickness. The heater has a 8 inch inner diameter and will be placed around the entire reactor.

Temperatures and pressures

$T_{pyrolysis} := 500K + 273K$

The design parameters are set for a bed temperature of 500C and operating at atmospheric pressure

$P_{pyrolysis} := 14.696psi$

$T_{atm} := 25K + 273K$

$T_{bed} := T_{pyrolysis}$

Fluid Bed Properties

$\rho_p := 2600\frac{kg}{m^3}$ $dv := 500 \cdot 10^{-6}m$

dv= volume diameter of particle

$\rho_{bulk} := 400\left(\frac{kg}{m^3}\right)$ $dv_{char} := 52 \cdot 10^{-6}m$

$\mu(T) \equiv \left[52.584 + 0.262\left(\frac{T}{R}\right) - 2.954 \cdot 10^{-5} \cdot \left(\frac{T}{R}\right)^2\right] \cdot 10^{-7} \cdot \frac{newton \cdot sec}{m^2}$ $\varepsilon_{char} := 0.4$

$R_{Nitrogen} \equiv \frac{8.314 \cdot \frac{joule}{mole \cdot K}}{29.0 \cdot \frac{gm}{mole}}$ $\rho(T,P) \equiv \frac{P}{R_{Nitrogen} \cdot T}$ $\rho_{char} := \rho_{bulk} \cdot (1 - \varepsilon_{char})$

$\mu_f := \mu(T_{pyrolysis})$ $\rho_f := \rho(T_{pyrolysis}, P_{pyrolysis})$ $C_{pN2} := 1.05 \cdot 10^3 \frac{J}{kg \cdot K}$

These are just general fluid properties and also material properties for the sand and the char. The sand and char properties are assumed values that have come from previous experience. The char properties come from Joe Ritzert's thesis and the sand comes from general sand properties. The sand diameter was reduced to 500 microns in an attempt to meet the specification that U/Umf>=4.

Material Properties

$\varepsilon_{heater} := 0.9$ $\varepsilon_{wall} := .58$ $k_{shell} := 14.9 \frac{W}{m \cdot K}$ $\sigma := 5.67 \cdot 10^{-8} \frac{W}{m^2 K^4}$

The emissivity of the heaters is assumed to 0.9 while the emissivity of the stainless steel wall is assumed to be 0.67. The wall could vary from 0.2 to 0.9 depending on the condition of the reactor wall. If a coating can be applied to the outer surface of the reactor then the emissivity of the wall can be increased.

Heat Transfer information

$$h_{bed} := \begin{pmatrix} 100 \\ 150 \\ 200 \\ 250 \end{pmatrix} \frac{W}{m^2 K}$$

$$q_{req} := m_{biomass} \cdot 1.35 \cdot 10^6 \frac{J}{kg}$$

$q_{req} = 3 \times 10^3 \, W$

To investigate the entire spectrum of internal heat transfer coefficients, all of the calculations are being performed with a range of h_conv that spans from 100 to 250, with the main focus being placed on 150. This is occuring because 150 is a value that has been used by multiple people in designing fluidized bed reactors and if the convective heat transfer coefficient does end up being higher than that, this adds a factor of safety to the calculations.

Minimum Fluidization Velocity

$$Ar\_py := \frac{\rho_f \cdot dv^3 \cdot (\rho_p - \rho_f) \cdot g}{\mu_f^2}$$

$$U_{mf} := \left(\frac{\mu_f}{\rho_f \cdot dv} \right) \cdot \left[(1135.7 + 0.0408 \cdot Ar\_py)^{\frac{1}{2}} - 33.7 \right]$$

$Ar\_py = 1.125 \times 10^3$

$U_{mf} = 0.106 \frac{m}{s}$

Char Elutriation Calculations

$U_{super} := .2 \frac{m}{s}$ $Re_{py} := \frac{\rho_f \cdot U_{super} \cdot dv}{\mu_f}$ $C_d := \frac{10}{Re_{py}^{\frac{1}{2}}}$

$$V_t := \left[\frac{4 \cdot g \cdot dv_{char} \cdot (\rho_{char} - \rho_f)}{3 \cdot \rho_f \cdot C_d} \right]^{.5}$$

$V_t = 0.2 \frac{m}{s}$

The preceeding calculation was to ensure that the velocities with in the fluidized bed were high enough to elutriate the char from the bed. Once again Joe Ritzerts information was used to perform the calculation and the U_super was iterated to determine the velocity required.

Max Char particle size to be Elutriated

$dv_{guess} := 2.342 \cdot 10^{-4} m$ $\quad U_{maxd} := U_{mf} \cdot 4$

$Re_{pymaxd} := \rho_f \cdot U_{maxd} \cdot \frac{dv_{guess}}{\mu_f}$ $\quad C_{dmaxd} := \frac{10}{Re_{pymaxd}^{\frac{1}{2}}}$

$dv_{max} := \left[\frac{\left(U_{maxd}^{2} \cdot 3 \cdot \rho_f \cdot C_{dmaxd} \right)}{4 \cdot g \cdot \left(\rho_{char} - \rho_f \right)} \right]$

$dv_{max} = 2.341 \times 10^{-4} m$

Total Amount of Heat Required

$U_f := 4 \cdot U_{mf}$ $\quad Q_{N2} := U_f \cdot A_{cs}$ $\quad m_f := Q_{N2} \cdot \rho_f$ $\quad m_f = 13.026 \frac{kg}{hr}$

$q_{N2} := m_f \cdot C_{pN2} \cdot \left(T_{pyrolysis} - T_{atm} \right)$ $\quad q_{N2} = 1.805 \times 10^{3} W$ $\quad Q_{N2s} := Q_{N2} \cdot \left(\frac{T_{atm}}{T_{pyrolysis}} \right)$

$q_{tot} := q_{req} + q_{N2}$ $\quad q_{tot} = 4.805 \times 10^{3} W$ $\quad Q_{N2s} = 183.048 \frac{L}{min}$

To determine the total amount of heat that needs to be transfered into the reactor, the heat required to heat the fluidizing gas is calculated above. This was then added to the heat required to transform the biomass into pyrolysis gases.

Heat Transfer Information and Resistances

$q_{rad} := q_{tot}$

$r_{conv} := \frac{1}{h_{bed} \cdot A_{in}}$ $\quad r_{shell} := \frac{\ln\left(\frac{r_{out}}{r_{in}} \right)}{2 \cdot \pi \cdot k_{shell} \cdot z}$

This is just information concerning general heat transfer information that is used below to calculate the temperature of heater required to provide the required heat. The heater temperature has been iterated to solve for the h_conv=150.

Inside the Pyrolysis Reactor

$$T_{in} := q_{rad} \cdot r_{conv} + T_{bed}$$

$$T_{inC} := T_{in} - 273K$$

$$T_{inC} = \begin{pmatrix} 822.218 \\ 714.812 \\ 661.109 \\ 628.887 \end{pmatrix} K$$

Heat Transfer through the pipe

$$T_{out} := q_{rad} \cdot r_{shell} + T_{in}$$

$$T_{outC} := T_{out} - 273K$$

$$T_{outC} = \begin{pmatrix} 836.929 \\ 729.523 \\ 675.82 \\ 643.598 \end{pmatrix} K$$

These two calculate solve for the inner and outer temperatures of the reactor shell. The outer temperature will then be used to determine the temperature of the heater that is needed.

Radiative Heat Transfer

$T_{heater2} := 1161K$ Iterations done on h_bed=150

$$h_{rad} := \frac{\sigma \cdot \left(T_{heater2}^2 + T_{out}^2 \right) \cdot \left(T_{heater2} + T_{out} \right)}{\left(\frac{1}{\varepsilon_{wall}} \right) + \left(\frac{1 - \varepsilon_{heater}}{\varepsilon_{heater}} \right) \cdot \left(\frac{r_{out}}{r_{heater}} \right)} \qquad r_{rad} := \frac{1}{h_{rad} \cdot A_{out}}$$

$$R_{tot} := r_{rad} + r_{conv} + r_{shell}$$

$$T_{heater} := q_{rad} \cdot r_{rad} + T_{out} \qquad T_{heater} = \begin{pmatrix} 1.271 \times 10^3 \\ 1.188 \times 10^3 \\ 1.148 \times 10^3 \\ 1.124 \times 10^3 \end{pmatrix} K$$

$$T_{heaterC} := T_{heater} - 273K \qquad T_{heaterC} = \begin{pmatrix} 998.202 \\ 915.125 \\ 875.018 \\ 851.443 \end{pmatrix} K$$

The temperature that is required if h_conv=150 is 915.125 C. This is well below the 1023C that is the maximum temperature of the heaters that are being used for this design.

Distributor Plate Design

$\rho_{in} := \rho(T_{atm}, P_{pyrolysis})$ $Q_{N2\_25} := Q_{N2} \cdot \left(\frac{T_{atm}}{T_{bed}}\right)$ $Q_{N2\_25} = 183.048 \frac{L}{min}$ $\varepsilon_{mf} := .4$

$D_{plenum} := \frac{1}{8} in$ $N_{plenum} := 40$ $A_p := N_{plenum} \cdot \frac{\pi}{4} \cdot (D_{plenum})^2$ $A_p = 0.491\ in^2$

$d_{eq} := 3.371 in$ $U_{br} := 0.5 \cdot \sqrt{g \cdot d_{eq}}$ $H_{mf} := \frac{U_{br} \cdot z}{U_{br} + (U_f - U_{mf})}$

$D_{reactor} := dia$ $A_b := \left(\frac{\pi}{4}\right) \cdot D_{reactor}^2$ $v_{standard} := \frac{m_f}{\rho_{in}}$ $v_{standard} = 183.048 \frac{L}{min}$

Orifice Dimensions

$d_{or.i} := 3 \cdot dv$ $d_{or.i} = 0.059\ in$

$d_{or} := \left(\frac{1}{16}\right) in$ $A_{or} := \pi \cdot \left(\frac{d_{or}}{2}\right)^2$

$d_{bubble} := 0.54 (U_f - U_{mf})^{0.4} \cdot \left(z + 4\sqrt{A_{or}}\right)^{0.8} \cdot g^{-0.2}$ $d_{bubble} = 3.371\ in$

Pressure Drops Across Bed and Distributor

$\Delta P_{bed} := \rho_p \cdot g \cdot H_{mf} \cdot (1 - \varepsilon_{mf})$ $\Delta P_{distributor} := \Delta P_{bed} \cdot (.25)$

$\Delta P_{distributor} = 695.195\ Pa$

$\frac{\Delta P_{distributor}}{\Delta P_{bed}} = 0.25$ $C_{or} := 0.5$

$Up := \frac{Q_{N2\_25}}{A_b}$ $U_{or} := C_{or} \cdot \left(\frac{2 \cdot \Delta P_{distributor}}{\rho_f}\right)^{\frac{1}{2}}$

$N_{or} := \frac{Q_{N2\_25}}{U_{or} \cdot \frac{\pi}{4} \cdot d_{or}^2}$ $N_{or} = 55.901$ $\Delta P_{plenum} := \frac{\rho_{in}}{2} \cdot \left(\left(Q_{N2\_25} \cdot \frac{1}{A_p}\right)\right)^2$

$\frac{\Delta P_{distributor}}{\Delta P_{plenum}} = 12.633$ $\Delta P_{plenum} = 7.982 \times 10^{-3}\ psi$

Height of Freeboard Calculation

$H_{settled} := H_{mf} \cdot \left(1 - \varepsilon_{mf}\right)$

$TDH := 1200 \cdot H_{settled} \cdot Re_{py}^{1.55} \cdot Ar\_py^{-1.1}$ $\quad TDH = 3.288\,in$

Volume Flow of Bio-oil coming out of the reactor

$M_{biomass} := 98.9 \frac{gm}{mol}$ $\quad R_{biooil} := \frac{8.314 \cdot \frac{joule}{mole \cdot K}}{M_{biomass}}$ $\quad Q_{biooilvapor} := \frac{m_{biomass} \cdot R_{biooil} \cdot \left(T_{bed}\right) \cdot 0.065}{P_{pyrolysis}}$

$Q_{biooilaerosol} := m_{biomass} \cdot \frac{.585}{(1.2) \cdot \frac{kg}{L}}$ $\quad Q_{biooilaerosol} = 1.083 \times 10^{-6} \frac{m^3}{s}$

$Q_{biooilvapor} = 5.558 \frac{L}{min}$

This is a calculation to determine the volume flow of bio-oil in the vapor form when it leaves the reactor and proceeds to the cyclones.

$M_{gases} := 29.4 \frac{gm}{mol}$ $\quad R_{gases} := \frac{8.314 \cdot \frac{joule}{mole \cdot K}}{M_{gases}}$ $\quad Q_{gases} := \frac{m_{biomass} \cdot R_{gases} \cdot \left(T_{bed}\right) \cdot 0.10}{P_{pyrolysis}}$

$Q_{gases} = 28.765 \frac{L}{min}$

Cyclone Design

Cyclone Separator Design: Cyclone 1 $Q := Q_{N2} + Q_{biooilaerosol} + Q_{biooilvapor} + Q_{gases}$

Total Estimated Gas Flow through Cyclone

$Q_{design} := 500\frac{L}{min}$ $Q = 509.207\frac{L}{min}$ $Q_{N2} = 474.819\frac{L}{min}$ $Q_{biooilvapor} = 5.558\frac{L}{min}$

For a High Efficiency cyclone Use St_50 of **1.17*10^-4**, for High Flow Rate Use St_50 of **0.006**

$St_{50\_1} := 0.006$

Maximum acceptable pressure drop across the cyclor

$\delta P\_1 := 0.05psi$

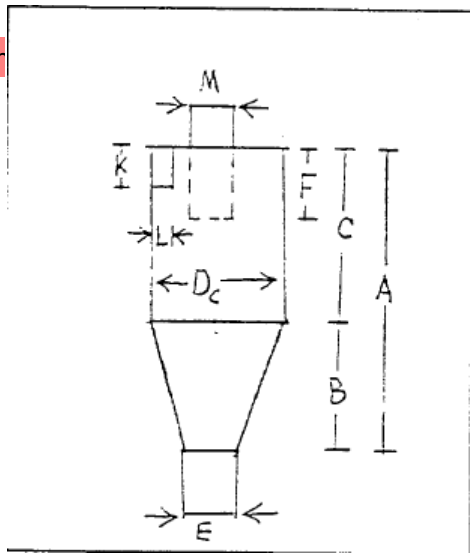

Euler number

$$Eu\_1 := \left(\frac{12}{St_{50\_1}}\right)^{\frac{1}{2}}$$

Characteristic flow velocity

$$U\_1 := \left(\frac{2\cdot\delta P\_1}{Eu\_1\cdot\rho_f}\right)^{\frac{1}{2}} \qquad U\_1 = 5.807\frac{m}{s}$$

Diameter of the cyclone

$$D_{c\_1} := \left(\frac{4\cdot Q_{design}}{\pi\cdot U\_1}\right)^{\frac{1}{2}} \qquad D_{c\_1} = 1.683\,in$$

Check the particle diameter, d_50, the minimum diameter at which particle are filtered with a 50% effieicency. Particles larger than this diameter will be filtered with greater than 50% efficiency. If d_50 is too large divide Q by two, using two cyclones of equal size and re-compute D_c.

$$d_{50\_1} := \left(\frac{St_{50\_1}\cdot 18\cdot\mu_f\cdot D_{c\_1}}{\rho_{char}\cdot U\_1}\right)^{\frac{1}{2}} \qquad d_{50\_1} = 1.092\times 10^{-5}\,m$$

Other relevant dimensions of the cyclone

$$\begin{pmatrix} A\_1 \\ B\_1 \\ C\_1 \\ E\_1 \\ F\_1 \\ L\_1 \\ K\_1 \\ M\_1 \end{pmatrix} := \begin{cases} \begin{pmatrix} 4 \\ 2.5 \\ 1.5 \\ 0.375 \\ 0.5 \\ 0.2 \\ 0.5 \\ 0.5 \end{pmatrix} \cdot D_{c\_1} & \text{if } St_{50\_1} < 0.005 \\ \begin{pmatrix} 4 \\ 2.5 \\ 1.5 \\ 0.375 \\ 0.875 \\ 0.375 \\ 0.75 \\ 0.75 \end{pmatrix} \cdot D_{c\_1} & \text{otherwise} \end{cases}$$

$$\begin{pmatrix} A\_1 \\ B\_1 \\ C\_1 \\ E\_1 \\ F\_1 \\ L\_1 \\ K\_1 \\ M\_1 \end{pmatrix} = \begin{pmatrix} 6.732 \\ 4.207 \\ 2.524 \\ 0.631 \\ 1.473 \\ 0.631 \\ 1.262 \\ 1.262 \end{pmatrix} \text{ in}$$

$$\eta(d_{px}) := \frac{100}{1 + \left(\frac{d_{50\_1} \cdot 10^6}{d_{px}} \right)^{6.4}}$$

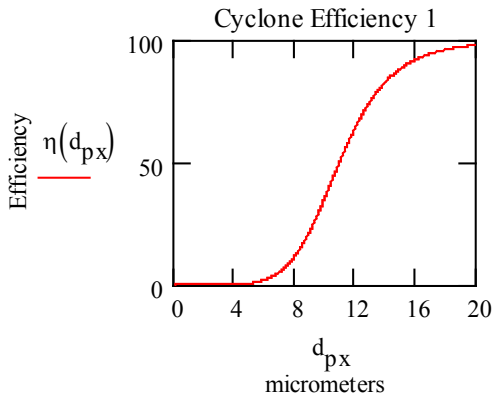

The first cyclone will be used to remove the majority of the char from the flow. Meanwhile the second cyclone will remove the rest of the char from the flow. There will still be some char left because the cyclones aren't perfect in removing particulate from the flow.

Cyclone Separator Design: Cyclone 2

For a High Efficiency cyclone Use St_50 of **1.17*10^-4**, for High Flow Rate Use St_50 of **0.006**

$$St_{50\_2} := 1.17 \cdot 10^{-4}$$

Maximum acceptable pressure drop across the cyclone

$$\delta P\_2 := .30 psi$$

Euler number

$$Eu\_2 := \left(\frac{12}{St_{50\_2}} \right)^{\frac{1}{2}}$$

Characteristic flow velocity

$$U\_2 := \left(\frac{2 \cdot \delta P\_2}{Eu\_2 \cdot \rho_f} \right)^{\frac{1}{2}} \qquad U\_2 = 5.315 \frac{m}{s}$$

Diameter of the cyclone

$$D_{c\_2} := \left(\frac{4 \cdot Q_{design}}{\pi \cdot U\_2} \right)^{\frac{1}{2}} \qquad D_{c\_2} = 1.759 in$$

$$d_{50\_2} := \left(\frac{St_{50\_2} \cdot 18 \cdot \mu_f \cdot D_{c\_2}}{\rho_{char} \cdot U\_2} \right)^{\frac{1}{2}} \qquad d_{50\_2} = 1.629 \times 10^{-6} m$$

Other relevant dimensions of the cyclone

$$\begin{pmatrix} A\_2 \\ B\_2 \\ C\_2 \\ E\_2 \\ F\_2 \\ L\_2 \\ K\_2 \\ M\_2 \end{pmatrix} := \begin{cases} \begin{pmatrix} 4 \\ 2.5 \\ 1.5 \\ 0.375 \\ 0.5 \\ 0.2 \\ 0.5 \\ 0.5 \end{pmatrix} \cdot D_{c\_2} & \text{if } St_{50\_2} < 0.005 \\ \begin{pmatrix} 4 \\ 2.5 \\ 1.5 \\ 0.375 \\ 0.875 \\ 0.375 \\ 0.75 \\ 0.75 \end{pmatrix} \cdot D_{c\_2} & \text{otherwise} \end{cases}$$

$$\begin{pmatrix} A\_2 \\ B\_2 \\ C\_2 \\ E\_2 \\ F\_2 \\ L\_2 \\ K\_2 \\ M\_2 \end{pmatrix} = \begin{pmatrix} 7.036 \\ 4.398 \\ 2.639 \\ 0.66 \\ 0.88 \\ 0.352 \\ 0.88 \\ 0.88 \end{pmatrix} \text{ in}$$

$$n(d_{px}) := \frac{100}{1 + \left(\frac{d_{50\_2} \cdot 10^6}{d_{px}} \right)^{6.4}}$$

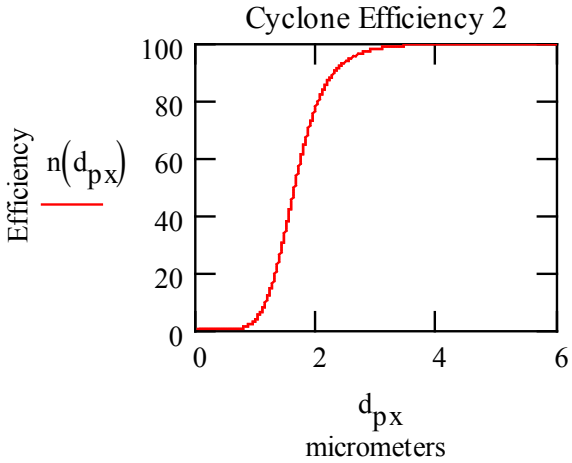

Condenser 1 Design

Problem Definition: Predict the surface area needed to both cool and condense pyrolysis bio-oil from a mixture of gases. Initially, condense the levoglucosan from the mixture. The inlet temperature of the gas is 250C and the outlet temperature of the gas is 150C. The wall temperature will be held constant at 85C. The initial partial pressure of the levoglucosan is 0.008 and the levoglucosan is produced at a mass flow rate of .75 kg/hr. The mass flowrate of the bulk gases is equal to 19 kg/hr and can be approximated as nitrogen gas and the given temperature. The concentration at the walls is assumed to be equal to 0 and 95% of the levoglucosan is removed.

Given:

Flow Temperatures:

$T_{in} := (400 + 273)K$ Temperature of the incoming gas

$T_{out} := (150 + 273)K$ Temperature of the outflowing gas

$T_w := (85 + 273)K$ Temperature of the walls

Mass Flow Rates:

$m_{biomass} := 8$

$m_{N2} := \left(13 + m_{biomass} \cdot .75\right)\frac{kg}{hr}$ Mass flow of the nitrogen

$m_L := m_{biomass} \cdot .094\,\frac{kg}{hr}$ Theoretical mass flow of the levoglucosan

Partial Pressures:

$P_{sat} := 0.000001$ Saturation Pressure at Wall Temperater

$P_{in} := .008$ Incoming partial pressure

$P_{out} := P_{in} \cdot .05$ Out flowing partial pressure

Required Properties:

$Cp_{N2} := 1.065\,\frac{J}{gm \cdot K}$

$D_{AB} := .638\,\frac{cm^2}{sec}$

$H_{vapL} := .56835 \times 1000\,\frac{J}{gm}$

$\nu_{N2} := 44.86 \cdot 10^{-6}\,\frac{m^2}{sec}$

$\mu_{N2} := 0.00002677\,\frac{kg}{m \cdot s}$

$M_L := 162.4\,\frac{kg}{mol}$

$k_{N2} := 41.7 \cdot 10^{-3}\,\frac{W}{m \cdot K}$

$M_{N2} := 14\,\frac{kg}{mol}$

$\rho_{N2} := 0.6124\,\frac{kg}{m^3}$

$Pr_{N2} := .7061$

Heat Transfer:

The total heat must contain both the sensible heat of the gas flow cooling and the latent hea of the levoglucosan. The equation above contains first the sensible heat. This assumes tha the entire flow is nitrogen and is cooling from 400 to 150. The latent heat assumes that only 95% of the levoglucosan is removed.

q_{total} =(Sensible heat for Nitrogen)+(Latent Heat for levoglucosan)

$$q_{total} := m_{N2} \cdot Cp_{N2} \cdot \left(T_{in} - T_{out}\right) + .95 m_L \cdot H_{vapL}$$

Heat transfer for Condenser Design:

The condenser is being designed as a constant surface temperature, shell and tube heat exchanger. The flow will be designed to be laminar to reduce the chance that aerosols will impinge on the condenser walls. The flow is made of mainly nitrogen and there is levoglcosan vapors present that will be condensed from the flow.

$q_{total} = h_d \cdot A_s \cdot \Delta T_{lm}$

Where:

q_{total}= total heat removed

h_d= convective heat transfer coefficient

A_s= Surface area

ΔT_{lm}= Log-mean temperature difference

The goal is to determine the amount of surface area required to remove the required heat. This will be done by following the procedure listed below:

1. Assume D and L the tubes and the number of tubes
2. Calculate the Reynolds number and adjust D and number of tubes to ensure that flow is laminar
3. Find correlation for Nu and Calculate Nu
4. Determine h_d
5. Calculate ΔT_{lm}
6. Calculate A_s
7. Calculate L and iterate it back. If ok porceed to mass transfer analysis

1. Assume Diameter, Length and Number of Tubes

$D := 1in \qquad N := 30 \qquad L := 24in$

2. Reynolds Number:

The calculation of the Reynolds Number is important to perform first to check to see if the flow is laminar of turbulent. The outcome of this calculation will help us decide what Nussetl number will be used with the problem. Initial assumptions include that the entire flow is nitrogen.

$$Re_d := \frac{4 \cdot m_{N2}}{\pi \cdot D \cdot \mu_{N2} \cdot N}$$

$Re_d = 329.426$ **Adjust D and N if not laminar**

3. Nussetl Number

$$Nu_d := 1.86\left(\frac{Re_d \cdot Pr_{N2}}{\frac{L}{D}}\right)^{\frac{1}{3}} \qquad Nu_d = 3.966$$

Because the flow is laminar through the tubes and fully developed the preceeding correlation can be used to calculate the Nussetl Number. This correlation can be found in Incropera (equation 8.57)

4. Heat Transfer Coefficient:

$$Nu_d = \frac{h_d \cdot k_{N2}}{D} \qquad h_d := \frac{k_{N2}}{D} \cdot Nu_d \qquad h_d = 6.511 \frac{W}{m^2 K}$$

The Nussetl number can then be used to calculate a heat transfer coefficient. This heat transfer coefficient is then insterted into the heat equation.

5. Log-Mean Temerature Difference:

$$\Delta T_{lm} := \frac{(T_{out} - T_w) - (T_{in} - T_w)}{\ln\left[\frac{(T_{out} - T_w)}{(T_{in} - T_w)}\right]} \qquad \Delta T_{lm} = 158.41\,K$$

$T_{in} = 673\,K$

$T_{out} = 423\,K$

$T_w = 358\,K$

The final piece of information needed to calculate the required area is the log-mean temperature difference. This equation comes from simple heat exchanger design. This takes into account the changing temperature within the tube. The wall temperature is held constant.

6. and 7. Surface Area and Tube Length

$$A_s := \frac{q_{total}}{h_d \cdot \Delta T_{lm}} \qquad L := \frac{A_s}{\pi \cdot D \cdot N^*}$$

$A_s = 2.281 \times 10^3\,in^2$ $\qquad L = 24.206\,in$

The surface area required to achomplish the desired heat removal is shown above, along with length of tubes required to achomplish the heat transfer. Note that the length of tube is not effected bv diameter.

Mass Transfer for Condenser Design:

The mass transfer based design of the condensers is going to utilize the Reynold's Analogy to derive correlations between Heat Transfer and Mass Transfer.

Reynold's Analogy

The Reynold's Analogy is a way that simple heat translated into mass transfer through a simple transformation. The key to this transformation is the fact that the ratios of dimensionless value are equal.

$$\frac{Nu}{Pr^n} = \frac{Sh}{Sc^n}$$

Knowing that this ratio holds true, any convective correlation can be translated into a heat transfer correlation. The equation below shows how the Nussetl correlation that was used previously for the heat transfer can be transformed into a Sherwood number correlation that can then be used for mass transfer.

$$Nu_d = 186\left(\frac{Re_d \cdot Pr_{N2}}{\frac{L}{D}}\right)^{\frac{1}{3}} \quad \text{====>} \quad Sh_d = 186\left(\frac{Re_d \cdot Sc}{\frac{L}{D}}\right)^{\frac{1}{3}}$$

Getting mass transfer coefficients is very similar to getting heat transfer coefficients except that the mass transfer coefficient is a function of diffusivity instead of conductivity.

$$Nu_d = \frac{h_d \cdot k_{N2}}{D} \quad \text{====>} \quad Sh_d = \frac{h_m \cdot D_{AB}}{D}$$

Heat transfer is driven by temperature gradients. Similarly, mass transfer is driven by concentration or pressure gradients. Thus the Log-Mean Temperature Difference can be modified to become a Log-Mean Pressure Difference

$$C_{levoglcosan} \cdot \frac{1}{M_L} \cdot \frac{1}{\rho_{N2}} \cdot M_{N2} = P$$

$$\Delta T_{lm} := \frac{(T_{out} - T_w) - (T_{in} - T_w)}{\ln\left[\frac{(T_{out} - T_w)}{(T_{in} - T_w)}\right]} \quad \text{====>} \quad \Delta P_{lm} := \frac{(P_{out} - P_{sat}) - (P_{in} - P_{sat})}{\ln\left[\frac{(P_{out} - P_{sat})}{(P_{in} - P_{sat})}\right]}$$

FInally all of this combined becomes out mass flow instead of our heat flow.

$$q_{total} = h_d \cdot A_s \cdot \Delta T_{lm} \quad \text{====>} \quad m_{total} = h_m \cdot A_s \cdot \Delta C_{lm}$$

The procedure of design based on mass transfer is similar to the design based on heat transfer.

1. Use tube dimensions and Reynolds number from previous work.
2. Calculate Sc Number
3. Find correlation for Sh and Calculate Sh
4. Determine h_m
5. Calculate ΔP_{lm}
6. Calculate A_s
7. Calculate L and iterate it back. If ok porceed to mass transfer analysis

1. Tube Dimensions and Reynold's Number

The tube dimensions are taken from the heat transfer design. The goal of these calculations are to calculate the required area.

$D = 1\,in \qquad L := 24in \qquad N = 30$

2. Schmidt Number:

The Schmidt number is the ratio of the momentum and mass diffusivities. This dimensionless value is used to calculate a Sherwood number and is calculated from known/assumed properties.

$$Sc := \frac{\nu_{N2}}{D_{AB}} \qquad Sc = 0.703$$

3. Sherwood Number:

The Sherwood Number is a dimensionless value that is analogus to the Nusselt number. It is a dimensionless concentration gradient on the surface in which the condensation is taking place. This value will allow us to calculate a mass transfer coefficient.

$$Sh_d := 1.86\left(\frac{Re_d \cdot Sc}{\frac{L}{D}}\right)^{\frac{1}{3}} \qquad Sh_d = 3.96$$

4. Mass Transfer Coefficient:

The mass transfer coefficient is similar to the convective heat transfer coefficient.

$$h_m := \frac{Sh_d \cdot D_{AB}}{D} \qquad h_m = 9.947 \times 10^{-3}\,\frac{m}{s}$$

5. Log-Mean Partial Pressure Difference:
   The purpose of this value is to take into account the change in partial pressures through the condenser. The pressure at the wall is the saturation pressure.

$$\Delta P_{lm} := \frac{\left(P_{out} - P_{sat}\right) - \left(P_{in} - P_{sat}\right)}{\ln\left[\frac{\left(P_{out} - P_{sat}\right)}{\left(P_{in} - P_{sat}\right)}\right]} \qquad \Delta P_{lm} = 2.535 \times 10^{-3}$$

$$P_{out} = 4 \times 10^{-4}$$

$$P_{in} = 8 \times 10^{-3}$$

$$P_{sat} = 1 \times 10^{-6}$$

6. and 7. Surface Area Check and Length Calculation:

$$A_{s\_check} := \frac{m_L \cdot M_{N2}}{h_m \cdot \rho_{N2} \cdot M_L \cdot \Delta P_{lm}} \qquad L := \frac{A_{s\_check}}{\pi \cdot D \cdot N}*$$

$$A_{s\_check} = 1.808 \times 10^{3}\,in^2 \qquad L = 19.179\,in$$

Assumes that cooling occurs first and mass is transfered second.

Condenser 2 Design

Problem Definition: Predict the surface area needed to both cool and condense pyrolysis bio-oil from a mixture of gases. The second condenser will condense the phenols from the gas stream. The inlet temperature of the gas is 150C and the outlet temperature of the gas is 100C. The wall temperature will be held constant at 65C. The initial partial pressure of the phenol is 0.029. The mass flowrate of the bulk gases is equal to 19 kg/hr and can be approximated as nitrogen gas and the given temperature. The concentration at the walls is assumed to be equal to 0 and 95% of the Phenol is removed.

Given:

Flow Temperatures:

$T_{in} := (150 + 273)K$ Temperature of the incoming gas

$T_{out} := (100 + 273)K$ Temperature of the outflowing gas

$T_w := (65 + 273)K$ Temperature of the walls

Mass Flow Rates:

$m_{biomass} := 8$

$m_{N2} := \left(13 + m_{biomass} \cdot .75\right)\frac{kg}{hr}$ Mass flow of the nitrogen

$m_L := (8 \cdot .24)\frac{kg}{hr}$ Theoretical mass flow of the Phenol

Partial Pressures:

$P_{sat} := .015$ Saturation Pressure at Wall Temperater

$P_{in} := .029$ Incoming partial pressure

$P_{out} := .0175$ Out flowing partial pressure

Required Properties:

$Cp_{N2} := 1.045\frac{J}{gm \cdot K}$

$H_{vapL} := 488.46\frac{J}{gm}$

$\mu_{N2} := 220.4 \cdot 10^{-7}\frac{N \cdot sec}{m^2}$

$k_{N2} := 32.7 \cdot 10^{-3}\frac{W}{m \cdot K}$

$\rho_{N2} := .8425\frac{kg}{m^3}$

$D_{AB} := .399\frac{cm^2}{sec}$

$\nu_{N2} := 26.16 \cdot 10^{-6}\frac{m^2}{sec}$

$M_L := 94.11\frac{gm}{mol}$

$M_{N2} := 14\frac{kg}{mol}$

$Pr_{N2} := .711$

Heat Transfer:

The total heat must contain both the sensible heat of the gas flow cooling and the latent heat of the Phenol. The equation above contains first the sensible heat. This assumes that the entire flow is nitrogen and is cooling from 400 to 150. The latent heat assumes that only 95% of the Phenol is removed.

q_{total} =(Sensible heat for Nitrogen)+(Latent Heat for Phenol)

$$q_{total} := m_{N2} \cdot Cp_{N2} \cdot \left(T_{in} - T_{out}\right) + .4 m_L \cdot H_{vapL}$$

Heat transfer for Condenser Design:

The condenser is being designed as a constant surface temperature, shell and tube heat exchanger. The flow will be designed to be laminar to reduce the chance that aerosols will impinge on the condenser walls. The flow is made of mainly nitrogen and there is phenol vapors present that will be condensed from the flow.

$q_{total} = h_d \cdot A_s \cdot \Delta T_{lm}$

Where:

q_{total}= total heat removed

h_d= convective heat transfer coefficient

A_s= Surface area

ΔT_{lm}= Log-mean temperature difference

The goal is to determine the amount of surface area required to remove the required heat. This will be done by following the procedure listed below:

1. Assume D and L the tubes and the number of tubes
2. Calculate the Reynolds number and adjust D and number of tubes to ensure that flow is laminar
3. Find correlation for Nu and Calculate Nu
4. Determine h_d
5. Calculate ΔT_{lm}
6. Calculate A_s
7. Calculate L and iterate it back. If ok porceed to mass transfer analysis

1. Assume Diameter, Length and Number of Tubes

$D := 1in \qquad N := 23 \qquad L := 24in$

2. Reynolds Number:

The calculation of the Reynolds Number is important to perform first to check to see if the flow is laminar of turbulent. The outcome of this calculation will help us decide what Nussetl number will be used with the problem. Initial assumptions include that the entire flow is nitrogen.

$$Re_d := \frac{4 \cdot m_{N2}}{\pi \cdot D \cdot \mu_{N2} \cdot N} \qquad Re_d = 521.901$$

Adjust D and N if not laminar

3. Nussetl Number

$$Nu_d := 1.86\left(\frac{Re_d \cdot Pr_{N2}}{\frac{L}{D}}\right)^{\frac{1}{3}} \qquad Nu_d = 4.634$$

Because the flow is laminar through the tubes and fully developed the preceeding correlation can be used to calculate the Nussetl Number. This correlation can be found in Incropera (equation 8.57)

4. Heat Transfer Coefficient:

$$Nu_d = \frac{h_d \cdot k_{N2}}{D} \qquad h_d := \frac{k_{N2}}{D} \cdot Nu_d \qquad h_d = 5.965 \frac{W}{m^2 K}$$

The Nussetl number can then be used to calculate a heat transfer coefficient. This heat transfer coefficient is then insterted into the heat equation.

5. Log-Mean Temerature Difference:

$$\Delta T_{lm} := \frac{(T_{out} - T_w) - (T_{in} - T_w)}{\ln\left[\frac{(T_{out} - T_w)}{(T_{in} - T_w)}\right]} \qquad \Delta T_{lm} = 56.351\,K$$

$T_{in} = 423\,K$

$T_{out} = 373\,K$

$T_w = 338\,K$

The final piece of information needed to calculate the required area is the log-mean temperature difference. This equation comes from simple heat exchanger design. This takes into account the changing temperature within the tube. The wall temperature is held constant.

6. and 7. Surface Area and Tube Length

$$A_s := \frac{q_{total}}{h_d \cdot \Delta T_{lm}} \qquad L := \frac{A_s}{\pi \cdot D \cdot N^*}$$

$A_s = 1.752 \times 10^3\,in^2$ $\qquad L = 24.247\,in$

The surface area required to achomplish the desired heat removal is shown above, along with length of tubes required to achomplish the heat transfer. Note that the length of tube is not effected by diameter.

The procedure of design based on mass transfer is similar to the design based on heat transfer.

1. Use tube dimensions and Reynolds number from previous work.
2. Calculate Sc Number
3. Find correlation for Sh and Calculate Sh
4. Determine h_m
5. Calculate ΔP_{lm}
6. Calculate A_s
7. Calculate L and iterate it back. If ok porceed to mass transfer analysis

1. Tube Dimensions and Reynold's Number

The tube dimensions are taken from the heat transfer design. The goal of these calculations are to calculate the required area.

$D = 1\,in \qquad L = 24.247\,in \qquad N = 23$

2. Schmidt Number:

The Schmidt number is the ratio of the momentum and mass diffusivities. This dimensionless value is used to calculate a Sherwood number and is calculated from known/assumed properties.

$$Sc := \frac{\nu_{N2}}{D_{AB}} \qquad Sc = 0.656$$

3. Sherwood Number:

The Sherwood Number is a dimensionless value that is analogus to the Nusselt number. It is a dimensionless concentration gradient on the surface in which the condensation is taking place. This value will allow us to calculate a mass transfer coefficient.

$$Sh_d := 1.86\left(\frac{Re_d \cdot Sc}{\frac{L}{D}}\right)^{\frac{1}{3}} \qquad Sh_d = 4.495$$

4. Mass Transfer Coefficient:
The mass transfer coefficient is similar to the convective heat transfer coefficient.

$$h_m := \frac{Sh_d \cdot D_{AB}}{D} \qquad h_m = 7.061 \times 10^{-3}\,\frac{m}{s}$$

5. Log-Mean Partial Pressure Difference:
The purpose of this value is to take into account the change in partial pressures through the condenser. The pressure at the wall is the saturation pressure.

$$\Delta P_{lm} := \frac{\left(P_{out} - P_{sat}\right) - \left(P_{in} - P_{sat}\right)}{\ln\left[\frac{\left(P_{out} - P_{sat}\right)}{\left(P_{in} - P_{sat}\right)}\right]} \qquad \Delta P_{lm} = 6.675 \times 10^{-3}$$

$P_{out} = 0.018$

$P_{in} = 0.029$

$P_{sat} = 0.015$

6. and 7. Surface Area Check and Length Calculation:

$$A_{s\_check} := \frac{m_L \cdot M_{N2}}{h_m \cdot \rho_{N2} \cdot M_L \cdot \Delta P_{lm}} \qquad L := \frac{A_{s\_check}}{\pi \cdot D \cdot N}*$$

$$A_{s\_check} = 3.097 \times 10^{6}\ in^2 \qquad L = 4.286 \times 10^{4}\ in$$

Assumes that cooling occurs first and mass is transfered second.

ESP Design

ESP 1

ε := "Permitivity of Phenol from CRC Handbook"

$\varepsilon := 12.4$

L_t := "Length of Tube"

Δw := "Change in Voltage Input"

$\Delta w := 25000V$

$L_t := 48in$

d := "Diameter of Aerosol Particles"

$d := 3 \cdot 10^{-6} m$

η := "Vescosity"

$\eta := 1.76 \cdot 10^{-5} N \cdot \frac{s}{m^2}$

K_e := "Electrostatic Constant of Proportionality"

$K_e := 9 \cdot 10^{9} N \cdot \frac{m^2}{C^2}$

C_c := "Slip Correction Factor"

$C_c := 1.051$

e := "Electron"

$e := 1.6 \cdot 10^{-19} C$

Q := "Volumetric Flow Rate"

$Q := 260 \frac{liter}{min}$

Z_i := "Ion Mobility"

$Z_i := .00015 \frac{m^2}{V \cdot s}$

N_i := "Ion Number Concentration"

$N_i := \frac{10^{13}}{m^3}$

d_t := "Diameter of Tube"

$d_t := 6.357in$

d_w := "Diameter of Wire"

$d_w := 1in$

R := "Radius of Tube"

$R := \frac{d_t}{2}$

A_t := "Area of Tube"

$A_t := \pi \cdot R^2$

$E := \text{"Electric Field"}$ $t_t := \text{"Total Time in Apparatus"}$ $t := \text{"Time Exposed to Electrode"}$

$$E := \frac{\Delta w}{R \cdot \ln\left(\frac{d_t}{d_w}\right)} \qquad t_t := \frac{(A_t \cdot L_t)}{Q} \qquad t := \frac{t_t}{2}$$

$$E = 167423.516 \frac{V}{m} \qquad t_t = 5.761\,s \qquad t = 2.881\,s$$

$n := \text{"Number of Charges"}$

$$n := \left[\frac{(3 \cdot \varepsilon)}{\varepsilon + 2}\right] \cdot \left[\frac{\left(E \cdot d^2\right)}{(4 \cdot K_e \cdot e)}\right] \cdot \left[\frac{(\pi \cdot K_e \cdot e \cdot Z_i \cdot N_i \cdot t)}{1 + \pi \cdot K_e \cdot e \cdot Z_i \cdot N_i \cdot t}\right]$$

$n = 642.908$

$V_{TE} := \text{"Thermal Electric Velocity"}$

$$V_{TE} := \frac{(n \cdot e \cdot E \cdot C_c)}{3 \cdot \pi \cdot \eta \cdot d}$$

$$V_{TE} = 3.637 \frac{cm}{sec}$$

$E := \text{"Efficiency"}$

$$E := 1 - \exp\left[\left[\frac{-(V_{TE} \cdot 2 \cdot \pi \cdot R \cdot L_t)}{Q}\right]\right]$$

$E = 0.994$

$$\eta := 1 - \exp\left[-\left[\frac{V_{TE} \cdot (2 \cdot \pi \cdot R \cdot L_t)}{Q}\right]^{\frac{1}{2}}\right]$$

$\eta = 0.898$

$$\frac{2 \cdot \pi \cdot R \cdot L_t}{Q} = 39.645 \frac{m^2}{1000 \frac{m^3}{hr}}$$

APPENDIX B

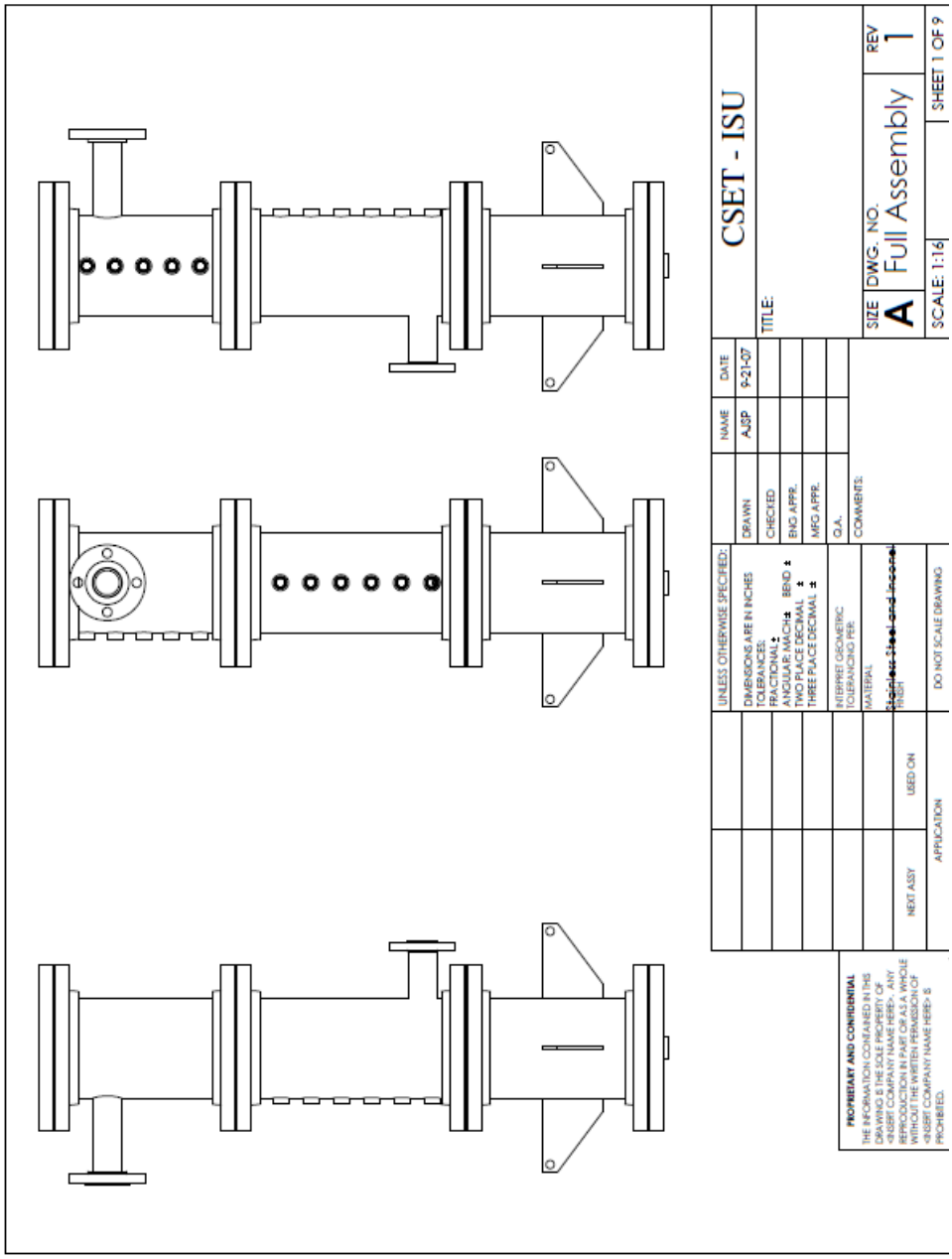
CSET - ISU
TITLE:
SIZE A
DWG. NO. Full Assembly
REV 1
SCALE: 1:16
SHEET 1 OF 9
DRAWN AJSP 9-21-07
CHECKED
ENG APPR.
MFG APPR.
Q.A.
COMMENTS:
UNLESS OTHERWISE SPECIFIED:
DIMENSIONS ARE IN INCHES
TOLERANCES:
FRACTIONAL ±
ANGULAR: MACH ± BEND ±
TWO PLACE DECIMAL ±
THREE PLACE DECIMAL ±
INTERPRET GEOMETRIC TOLERANCING PER:
MATERIAL
Stainless Steel and Inconel
FINISH
DO NOT SCALE DRAWING
NEXT ASSY
USED ON
APPLICATION
PROPRIETARY AND CONFIDENTIAL
THE INFORMATION CONTAINED IN THIS DRAWING IS THE SOLE PROPERTY OF <INSERT COMPANY NAME HERE>. ANY REPRODUCTION IN PART OR AS A WHOLE WITHOUT THE WRITTEN PERMISSION OF <INSERT COMPANY NAME HERE> IS PROHIBITED.

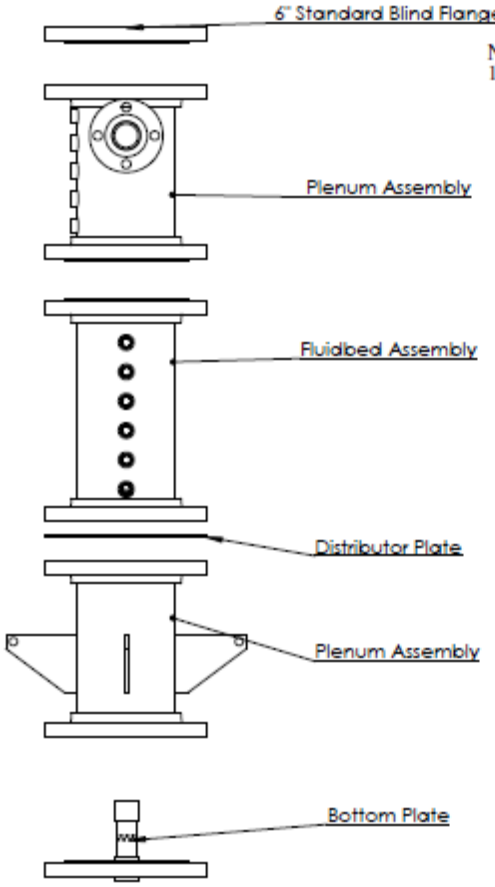

Notes:
1. The Gussets, half couplings, and 2 large ports must all be 90 degrees from one another.

		DIMENSIONS ARE IN INCHES		NAME	DATE
		TOLERANCES:	DRAWN		
		FRACTIONAL ±	CHECKED		
		ANGULAR: MACH ± BEND ±	ENG APPR.		
		TWO PLACE DECIMAL ±	MFG APPR.		
		THREE PLACE DECIMAL ±	Q.A.		
		MATERIAL	COMMENTS:		
		FINISH			
NEXT ASSY	USED ON				
APPLICATION		DO NOT SCALE DRAWING			

SIZE	DWG. NO.	REV.
A	Full Assembly	
SCALE: 1/4	WEIGHT:	SHEET 2 OF 9

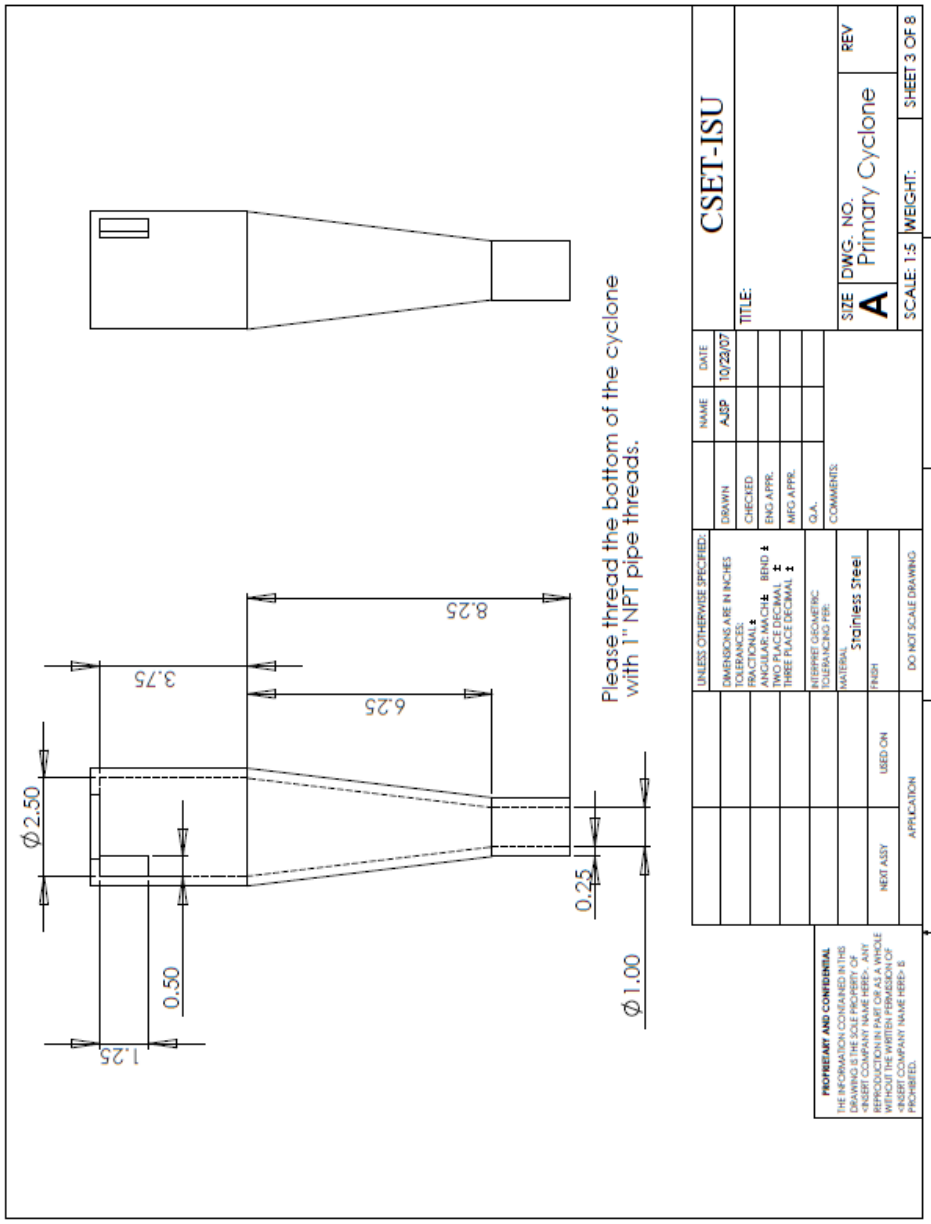
Please thread the bottom of the cyclone with 1" NPT pipe threads.
8.25
6.25
3.75
Ø2.50
0.50
1.25
0.25
Ø1.00
CSET-ISU
TITLE:
SIZE A
DWG. NO. Primary Cyclone
REV
SCALE: 1:5
WEIGHT:
SHEET 3 OF 8
UNLESS OTHERWISE SPECIFIED:
DIMENSIONS ARE IN INCHES
TOLERANCES:
FRACTIONAL ±
ANGULAR: MACH ± BEND ±
TWO PLACE DECIMAL ±
THREE PLACE DECIMAL ±
INTERPRET GEOMETRIC TOLERANCING PER:
MATERIAL
Stainless Steel
FINISH
DO NOT SCALE DRAWING
DRAWN
CHECKED
ENG APPR.
MFG APPR.
Q.A.
COMMENTS:
NAME
AJSP
DATE
10/29/07
NEXT ASSY
USED ON
APPLICATION
PROPRIETARY AND CONFIDENTIAL
THE INFORMATION CONTAINED IN THIS DRAWING IS THE SOLE PROPERTY OF <INSERT COMPANY NAME HERE>. ANY REPRODUCTION IN PART OR AS A WHOLE WITHOUT THE WRITTEN PERMISSION OF <INSERT COMPANY NAME HERE> IS PROHIBITED.

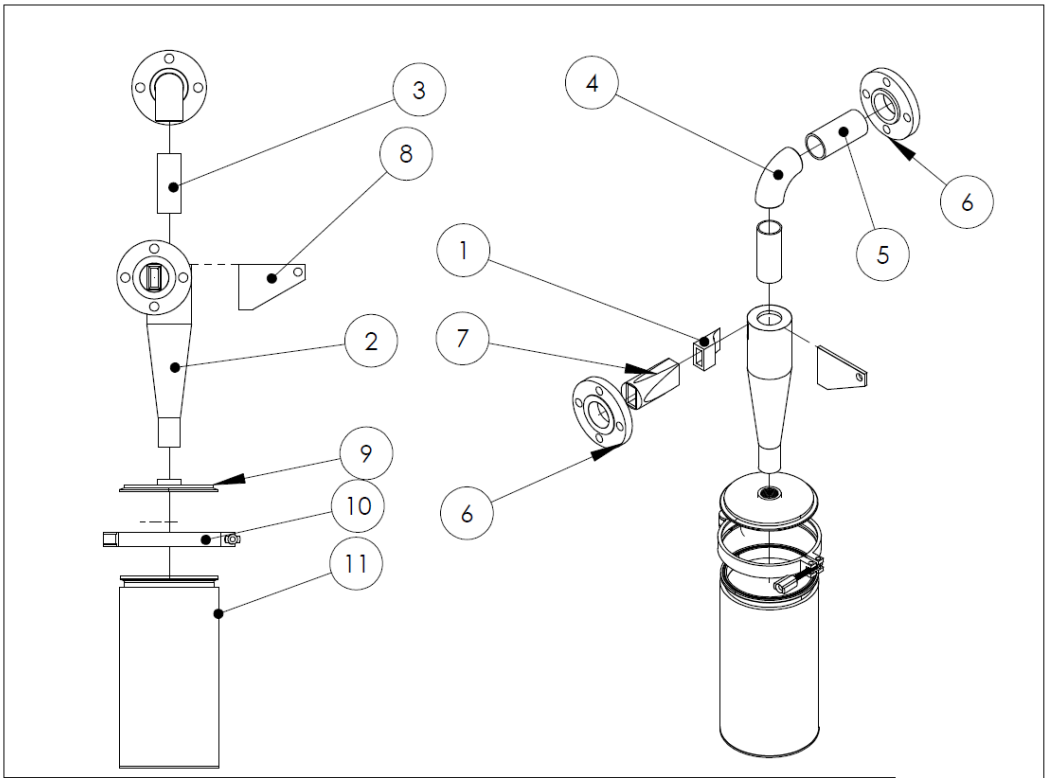

ITEM NO.	PART NUMBER	DESCRIPTION	QTY.
1	Primary Entry	Stainless Steel	1
2	Primary Cyclone	Stainless Steel	1
3	1.25" X 4" Sch. 10	Stainless Steel	1
4	1.5" pipe 90	Stainless Steel	1
5	1.5" X 4" pipe	Stainless Steel	1
6	1.5" Flange	Stainless Steel	2
7	Primary Transition	Stainless Steel	1
8	Primary Cyclone Gusset	Stainless Steel	1
9	6" Blind, Modified	Stainless Steel	1
10	6" Sanitary Clamp	Stainless Steel	1
11	Cyclone Catch	Stainless Steel	1

NEXT ASSY | USED ON
APPLICATION

DIMENSIONS ARE IN INCHES
TOLERANCES:
FRACTIONAL ±
ANGULAR: MACH ± BEND ±
TWO PLACE DECIMAL ±
THREE PLACE DECIMAL ±
MATERIAL
FINISH
DO NOT SCALE DRAWING

	NAME	DATE
DRAWN		
CHECKED		
ENG APPR.		
MFG APPR.		
Q.A.		

COMMENTS:

SIZE A | DWG. NO. Primary Cyclone Assem. | REV.
SCALE:1:5 | WEIGHT: | SHEET 1 OF 8

APPENDIX C

Table 11 Fast Pyrolysis Mass Balance

Test #	Biomass	Char 1	SF1	SF2	SF3	SF4	SF5	NCG
1-20090619	Red Oak	23.0%	12.4%	14.0%	3.3%	6.5%	20.5%	25.0%
1-20090622	Red Oak	24.0%	11.9%	12.3%	2.9%	8.1%	21.8%	26.5%
1-20090731	Red Oak	19.9%	11.0%	18.0%	2.9%	4.0%	18.0%	29.3%
	Average	**22.3%**	**11.7%**	**14.8%**	**3.0%**	**6.2%**	**20.1%**	**26.9%**
1-20090629	Cornstover	31.0%	3.9%	8.0%	1.8%	5.6%	26.2%	28.1%
1-20090630	Cornstover	27.3%	9.0%	7.9%	2.6%	5.1%	25.4%	29.9%
1-20090702	Cornstover	27.9%	9.1%	9.0%	2.6%	5.2%	26.7%	31.1%
	Average	**28.8%**	**7.3%**	**8.3%**	**2.3%**	**5.3%**	**26.1%**	**29.7%**
1-20090707	Switchgrass	22.5%	8.5%	12.2%	3.3%	5.3%	23.0%	36.8%
1-20090709	Switchgrass	32.2%	10.5%	13.2%	2.9%	5.3%	23.3%	24.9%
1-20090710	Switchgrass	23.8%	9.5%	14.3%	3.1%	4.1%	24.4%	22.8%
	Average	**26.2%**	**9.5%**	**13.3%**	**3.1%**	**4.9%**	**23.6%**	**28.2%**

Table 12 Bio-oil Analysis 1-20090619

1-20090619-Red Oak						
Fraction	**SF1**	**SF2**	**SF3**	**SF4**	**SF5**	**Total**
Mass Balance (kg)	0.93	1.05	0.25	0.49	1.53	4.25
Char Collected (kg)	1.72					
Non-Condensable Gases (kg)	1.87					
	SF1	**SF2**	**SF3**	**SF4**	**SF5**	**Mass Averaged Total**
Karl Fischer (% Moisture)	7.4	7.2	9.5	12.7	63.5	28.3
MAN (mg KOH/g)	35.9	30.6	82.1	112.9	120.3	76.6
Insolubles (%)	0.4	0.5	0.1	0.1	0.0	0.2
Solids (%)	0.0	0.0	0.0	0.0	0.0	0.0
HHV (MJ/kg)	23.8	24.4	20.1	19.1	7.2	17.2
Elemental (%wt, Wet Basis)						
C	62.2	64.1	52.0	51.4	42.3	53.7
H	5.5	5.4	5.8	5.6	1.8	4.2
N	0.1	0.1	0.0	0.0	-0.2	0.0
S	0.0	0.0	0.0	0.0	0.0	0.0
O by Difference	27.8	27.8	37.5	35.6	19.3	26.2
Ash	1.8	0.0	0.2	1.4	0.1	0.6
Other Analysis (wt% bio-oil)						
Water	7.4	7.2	9.5	12.7	63.5	28.3
Solids	2.4	4.7	0.7	1.4	0.5	2.1
Water Insolubles	40.0	46.4	6.9	12.9	0.8	22.4
Undetectable	9.6	16.1	43.9	37.9	27.8	23.0
GC/MS Detectable Compounds						
Levoglucosan	10.8	6.5	1.1	1.1	0.0	4.2
Acetic Acid	2.3	2.7	11.0	12.3	0.4	3.4
Furans	2.8	2.9	4.4	3.6	0.2	2.1
Phenols	2.2	0.9	1.7	3.4	0.3	1.3
Guiacols	2.7	1.3	2.3	0.9	0.4	1.3
Syringols	6.6	3.1	2.6	0.8	0.3	2.6
Other GS/MS Detected Compounds	13.1	8.0	16.1	13.0	5.8	9.4

Table 13 Bio-oil Analysis 1-20090622

1-20090622-Red Oak						
Fraction	**SF1**	**SF2**	**SF3**	**SF4**	**SF5**	**Total**
Mass Balance (kg)	0.80	0.83	0.20	0.55	1.48	3.85
Char Collected (kg)	1.62					
Non-Condensable Gases (kg)	1.79					
	SF1	**SF2**	**SF3**	**SF4**	**SF5**	**Mass Averaged Total**
Karl Fischer (% Moisture)	4.9	9.5	8.2	10.3	63.3	29.2
MAN (mg KOH/g)	33.4	30.6	71.6	93.9	118.0	75.7
Insolubles (%)	0.4	0.5	0.1	0.2	0.0	0.2
Solids (%)	0.0	0.0	0.0	0.0	0.0	0.0
HHV (MJ/kg)	24.1	24.5	20.3	20.7	7.0	17.0
Elemental (%wt, Dry Basis)						
C	62.1	65.2	52.5	55.3	43.2	54.1
H	5.7	5.2	6.0	5.6	1.8	4.1
N	0.1	0.1	0.0	0.0	-0.3	0.0
S	0.0	0.0	0.0	0.0	0.0	0.0
O by Difference	25.7	24.8	37.2	33.5	19.2	24.7
Ash	4.8	1.6	0.4	1.1	0.0	1.5
Other Analysis (wt% bio-oil)						
Water	4.9	9.5	8.2	10.3	63.3	29.2
Solids	0.0	0.0	0.0	0.0	0.0	0.0
Water Insolubles	44.0	45.7	11.5	23.3	0.8	23.2
Undetectable	35.8	32.9	51.4	32.8	7.6	24.7
GC/MS Detectable Compounds						
Levoglucosan	5.3	2.6	2.5	1.2	1.0	2.3
Acetic Acid	0.0	0.0	6.8	8.7	12.4	6.3
Furans	0.5	0.5	3.3	3.4	1.1	1.3
Phenols	1.3	1.1	1.8	7.6	0.6	1.9
Guiacols	1.3	1.2	1.9	0.9	0.5	0.9
Syringols	3.0	2.7	2.4	0.8	1.2	1.9
Other GS/MS Detected Compounds	4.0	3.8	10.2	11.1	11.5	8.2

Table 14 Bio-oil Analysis 1-20090731

1-20090731-Red Oak						
Fraction	**SF1**	**SF2**	**SF3**	**SF4**	**SF5**	**Total**
Mass Balance (kg)	2.19	3.59	0.59	0.80	3.60	10.76
Char Collected (kg)	3.97					
Non-Condensable Gases (kg)	5.84					
	SF1	**SF2**	**SF3**	**SF4**	**SF5**	**Mass Averaged Total**
Karl Fischer (% Moisture)	4.7	6.8	10.3	21.3	65.9	27.4
MAN (mg KOH/g)	35.4	33.7	83.5	144.4	110.7	70.7
Insolubles (%)	0.5	0.4	0.1	0.0	0.0	0.3
Solids (%)	0.0	0.0	0.0	0.0	0.0	0.0
HHV (MJ/kg)	24.7	24.4	20.2	16.3	6.5	17.7
Elemental (%wt, Dry Basis)						
C	62.5	63.1	52.2	47.9	42.2	54.3
H	5.8	5.7	5.9	4.8	1.6	4.3
N	0.5	0.1	0.0	0.0	-0.2	0.1
S	0.0	0.0	0.0	0.0	0.0	0.0
O by Difference	29.0	28.4	36.7	32.1	18.1	25.8
Ash	0.4	0.3	0.3	5.2	0.2	0.7
Other Analysis (wt% bio-oil)						
Water	4.7	6.8	10.3	21.3	65.9	27.4
Solids	0.0	0.0	0.0	0.0	0.0	0.0
Water Insolubles	48.6	43.8	6.3	3.1	0.7	25.3
Undetectable	3.4	20.5	43.9	35.4	-2.5	11.7
GC/MS Detectable Compounds						
Levoglucosan	14.1	8.5	1.3	0.8	0.0	5.9
Acetic Acid	2.9	3.8	8.2	19.1	14.6	8.6
Furans	3.2	2.9	4.5	3.4	3.6	3.3
Phenols	2.3	1.0	1.8	3.1	0.4	1.3
Guiacols	3.2	1.7	2.7	0.6	0.6	1.6
Syringols	6.3	3.5	2.9	0.6	0.0	2.7
Other GS/MS Detected Compounds	11.3	7.4	18.1	12.7	16.7	12.3

Table 15 Bio-oil Analysis 1-20090629

1-20090629-Cornstover						
Fraction	**SF1**	**SF2**	**SF3**	**SF4**	**SF5**	**Total**
Mass Balance (kg)	1.02	0.89	0.29	0.58	2.88	5.67
Char Collected (kg)	0.98					
Non-Condensable Gases (kg)	0.89					
	SF1	**SF2**	**SF3**	**SF4**	**SF5**	**Mass Averaged Total**
Karl Fischer (% Moisture)	5.6	6.8	12.2	23.2	79.9	45.7
MAN (mg KOH/g)	23.9	23.6	45.2	82.0	42.1	40.2
Insolubles (%)	0.7	0.6	0.3	0.1	0.0	0.2
Solids (%)	0.1	0.1	0.0	0.0	0.0	0.0
HHV (MJ/kg)	26.8	27.4	23.2	19.1	4.0	14.3
Elemental (%wt, Dry Basis)						
C	67.2	69.3	60.7	55.5	41.6	53.0
H	5.9	6.0	6.0	5.2	-0.1	2.8
N	1.5	0.8	0.7	0.3	-0.4	0.4
S	0.0	0.0	0.1	0.1	0.1	0.1
O by Difference	23.3	21.1	27.6	27.0	11.9	17.8
Ash	0.3	0.9	0.2	2.1	0.0	0.4
Other Analysis (wt% bio-oil)						
Water	5.6	6.8	12.2	23.2	79.9	45.7
Solids	0.1	0.1	0.0	0.0	0.0	0.0
Water Insolubles	66.4	61.3	26.4	14.3	0.6	24.8
Undetectable	1.6	6.9	25.3	28.2	-3.6	3.7
GC/MS Detectable Compounds						
Levoglucosan	4.5	4.3	1.2	1.0	0.0	1.7
Acetic Acid	4.6	1.7	5.1	7.9	4.0	4.2
Furans	3.7	3.4	4.3	4.8	0.8	2.3
Phenols	2.2	2.5	4.3	4.3	0.6	1.8
Guiacols	1.6	1.9	2.5	0.9	0.4	1.0
Syringols	2.2	2.4	2.1	0.7	0.0	0.9
Other GS/MS Detected Compounds	7.5	8.7	16.6	14.7	17.3	13.9

Table 16 Bio-oil Analysis 1-20090630

1-20090630-Cornstover						
Fraction	**SF1**	**SF2**	**SF3**	**SF4**	**SF5**	**Total**
Mass Balance (kg)	1.03	1.02	0.30	0.60	3.04	5.99
Char Collected (kg)	3.10					
Non-Condensable Gases (kg)	3.40					
	SF1	**SF2**	**SF3**	**SF4**	**SF5**	**Mass Averaged Total**
Karl Fischer (% Moisture)	5.8	4.2	13.2	18.3	76.9	43.2
MAN (mg KOH/gram)	23.5	21.2	48.4	89.7	42.4	40.5
Insolubles (%)	0.7	0.6	0.2	0.2	0.0	0.3
Solids (%)	0.1	0.1	0.0	0.0	0.0	0.0
HHV (MJ/kg)	26.8	27.6	22.9	16.8	4.2	14.3
Elemental (%wt, Dry Basis)						
C	68.1	68.0	60.3	43.3	35.3	48.6
H	5.9	6.2	6.0	6.0	0.1	3.0
N	1.6	0.9	0.5	0.2	-0.2	0.4
S	0.0	0.0	0.1	0.1	0.1	0.0
O by Difference	22.3	23.3	27.6	37.5	14.9	20.5
Ash	0.4	0.3	0.4	3.0	0.2	0.6
Other Analysis (wt% bio-oil)						
Water	5.8	4.2	13.2	18.3	76.9	43.2
Solids	5.3	8.7	0.5	0.8	0.6	2.8
Water Insolubles	70.1	63.3	21.6	17.1	3.0	27.2
Undetectable	-2.3	0.9	22.3	30.7	-3.6	2.1
GC/MS Detectable Compounds						
Levoglucosan	2.9	3.9	1.0	0.9	0.0	1.3
Acetic Acid	1.1	1.3	6.2	8.9	4.0	3.6
Furans	3.3	3.3	4.9	4.2	0.8	2.2
Phenols	2.3	2.1	5.1	3.5	0.6	1.7
Guiacols	1.7	1.4	2.9	0.7	0.5	1.0
Syringols	2.2	2.3	2.1	0.6	0.0	0.9
Other GS/MS Detected Compounds	7.8	8.9	20.2	14.2	17.3	14.1

Table 17 Bio-oil Analysis 1-20090702

1-20090702-Cornstover						
Fraction	**SF1**	**SF2a**	**SF3**	**SF4**	**SF5**	**Total**
Mass Balance (kg)	1.03	1.02	0.30	0.60	3.04	5.99
Char Collected (kg)	3.18					
Non-Condensable Gases (kg)	3.54					
	SF1	**SF2**	**SF3**	**SF4**	**SF5**	**Mass Averaged Total**
Karl Fischer (% Moisture)	5.8	7.1	13.4	24.5	79.6	45.7
MAN (mg KOH/gram)	26.8	27.2	58.5	102.1	47.1	46.3
Insolubles (%)	0.7	0.6	0.2	0.1	0.0	0.2
Solids (%)	0.1	0.1	0.0	0.0	0.0	0.0
HHV (MJ/kg)	26.7	27.1	21.6	17.1	4.1	14.1
Elemental (%wt, Dry Basis)						
C	66.8	69.1	57.6	50.8	42.9	53.0
H	5.9	6.0	6.0	5.2	0.0	2.9
N	1.5	0.9	0.4	0.3	-0.3	0.4
S	0.0	0.0	0.1	0.1	0.1	0.1
O by Difference	24.0	20.8	29.0	28.5	11.5	17.8
Ash	0.0	1.2	1.5	4.2	0.8	1.1
Other Analysis (wt% bio-oil)						
Water	5.8	7.1	13.4	24.5	79.6	45.7
Solids	7.2	6.5	0.1	0.2	0.1	2.4
Water Insolubles	66.0	60.8	16.5	10.6	0.4	23.8
Undetectable	-0.5	1.9	28.2	20.7	-3.7	1.8
GC/MS Detectable Compounds						
Levoglucosan	2.3	3.2	1.0	0.0	0.0	1.0
Acetic Acid	1.3	2.4	7.5	12.3	5.0	4.8
Furans	3.5	3.4	4.3	4.3	0.9	2.3
Phenols	2.1	2.1	3.3	3.1	0.6	1.5
Guiacols	1.8	1.8	2.3	2.4	0.4	1.2
Syringols	2.4	2.4	1.9	1.9	0.0	1.1
Other GS/MS Detected Compounds	8.4	8.4	21.4	20.1	16.7	14.4

Table 18 Bio-oil Analysis 1-20090707

1-20090707-Switchgrass						
Fraction	**SF1**	**SF2**	**SF3**	**SF4**	**SF5**	**Total**
Mass Balance (kg)	1.46	2.20	0.47	0.63	3.74	6.30
Char Collected (kg)	4.76					
Non-Condensable Gases (kg)	7.78					
	SF1	**SF2**	**SF3**	**SF4**	**SF5**	**Mass Averaged Total**
Karl Fischer (% Moisture)	5.5	5.8	12.6	22.0	76.9	52.0
MAN (mg KOH/gram)	33.9	38.5	72.5	126.4	68.8	80.2
Insolubles (%)	0.6	0.5	0.1	0.1	0.0	0.3
Solids (%)	0.1	0.0	0.0	0.0	0.0	0.0
HHV (MJ/kg)	25.1	25.5	20.3	15.1	3.1	19.6
Elemental (%wt, Dry Basis)						
C	64.7	65.2	53.3	48.3	45.2	73.4
H	5.9	6.1	5.8	5.0	0.6	4.8
N	1.3	0.8	0.3	0.2	0.0	0.6
S	0.0	0.0	0.2	0.1	0.0	0.1
O by Difference	26.0	25.7	34.5	34.1	12.0	28.2
Ash	0.5	0.5	0.1	4.3	0.0	0.7
Other Analysis (wt% bio-oil)						
Water	5.5	5.8	12.6	22.0	76.9	52.0
Solids	5.3	4.3	0.9	0.3	0.4	3.0
Water Insolubles	64.9	50.9	7.8	5.5	1.2	34.6
Undetectable	-13.3	-4.3	13.1	18.9	-0.7	-2.1
GC/MS Detectable Compounds						
Levoglucosan	2.1	6.8	2.0	0.0	0.0	3.0
Acetic Acid	2.8	2.7	10.0	15.0	6.9	7.9
Furans	4.1	5.5	6.8	6.0	0.6	4.3
Phenols	3.5	4.2	5.2	4.7	0.9	3.7
Guiacols	4.9	4.9	5.2	4.9	0.9	4.3
Syringols	2.5	2.6	2.4	1.1	0.0	1.8
Other GS/MS Detected Compounds	17.7	16.7	34.1	21.7	12.9	22.3

Table 19 Bio-oil Analysis 1-20090709

1-20090709-Switchgrass						
Fraction	**SF1**	**SF2**	**SF3**	**SF4**	**SF5**	**Total**
Mass Balance (kg)	1.23	1.55	0.70	1.11	4.87	9.45
Char Collected (kg)	3.76					
Non-Condensable Gases (kg)	2.92					
	SF1	**SF2**	**SF3**	**SF4**	**SF5**	**Mass Averaged Total**
Karl Fischer (% Moisture)	4.0	4.7	13.8	27.8	76.1	44.8
MAN (mg KOH/gram)	38.5	39.7	73.8	129.1	68.2	67.3
Insolubles (%)	0.5	0.5	0.1	0.0	0.0	0.2
Solids (%)	0.0	0.0	0.0	0.0	0.0	0.0
HHV (MJ/kg)	24.8	25.8	18.1	15.2	5.1	13.2
Elemental (%wt, Dry Basis)						
C	63.2	64.3	52.8	47.8	43.2	50.5
H	6.0	6.2	5.7	4.5	0.7	3.1
N	1.2	0.8	0.3	0.2	-0.2	0.3
S	0.0	0.0	0.2	0.1	0.0	0.1
O by Difference	27.6	26.5	34.6	28.8	12.8	20.4
Ash	0.5	0.5	0.1	5.9	0.4	1.1
Other Analysis (wt% bio-oil)						
Water	4.0	4.7	13.8	27.8	76.1	44.8
Solids	2.8	4.6	0.4	0.1	0.1	1.1
Water Insolubles	52.8	49.6	7.2	4.2	0.1	16.0
Undetectable	17.7	18.9	40.1	32.8	2.5	13.5
GC/MS Detectable Compounds						
Levoglucosan	1.7	2.8	0.9	0.9	0.0	0.9
Acetic Acid	3.2	2.4	8.6	14.4	6.4	6.4
Furans	3.4	3.3	5.0	3.4	1.0	2.2
Phenols	1.6	1.5	2.2	3.0	0.4	1.2
Guiacols	1.8	1.8	2.5	0.7	0.4	1.0
Syringols	1.7	1.8	1.5	0.6	0.0	0.7
Other GS/MS Detected Compounds	9.2	8.7	17.9	11.9	13.0	12.0

Table 20 Bio-oil Analysis 1-20090710

1-20090710-Switchgrass						
Fraction	**SF1**	**SF2**	**SF3**	**SF4**	**SF5**	**Total**
Bio-oil Mass Balance (kg)	1.46	2.16	0.47	0.63	3.74	8.46
Char Collected (kg)	3.65					
Non-Condensable Gases (kg)	3.50					
	SF1	**SF2**	**SF3**	**SF4**	**SF5**	**Mass Averaged Total**
Karl Fischer (% Moisture)	5.4	4.0	11.9	24.8	70.5	35.6
MAN (mg KOH/gram)	35.2	39.3	68.2	125.6	75.7	62.7
Insolubles (%)	0.7	0.5	0.1	0.0	0.0	0.3
Solids (%)	0.1	0.0	0.0	0.0	0.0	0.0
HHV (MJ/kg)	25.5	26.5	20.3	15.3	5.6	15.9
Elemental (%wt, Dry Basis)						
C	65.0	64.4	53.4	46.8	41.0	52.2
H	5.7	6.3	5.9	4.7	0.8	3.6
N	1.3	0.8	0.2	0.2	0.1	0.4
S	0.0	0.0	0.2	0.2	0.1	0.1
O by Difference	25.4	27.0	34.6	30.5	16.5	22.8
Ash	0.8	0.2	0.3	6.0	0.7	1.0
Other Analysis (wt% bio-oil)						
Water	5.4	4.0	11.9	24.8	70.5	35.6
Solids	6.8	5.0	0.9	0.6	0.2	2.6
Water Insolubles	67.0	53.0	9.0	3.3	0.6	26.1
Undetectable	-0.1	14.9	39.5	36.9	-6.1	6.1
GC/MS Detectable Compounds						
Levoglucosan	1.8	4.0	0.9	0.9	0.0	1.5
Acetic Acid	3.3	2.6	8.4	14.0	9.5	6.9
Furans	3.3	3.2	4.3	3.7	3.5	3.5
Phenols	1.7	1.7	2.8	2.6	0.5	1.3
Guiacols	1.5	1.7	2.4	0.6	0.6	1.2
Syringols	1.6	1.6	1.4	0.5	0.0	0.8
Other GS/MS Detected Compounds	7.8	8.2	18.4	12.0	20.7	14.5

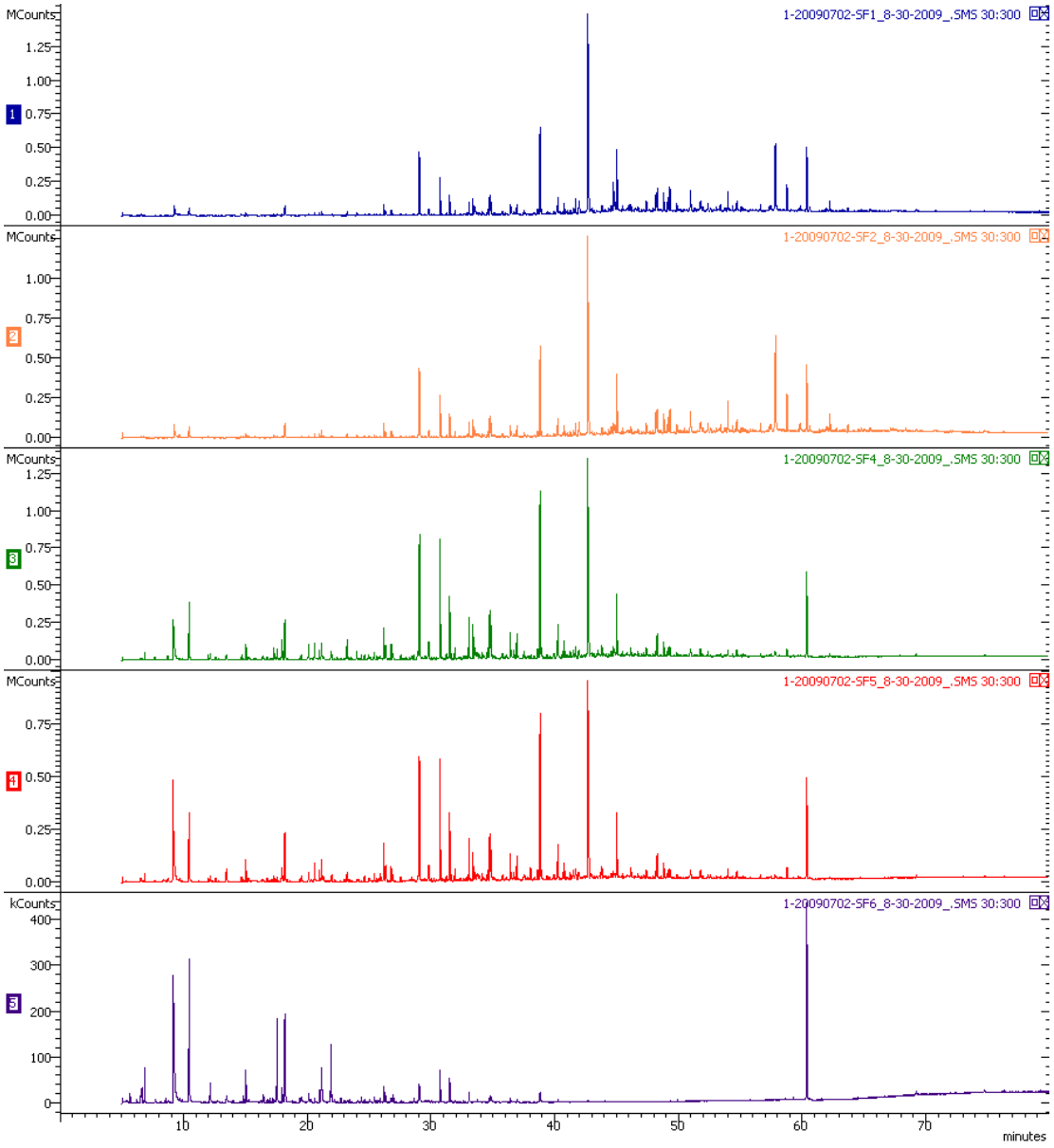

Figure 65 GC/MS Chromatogram for 1-20090702

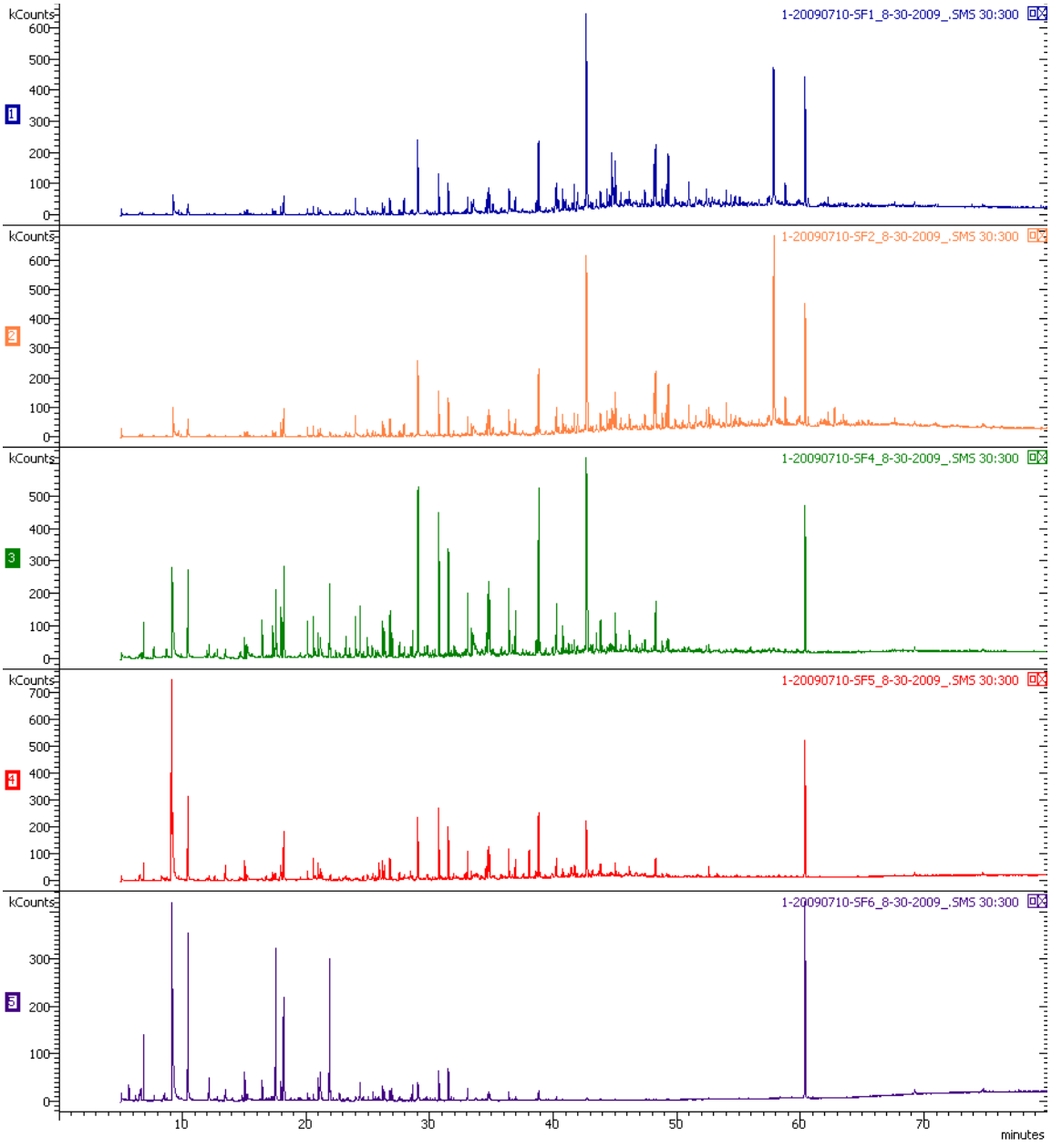

Figure 66 GC/MS Chromatograph for 1-20090710

APPENDIX D

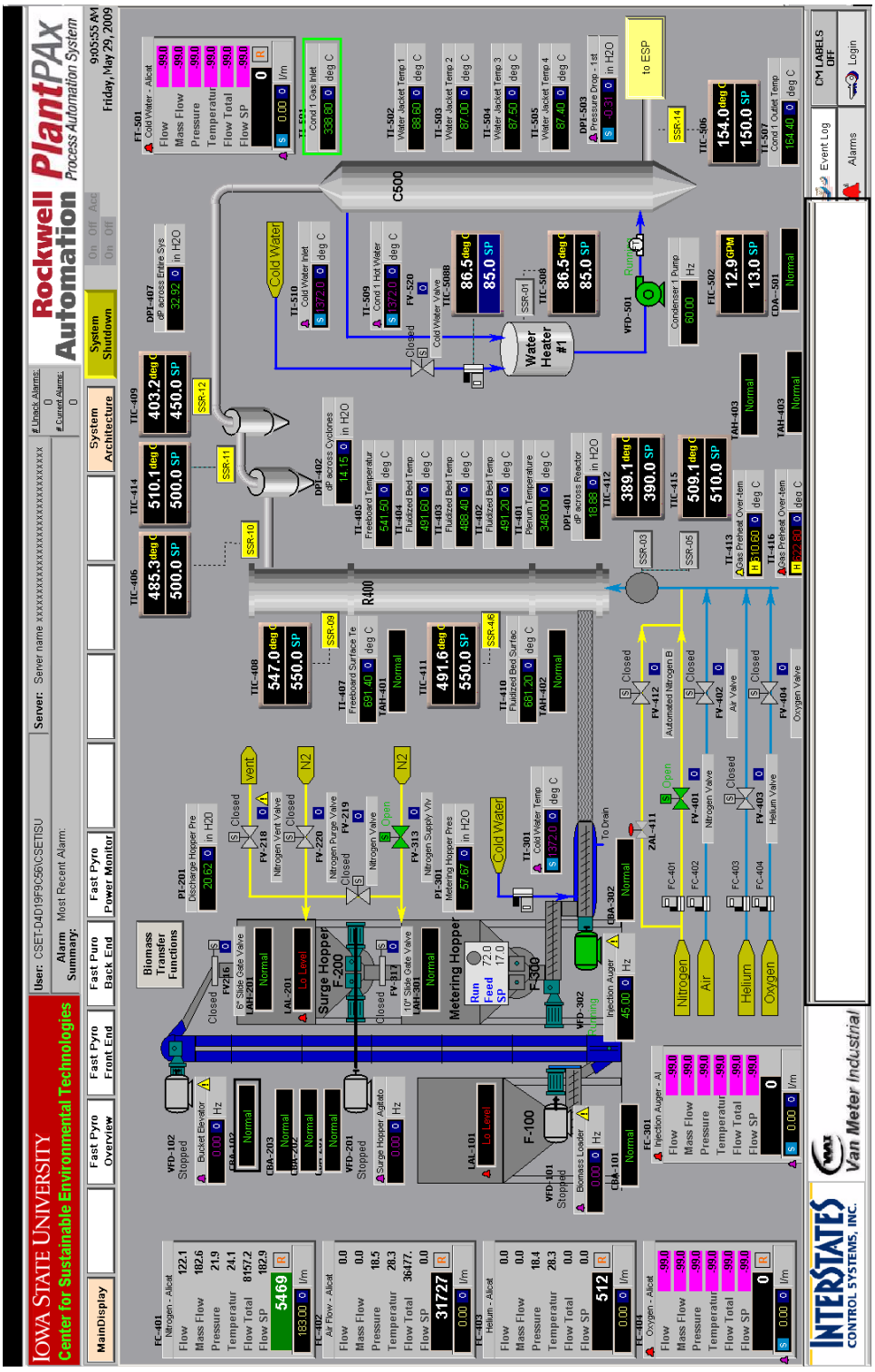
IOWA STATE UNIVERSITY
Center for Sustainable Environmental Technologies
Rockwell Automation
PlantPAx
Process Automation System
MainDisplay
Fast Pyro Overview
Fast Pyro Front End
Fast Puro Back End
Fast Pyro Power Monitor
System Architecture
System Shutdown
Biomass Transfer Functions
Surge Hopper F-200
Metering Hopper F-300
F-100
R400
C500
Water Heater #1
to ESP
Nitrogen
Air
Helium
Oxygen
INTERSTATES
CONTROL SYSTEMS, INC.
Van Meter Industrial

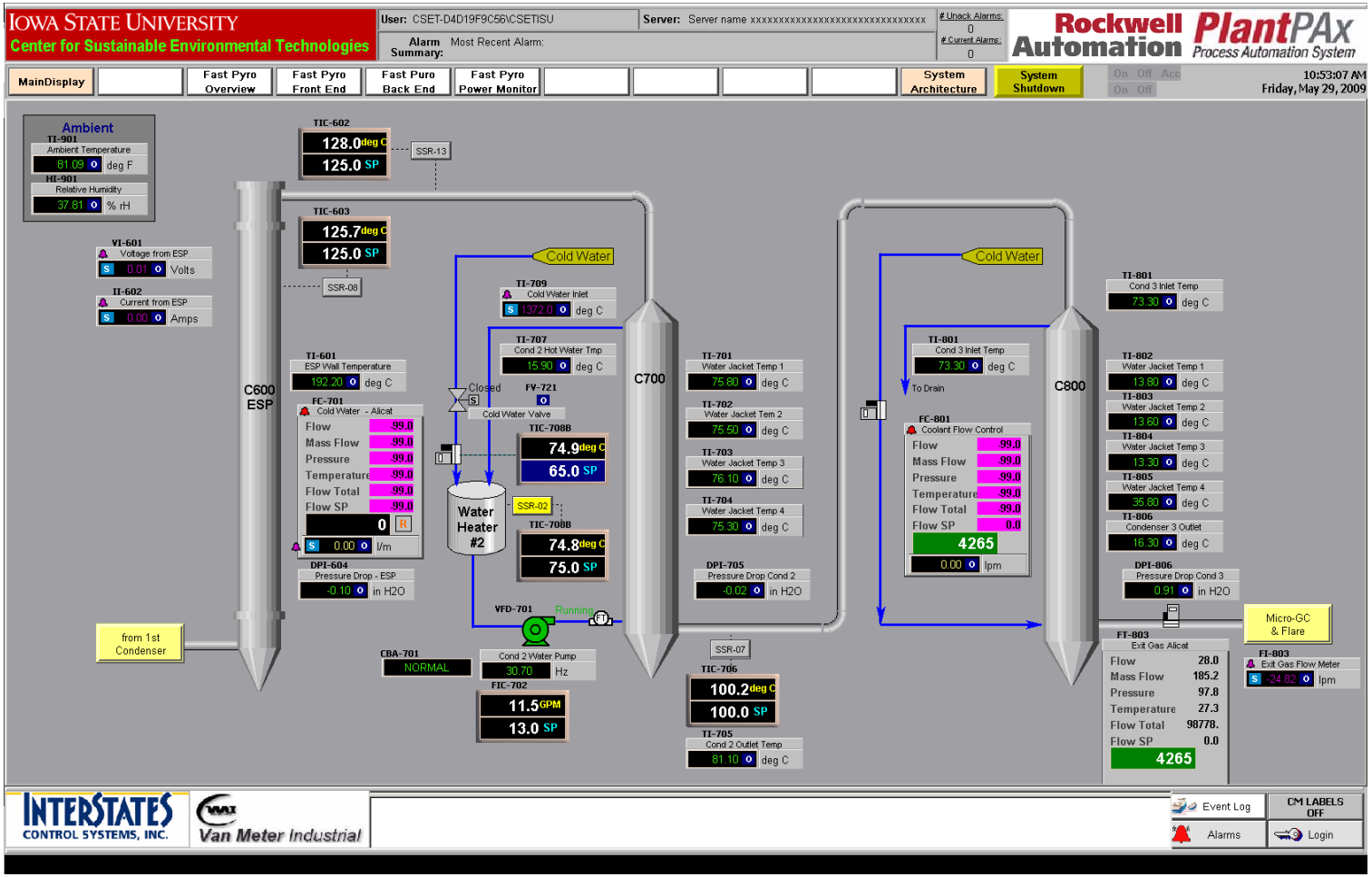
IOWA STATE UNIVERSITY
Center for Sustainable Environmental Technologies
User: CSET-D4D19F9C56\CSETISU
Server: Server name xxxxxxxxxxxxxxxxxxxxxxxxxxxxxxxx
Alarm Summary: Most Recent Alarm:
Unack Alarms: 0
Current Alarms: 0
Rockwell Automation PlantPAx Process Automation System
MainDisplay
Fast Pyro Overview
Fast Pyro Front End
Fast Puro Back End
Fast Pyro Power Monitor
System Architecture
System Shutdown
10:53:07 AM
Friday, May 29, 2009
Ambient
TI-901 Ambient Temperature 81.09 deg F
HI-901 Relative Humidity 37.81 % rH
VI-601 Voltage from ESP 0.01 Volts
II-602 Current from ESP 0.00 Amps
TIC-602 128.0 deg C 125.0 SP
SSR-13
TIC-603 125.7 deg C 125.0 SP
SSR-08
TI-601 ESP Wall Temperature 192.20 deg C
C600 ESP
FC-701 Cold Water - Alicat
Flow -99.0
Mass Flow -99.0
Pressure -99.0
Temperature -99.0
Flow Total -99.0
Flow SP -99.0
0 R
0.00 l/m
DPI-604 Pressure Drop - ESP -0.10 in H2O
from 1st Condenser
Cold Water
TI-709 Cold Water Inlet 1372.0 deg C
TI-707 Cond 2 Hot Water Tmp 15.90 deg C
Closed
FV-721 Cold Water Valve
TIC-708B 74.9 deg C 65.0 SP
Water Heater #2
SSR-02
TIC-708B 74.8 deg C 75.0 SP
VFD-701 Running
CBA-701 NORMAL
Cond 2 Water Pump 30.70 Hz
FIC-702 11.5 GPM 13.0 SP
C700
TI-701 Water Jacket Temp 1 75.80 deg C
TI-702 Water Jacket Tem 2 75.50 deg C
TI-703 Water Jacket Temp 3 76.10 deg C
TI-704 Water Jacket Temp 4 75.30 deg C
DPI-705 Pressure Drop Cond 2 -0.02 in H2O
SSR-07
TIC-706 100.2 deg C 100.0 SP
TI-705 Cond 2 Outlet Temp 81.10 deg C
Cold Water
TI-801 Cond 3 Inlet Temp 73.30 deg C
To Drain
FC-801 Coolant Flow Control
Flow -99.0
Mass Flow -99.0
Pressure -99.0
Temperature -99.0
Flow Total -99.0
Flow SP 0.0
4265
0.00 lpm
C800
TI-801 Cond 3 Inlet Temp 73.30 deg C
TI-802 Water Jacket Temp 1 13.80 deg C
TI-803 Water Jacket Temp 2 13.60 deg C
TI-804 Water Jacket Temp 3 13.30 deg C
TI-805 Water Jacket Temp 4 35.80 deg C
TI-806 Condenser 3 Outlet 16.30 deg C
DPI-806 Pressure Drop Cond 3 0.91 in H2O
Micro-GC & Flare
FT-803 Exit Gas Alicat
Flow 28.0
Mass Flow 185.2
Pressure 97.8
Temperature 27.3
Flow Total 98778.
Flow SP 0.0
4265
FI-803 Exit Gas Flow Meter -24.82 lpm
INTERSTATES CONTROL SYSTEMS, INC.
Van Meter Industrial
Event Log
CM LABELS OFF
Alarms
Login

BIBLIOGRAPHY

1. Wang, S.; Gu, Y.; Liu, Q.; Yao, Y.; Guo, Z.; Luo, Z.; Cen, K., Separation of bio-oil by molecular distillation. *Fuel Processing Technology* **2009,** 90, (5), 738-745.
2. Bridgwater, A. V., Biomass Fast Pyrolysis. *Thermal Science* **2004,** 8, (2), 21-49.
3. Incropera, F. P.; Dewitt, D. P.; Bergman, T. L.; Lavine, A. S., *Fundamentals of Heat and Mass Transfer*. 6th ed.; John Wiley & Sons: Hoboken, 2007.
4. Sinha, S., Modeling of Pyrolysis in Wood: A Review. *Solar Energy Society of India (SESI)* **2002,** 10, 1-17.
5. Boateng, A. A.; Daugaard, D. E.; Goldberg, N. M.; Hicks, K. B., Bench-scale fluidized-bed pyrolysis of switchgrass for bio-oil production. *Industrial and Engineering Chemistry Research* **2007,** 46, (7), 1891-1897.
6. Luo, Z.; Wang, S.; Liao, Y.; Zhou, J.; Gu, Y.; Cen, K., Research on biomass fast pyrolysis for liquid fuel. *Biomass and Bioenergy* **2004,** 26, (5), 455-462.
7. Predel, M.; Kaminsky, W., Pyrolysis of rape-seed in a fluidized-bed reactor. *Bioresource Technology* **1998,** 66, (2), 113-117.
8. Scott, D. S.; Piskorz, J.; Bergougnou, M. A.; Graham, R.; Overend, R. P., ROLE OF TEMPERATURE IN THE FAST PYROLYSIS OF CELLULOSE AND WOOD. *Industrial & Engineering Chemistry Research* **1988,** 27, (1), 8-15.
9. Mohan, D.; Pittman Jr, C. U.; Steele, P. H., Pyrolysis of wood/biomass for bio-oil: A critical review. *Energy and Fuels* **2006,** 20, (3), 848-889.
10. Bridgwater, A. V., Czernik, S, Piskorz, J, An Overview of Fast Pyrolysis. *Progress in Thermochemical Biomass Conversion* **2001,** 2, 977-997.
11. Bridgewater, A. V.; Meier, D.; Radlein, D., An Overview of Fast Pyrolysis of Biomass. *Organic Geochemistry* **1999,** 30, 1479-1493.
12. Onay, O.; Koçkar, O. M., Pyrolysis of rapeseed in a free fall reactor for production of bio-oil. *Fuel* **2006,** 85, (12-13), 1921-1928.
13. Daugaard, D. E.; Brown, R. C., Enthalpy for pyrolysis for several types of biomass. *Energy and Fuels* **2003,** 17, (4), 934-939.
14. Geldart, D., *Gas Fluidization Technology*. John Wiley & Sons: New York, 1986.
15. Whitelock, D.; Buser, M., Preliminary Results of a Series Cyclone Test. In *2005ASAE Annual International Meeting*, Tampa, Florida, 2005.
16. Westerhof, R. J. M.; Kuipers, N. J. M.; Kersten, S. R. A.; Van Swaaij, W. P. M., Controlling the water content of biomass fast pyrolysis oil. *Industrial and Engineering Chemistry Research* **2007,** 46, (26), 9238-9247.
17. Zheng, J.-l.; Yi, W.-m.; Wang, N.-n., Bio-oil production from cotton stalk. *Energy Conversion and Management* **2008,** 49, (6), 1724-1730.
18. Lede, J.; Broust, F.; Ndiaye, F.-T.; Ferrer, M., Properties of bio-oils produced by biomass fast pyrolysis in a cyclone reactor. *Fuel* **2007,** 86, (12-13), 1800-1810.
19. Miao, X.; Wu, Q.; Yang, C., Fast pyrolysis of microalgae to produce renewable fuels. *Journal of Analytical and Applied Pyrolysis* **2004,** 71, (2), 855-863.

20. Gerdes, C.; Simon, C. M.; Ollesch, T.; Meier, D.; Kaminsky, W., Design, construction, and operation of a fast pyrolysis plant for biomass. *Chemical Engineering and Technology* **2002,** 25, (6), 167-174.
21. Guo, Z.-G.; Wang, S.-R.; Zhu, Y.-Y.; Luo, Z.-Y.; Cen, K.-F., Separation of acid compounds for refining biomass pyrolysis oil. *Ranliao Huaxue Xuebao/Journal of Fuel Chemistry and Technology* **2009,** 37, (1), 49-52.
22. Branca, C.; Giodicianni, P.; Di Blasi, C., GC/MS Characterization of Liquids Generated from Low-Temperature Pyrolysis of Wood. *Ind. Eng. Chem. Res.* **2003,** 42, 3190-3202.
23. Yanik, J.; Kornmayer, C.; Saglam, M.; Yüksel, M., Fast pyrolysis of agricultural wastes: Characterization of pyrolysis products. *Fuel Processing Technology* **2007,** 88, (10), 942-947.
24. Patwardhan, P. R.; Satrio, J. A.; Brown, R. C.; Shanks, B. H., Product distribution from fast pyrolysis of glucose-based carbohydrates. *Journal of Analytical and Applied Pyrolysis* In Press, Corrected Proof.
25. Wikipedia Acetic Acid. http://en.wikipedia.org/wiki/Acetic_acid (August 18, 2009),
26. Suuberg, E. M.; Oja, V. *Vapor Pressures and Heats of Vaporization of Primary Coal Tars*; Brown University: July, 1997, 1997.
27. Chapter 2-Basic Sugar Chemistry http://dwb4.unl.edu/Chem/CHEM869E/CHEM869ELinks/www.forestry.auburn.edu/elder/wood_chem/ch2/ch2.html (October 21),
28. Liu, Q.; Lv, C.; Yang, Y.; He, F.; Ling, L., Study on the pyrolysis of wood-derived rayon fiber by thermogravimetry-mass spectrometry. *Journal of Molecular Structure* **2005,** 733, (1-3), 193-202.
29. Wikipedia Formic Acid. http://en.wikipedia.org/wiki/Formic_acid (August 18, 2009),
30. Wikipedia Furan. http://en.wikipedia.org/wiki/Furan (August 18, 2009),
31. Biochemistry, M. C. D. o. C. Ch. 24 Phenols (Ar-OH). http://bio-che.mc.edu/valente/ch24.pdf (August 18, 2009),
32. Wikipedia Guaiacol. http://en.wikipedia.org/wiki/Guaiacol (August 18, 2009),
33. Wikipedia Syringol. http://en.wikipedia.org/wiki/Syringol (August 18th, 2009),
34. Ba, T.; Chaala, A.; Garcia-Perez, M.; Rodrigue, D.; Roy, C., Colloidal Properties of Bio-oils Obtained by Vacuum Pyrolysis of Softwood Bark. Characterization of Water-Soluble and Water-Insoluble Fractions. *Energy & Fuels* **2004,** 18, (3), 704-712.
35. Diebold, J. P. *A Review of the Chemical and Physical Mechanisms of the Storage Stability of Fast Pyrolysis Bio-oils*; NREL: Lakewood, Colorado, January 2000, 2000.
36. Aubin, H.; Roy, C., Study on the corrosiveness of wood pyrolysis oils. *Fuel Science and Technology International* **1990,** 8, (1), 77-86.
37. Hoffman, A. C.; Stein, L. E., *Gas Cyclones and Swirl Tubes*. Springer: Berlin, 2002.
38. Bridgwater, A. V.; Peacocke, G. V. C., Fast pyrolysis processes for biomass. *Renewable & sustainable energy reviews* **2000,** 4, (1), 1-73.
39. Spurny, K., *Advances in Aerosol Filtration*. Lewis Publishes: Boca Raton, 1998.

40. Brown, D. E. D. a. R. C. In *The transport phase of pyrolytic oil exiting a fast fluidized bed reactor*, Science of Thermal and Chemical Biomass Conversion Conference, Victoria, British Columbia, Canada, August 30,2004 - September 2, 2004, 2004; Victoria, British Columbia, Canada, 2004.
41. Lide, D. R., *CRC Handbook of Chemistry and Physics*. 76th ed.; CRC Press: Boca Raton, 1995.
42. Wikipedia Thermocouple. http://en.wikipedia.org/wiki/Thermocouple (August 24, 2009),
43. McGowan, T. F., *Biomass and Alternate Fuel Systems*. Wiley: 2009.
44. EERE, U. D. a. Biomass Feedstock Composition and Property Database. http://www1.eere.energy.gov/biomass/feedstock_databases.html (October 21),
45. ASTM, Standard Test Method for Kinematic Viscosity of Transparent and Opaque Liquids (and Calculation of Dynamic Viscosity). In 2009; Vol. D445.
46. ASTM, Standard Specifications and Operating Instructions for Glass Capillary Kinematic Viscometers. In 2007; Vol. D446.
47. ASTM, Standard Test Method for Kinematic Viscosity of Asphalts (Bitumens). In 2007; Vol. D2170.
48. Agblevor, F. A.; Besler, S.; Wiselogel, A. E., Fast Pyrolysis of Stored Biomass Feedstocks. *Energy & Fuels* **1995,** 9, (4), 635-640.
49. Wright, L.; Boundy, B.; Perlack, B.; Davis, S.; Saulsbury, B., *Biomass Energy Data Book*. 1st ed.; Oak Ridge National Labratory: 2006.
50. Diebold, J. P., A Review of the Toxicity o f Biomass Pyrolysis Liquids Formed at Low Temperatures. In *Fast Pyrolysis of Biomass: A Handbook*, Bridgewater, A. V.; Czernik, S.; Diebold, J. P.; Meier, D.; Oasmaa, A.; Peacocke, G. V. C.; Piskorz, J.; Radlein, D., Eds. cplPRESS: Newbury, 1999; Vol. 1.
51. Buranov, A. U.; Mazza, G., Lignin in straw of herbaceous crops. *Industrial Crops and Products* **2008,** 28, (3), 237-259.
52. Oasmaa, A.; Kuoppala, E.; Solantausta, Y., Fast Pyrolysis of Forestry Residue. 2. Physicochemical Composition of Product Liquid. *Energy & Fuels* **2003,** 17, (2), 433-443.
53. Sharma, R. K.; Bakhshi, N. N., Upgrading of pyrolytic lignin fraction of fast pyrolysis oil to hydrocarbon fuels over HZSM-5 in a dual reactor system. *Fuel Processing Technology* **1993,** 35, (3), 201-218.
54. Lu, Q.; Li, W.-Z.; Zhu, X.-F., Overview of fuel properties of biomass fast pyrolysis oils. *Energy Conversion and Management* **2009,** 50, (5), 1376-1383.